AGSO

BENTHIC CHAMBERS, NUTRIENT FLUXES & THE BIOGEOCHEMISTRY OF THE SEAFLOOR OF PORT PHILLIP BAY, 1995 & 1996

BY

W. BERELSON, T. KILGORE, D. HEGGIE,
G. SKYRING & P.FORD

RECORD 1996/17

AGSO

AUSTRALIAN
GEOLOGICAL SURVEY
ORGANISATION

AGSO RECORD 1996/17

BENTHIC CHAMBERS, NUTRIENT FLUXES & THE BIOGEOCHEMISTRY OF THE SEAFLOOR OF PORT PHILLIP BAY 1995 & 1996

W. Berelson[1], T. Kilgore[1], D. Heggie[2], G. Skyring[3] & P. Ford[4]

1. Department of Geological Sciences, University of Southern California, Los Angeles, California, USA
2. Division of Environmental Geoscience & Groundwater, Australian Geological Survey Organisation, GPO Box 378, Canberra, ACT, 2601
3. Skyring Environment Enterprises, 40 Atherton St, Downer, ACT, 2602
4. Division of Environmental Mechanics, CSIRO, Canberra, ACT, 2601

TABLE OF CONTENTS

EXECUTIVE SUMMARY

The first phase of benthic flux studies in Port Phillip Bay conducted during the summer of 1994, identified that sedimentary processes play a very important role in the bay-wide budgets for carbon, phosphate, silicate and nitrogen. Three of the most important findings were: (1) the ratio between oxygen consumed and carbon dioxide produced was indicative of the degradation of organic matter from diatomaceous phytoplankton; (2) benthic bio-irrigation played a very important role in aeration of the sediments and the transfer of nutrients to the overlying water column, and (3) denitrification, the sequential conversion of organic-N to N_2, occurred in most sediments of the Bay, and that denitrification efficiencies were high (50 to 90%) at most sites.

The second phase of the benthic flux studies conducted from February 1995 to January 1996 focused on (1) spatial and temporal consistency in benthic fluxes at key sites in Port Phillip Bay (2) benthic chamber calibration (3) bio-irrigation measurements (4) direct measurements of N_2 for independent assessments of denitrification rates and efficiencies at key sites. The most important results of the study are:

1. The general pattern in nutrient fluxes observed in 1994, is repeated in the 1995 data.
2. The flux data show no sensitivity toward paddle stir rate indicating that benthic processes are insensitive to diffusive boundary layer thickness over a scale factor of two. Deuterium (as D_2O) was the best indicator of chamber water-pore water exchange. Results with other tracers (Cs, and Br added simultaneously with the D_2O) were in excellent agreement with those for deuterium. All tracer data confirmed that leakage is a non-issue with this technology. The present and previous measurements of benthic and bio-irrigation processes are valid.
3. The measured N:C flux ratios for the February 1995 study, was always less than the predicted value and the missing N is interpreted to be the result of denitrification. Direct measurements by Gas Chromatography (GC) of N_2 fluxes generally supported this conclusion.
4. Added nitrate was advected into the sediments. Only the naturally formed nitrate was denitrified, suggesting that there are microbial microniches in which organic carbon oxidation, ammonification, nitrification and denitrification occurs simultaneously.
5. The mass spectrometric measurements of N_2 during January/December 1996 proved beyond doubt that denitrification occurs in the sediments of Port Phillip Bay. Gas chromatographic measurements of N_2/Ar were verified by mass spectrometer measurements providing a basis for more confident interpretation of the preceding GC analyses from February 1995 to January 1996.
6. There was a significant seasonal effect in the denitrification efficiencies (measured) at site 16 (Yarra Estuary) but seasonal effects on denitrification efficiencies in the central sediments (Site 37) were marginal.
7. Denitrifying efficiencies were consistently high in the central basin sediments.

The role of sedimentary processes in Port Phillip Bay, is once again found to be extremely important. Phytoplankton, feeding on the nutrients entering the Bay from riverine and sewage inputs, are readily degraded on reaching the sediments resulting in nutrients recycling by the benthic communities of macro- and micro-organisms. Without checks or balances this recycling system may run into problems of nutrient enrichment and eutrophication, especially since there is a long residence time of water in Port Phillip Bay. There is an ample supply of

P in Port Phillip Bay but a limited availability of N. The sediments play a crucial role in maintaining this limitation. A combination of factors, including high benthic productivity, low sediment accumulation rates, and very active bio-irrigation, keep ammonium and nitrate concentrations very low and the efficiency of denitrification high. Port Phillip Bay is extraordinary because high denitrification rates and efficiencies have been continuously maintained even with increased nutrient loads from agricultural and urban sources since European colonisation. It is clear from the present studies that the future management of Port Phillip Bay must ensure that denitrification remains a quantitatively important process.

The report is presented in three sections:

1. Benthic chambers, nutrient fluxes and the biogeochemistry of the seafloor of Port Phillip Bay
2. Direct denitrification measurements in sediments
3. Transport processes and tracer kinetics.

BENTHIC CHAMBERS, NUTRIENT FLUXES AND THE BIOGEOCHEMISTRY OF THE SEAFLOOR OF PORT PHILLIP BAY, SUMMER 1995

Introduction

The report on benthic fluxes during the summer of 1994 (Berelson, W. M., Kilgore, T. E., and Heggie, D. T., *June 1994*) indicated that microbial nitrification and denitrification controlled N transformations in the Bay and denitrification prevented the Bay from becoming a significant sink for N. The important consequence of these observations is that, if nitrification is prevented by oxygen depletion (one of the consequences of eutrophication of the sediments), then nitrification and denitrification cannot occur. The waters of the Bay would then become a sink for N because it would be effluxed from the sediments as ammonia which would be immediately available for the next round of phytoplankton bloom.

The interpretation of the measured nutrient fluxes in the benthic chambers was on the basis of Redfield stoichiometry (106C:16N:1P), the gross ratios between the CNP components of marine phytoplankton. There is strong circumstantial evidence that diatoms are the major contributors of fresh organic material to the sediments of Port Phillip Bay (T. O'Leary et al, 1994), and the Redfield assumption is reasonable.

The subsequent investigations in February/March, May, June and August/September of 1995 and for January 1996, were to positively identify all components of the N budget. To do this, direct measurements of N_2 and dissolved organic nitrogen (DON) fluxes from sediments were required in addition to the nutrient and respiratory end-product fluxes which were measured in the summer of 1994. Figure 1 shows all of the study sites; the sites re-examined during 1995-96 are shown as stars.

Benthic chamber technology and methods

The benthic incubation chamber utilised by the USC group, schematically depicted in Figure 2, has been described by Berelson et al. (1986, 1987a). The device was deployed from the Marine Science Laboratories (Victoria) research vessel *Melita* or the chartered vessel *Shearwater* by lowered hand-line. The PVC chamber (a 30-cm diameter cylinder) entered the sediment slowly with the chamber lid open to allow flushing through the cylinder. Chamber seating on the sea floor was confirmed by divers. During a typical deployment, the chamber lid remained open for a few hours to allow the oxygen electrode to equilibrate and any disturbed sediment to re-settle. On a pre-programmed signal from the micro-computer on the device, the lid closed, capturing 7-10 L of bottom water in contact with the sea floor. A rotating paddle at the top of the chamber ensured mixing. The rate of rotation was usually 5-6 revolutions per minute (rpm), a rate previously determined to set up an average diffusive boundary layer thickness of ~300 μm. One chamber was deployed with a paddle stirring rate of 2 rpm in order to compare the difference in fluxes attributable to boundary layer thickness. Six samplers, 3 of 130 mL and 3 of 300 mL, withdrew water from the chamber during the course of an incubation. A narrow tube (0.3 cm id) connecting the chamber to the ambient environment allows the inflow of bottom water during a chamber draw. Samples were stored in plastic (for nutrient analyses) or glass (for radon analysis) tubes or calibrated

Nylaflow® sample loops affixed to miniature 6-port valves (nitrogen gas analysis) until the instrument was recovered. Three sample draws, normally draws 1, 5, and 6 were routed through two 6-port valves connected in series, located between the chamber and the first nutrient sample tube. The chamber volume was determined by measuring the dilution of a spike of CsCl, added to the chamber during the incubation by calibrated syringe. Additional tracers included D_2O, Br and KNO_3. Polarographic electrodes, operated in a pulsed mode, measured oxygen concentration every 6 minutes in both the ambient and the chamber water. Determinations of nutrients (PO_4^{3+}, NO_3^-, NO_2^-, SiO_4 and NH_4^+, by autoanalyser techniques), pH, alkalinity (by Gran titration), cesium (atomic emission) and conductivity were done on a combined volume of 30 mL. Total CO_2 was calculated from alkalinity and pH measurements using standard carbonate equilibrium constants as described by Berelson et al. (1994). Radon was determined by scintillation counting using the techniques described by Berelson et al. (1987b) on 100-mL samples from each of the 300-mL draws. N_2 and N_2/Ar were measured by gas chromatographic techniques on 1 mL sample loops from the 6-port valves.

Benthic chamber results

The data presented in Figs. 3-12 and Figs. 13 & 14 summarise the flux chamber measurements of nutrients and oxygen. For all plots, the y-axis is concentration in μM, except alkalinity (μeq/L) and Cs (ppm). The first point plotted on the y-axis represents the value of bottom water obtained from measurements of water collected with a Niskin bottle. The x-axis is scaled in hours after the lid of the benthic chamber has closed. The oxygen electrode output plots include electrode data from before the lid has closed (negative time on the x-axis) and also shows, with vertical tic marks, the timing of sample collection. Because the uptake of oxygen and the flux of nutrients into and out of the sediments is not always a linear function of time, we have designated a portion of the incubation period as representative of the flux from the undisturbed sea floor and indicate this designation with the dashed horizontal line in Figs. 13 and 14. For some stations, the entire incubation period was deemed representative (e.g. Site 37*-Blue) and thus all 6 sample draws regressed to a linear function. For many other stations (e.g. Sites 14 and 16), only a portion of the incubation period was considered representative of a 'constant flux condition' and thus only a few samples were used to determine the nutrient fluxes. The portion of the oxygen electrode output underlined by this dashed line, represents the segment modelled for the flux calculation.

Flux calculations take into account the fact that successive sample draws have been increasingly diluted with the inflow of ambient bottom water, as described by Berelson et al. (1994). The data presented in Figs. 3-12 are corrected for this dilution and fluxes are calculated from this corrected data set. The measured, uncorrected values, appear in the Appendix along with the final flux values and the flux uncertainties. Some values in the data tables are struck through with a horizontal line, these indicate data that did not enter into the flux calculation. In almost all cases, this represents data that fall outside the incubation period deemed representative of the constant flux condition, as described above. In a few cases, spurious measurements were struck through. These tables also contain the values of nutrient concentrations in bottom water collected at each site. Although, in most cases, the first

chamber draw and the Niskin sample concentration values are in close agreement, the bottom water value was not used in determining the flux, only chamber samples were considered.

The oxygen electrode output was converted to oxygen concentration (Figs. 13 and 14) by calibration to the ambient oxygen concentration as determined by Winkler titrations on Niskin samples and by internal calibrations performed in the laboratory. In most cases the cross calibrations agree to within 10% but for some electrode outputs the uncertainty of calibration is 20%. In calculating oxygen fluxes, the electrodes with the greater calibration uncertainties have the greater flux uncertainty. The oxygen electrode exposed to ambient water worked satisfactorily in 4 of the 10 chamber deployments.

A summary of the calculated benthic fluxes for all chemical species measured appears in Tables 1 and 2. The flux is calculated as the product of the slope of a linear regression through the corrected data and the effective chamber height. Within the Appendix there is a row labelled 'Uncertainty' which identifies the concentration (±s.d.) of each analyte measured. The source of uncertainty in the linear regression fit of the data may be either the goodness of fit or the analytical uncertainty of the measurements. The source of the uncertainty is also identified in the Appendix. The radon flux was determined by fitting the dilution-corrected data to an equation that corrects for radon decay during incubation (Berelson et al., 1987c). The uncertainty in the height of each chamber also enters into the overall uncertainty in flux. The chamber heights and their uncertainties are also given in the Appendix. In some chamber deployments the Cs spike injection syringe failed, in which case the chamber height was assumed as some average value, although the uncertainty assigned to this value was proportionally larger than for chambers in which the Cs was injected and measured.

Figures 15 and 16 contain the radon-222 data and fits to the concentration versus time plots. Although problems with scintillation counter efficiencies increased the measurement uncertainties from 10 to 30%, the trend in increasing radon is generally observed and well fit by the equation describing radon flux and radioisotope decay. Again, the fits to these measured data were not forced through a time=0 point although their intersection with the y-axis indicates a reasonable prediction of the assumed bottom water radon value of about 0.2-1 dpm/L. The data from Site 8-Blue were too erratic to fit and the cause of this may be spurious measurement.

An important consideration is whether the USC chambers are restricting light penetration to the incubated sediments and how this may impact the fluxes measured. The data presented in this report shows no definitive example of oxygen production although some may be occurring towards the end of the experiment at site 6* (Figure 3). The comparison of light and dark chambers provided by Nicholson et al. (1996) will address this issue. Our examination of their results indicate that sea floor productivity may impact the net, 24 hour fluxes by 30%. Any final corrections to the data presented in this report must await final interpretation of the light/dark comparisons (Longmore et al; 1996 and Nicholson et al, 1996) but we note this potential for systematic though small overestimation of respiratory product fluxes.

Comparison of 1994 and 1995 fluxes

Figures 17 and 18 present the 1995 flux data and offer a comparison to the 1994 results. The 1995 data are averages of two chambers, where 2 chambers were deployed, but do not include the chambers that were spiked with KNO_3. The general pattern in nutrient fluxes observed in 1994 is repeated in the 1995 data. Fluxes at Werribee are generally: Site 6 >Site 8 and these are generally > Site 37 located in the central part of Port Phillip Bay. Fluxes at the Hobsons Bay Site 14 and Yarra River Site 16 are generally >> than the other sites. It is significant that the pattern of nutrient fluxes generally mimics the pattern of radon fluxes. Radon is not linked to carbon diagenesis, thus the similarity in flux patterns suggests that the transport of radon from pore waters is also controlling the transport of nutrient species across the sediment-water interface. This point will be discussed in more detail later in this report.

In 1994 we measured a very high oxygen flux at Site 6, one that was not easily explained by our stoichiometric balances, and the 1995 data indicate that this high value is about 2 times the average flux for this area. At sites 6, 8 and 37, there is no systematic trend in nutrient fluxes between 1994 and 1995. The total CO_2 flux was slightly greater at sites 6 and 8 in '94 compared to '95, but the temporal trend is reversed at Site 37.

The notable difference between the 1994 and 1995 results occurs in the Hobsons Bay-Yarra region. Although we have deployed only one chamber at each of these sites on both occasions, the difference in nutrient fluxes indicates that greater organic matter diagenesis occurred in 1995 compared to 1994. The silicate flux dramatically demonstrates this conclusion; fluxes are 3 times greater in 1995 relative to 1994. The enhanced flux at both Sites 14 and 16 indicate that the results are not an artefact of placing a chamber over some non-representative portion of the sea floor. Oxygen, nitrate, phosphate and TCO_2 fluxes also show that significantly greater diagenesis was occurring during February1995.

One reason for the increased nutrient fluxes in 1995 may have been an increase in benthic infaunal irrigation. As a test to the hypothesis that the intensity of benthic irrigation has increased, hence the higher in fluxes in 1995, we compare the radon fluxes from both years. The data suggested that irrigation was not the reason for increased nutrient fluxes. However, a comparison of the rate constant for Cs loss from the 1995 and 1994 Yarra River site indicates a significant difference in the bio-pumping rate. The apparent discrepancy between these tracers is due to an upper limit on radon flux imposed by radioactive decay rates (this and similar arguments are made latter in this report, see also Figure 22).

One conclusion we draw from the comparison of fluxes in the Hobsons Bay region is that there was a marked increase in the rate of pumping between 1994 and 1995. We suggest that some recent input of silica-rich organic matter (diatoms) to the Hobsons-Yarra region probably occurred, within weeks or months of the 1995 field program. This time frame is based on work previously published which indicates that the lifetime of organic carbon in shallow marine systems may be on the order of a few weeks.

Determination of carbon oxidation and stoichiometric considerations

The data in Tables 1 and 2 have been used to interpret the organic carbon oxidation rate (C_{ox}) using two models which probably represent end-member scenarios. The budget presented in Table 3 presents two scenarios that explain the source of alkalinity effluxing from the sediments of Port Phillip Bay. One model accounts for all the measured alkalinity flux, after corrections for nitrate and ammonia fluxes, as derived from $CaCO_3$ dissolution. A second model accounts for all the corrected alkalinity flux as derived from sulfate reduction.

As there is a positive alkalinity flux at all stations, the interpretation of the $CaCO_3$ dissolution scenario is that all sites undergo carbonate dissolution. The bay-averaged dissolution rate of around 5 mmol $CaCO_3/m^2/day$ (based on a value of alkalinity flux = 10 $meq/m^2/day$), would amount to a loss of carbonate shell material of $1x10^9$ g $CaCO_3$/day (for a bay of 2000 km^2). It is very likely that not all of the corrected alkalinity can be accounted for by carbonate dissolution and thus this figure probably represents an upper limit for bay-wide dissolution. According to this scenario, that part of the TCO_2 flux not attributed to carbonate dissolution must be due to organic C degradation (column 2 in Table 3). The relationship between oxygen uptake and carbon oxidised, given the carbonate dissolution scenario, is shown in Figure 19 by the solid circles. The relationship defined in this plot indicates that approximately one mole of oxygen is consumed in the production of one mole of CO_2. This stoichiometry is consistent with the organic carbon having a valance state of zero, but it also assumes that the ammonia produced during organic matter degradation remains unoxidized. Certainly some of the oxygen uptake is going towards ammonium oxidation, thus we investigate the alternative scenario.

The sulfate reduction scenario attributes all the corrected alkalinity flux to sulfate reduction and the precipitation of iron sulfide minerals. The following equation summarises the general stoichiometry of sulfate reduction:

$$15C_{org} + 2.5NH_3 + 8SO_4^{2-} + 4Fe(OH)_3 + H_2O = 4FeS_2 + 11.5\ HCO_3^- + 3.5\ CO_3^{2-} + 2.5NH_4^+$$

This equation is formulated assuming Redfield C:N stoichiometry, that $Fe(OH)_3$ is the oxidised form of iron, and that pyrite is the reduced product. These are not unreasonable assumptions; changes in the C:N ratio have small effects on the alkalinity:CO_2 balance, iron oxyhydroxide is a common form of Fe^{+3} and pyrite is the commonly found reduced iron solid within marine sediments.

The sulfate reduction scenario accounts for some of the TCO_2 flux as attributable to sulfate reduction and some to oxygen uptake. Table 13 shows the partitioning between these two electron transfer pathways. Sulfate reduction within Port Phillip Bay generally accounts for 5-50% of the carbon oxidised. If the CO_2 flux not attributed to sulfate reduction is due to oxygen uptake, the relationship between oxygen uptake:$C_{oxidised}$ (Figure 19) indicates a stoichiometry of around 1.0. This ratio is consistent with the reaction of oxygen and ammonia to produce nitrate. The very low flux of nitrate from the sediments indicates that nitrate is further reduced in denitrification reactions. Hence, by the sulfate reduction scenario, the

carbon oxidised by oxygen has its ammonia oxidised as well. The carbon oxidised by sulfate produces ammonium.

Although both scenarios are plausible, the sulfate reduction scenario is likely to more closely represent carbon diagenesis within the Bay for the reasons discussed above. However, it is possible that both processes occur to varying degrees; as yet, we do not have the analytical means or supporting data to differentiate the relative proportion of each process. In terms of calculating total carbon oxidised in this system, the difference between the two models is not great, a maximum of 20% at Site 16. Hereafter, we adopt the sulfate reduction model in considering how much organic carbon is oxidised at each site. If we were determined to examine how much sulfate reduction/carbonate dissolution were occurring in Port Phillip Bay, the following measurements could be made: a) measure the amount and accumulation rate of pyrite within the sediments, b) measure the production and burial rate of $CaCO_3$ in the Bay, c) measure the flux of Ca^{+2} within the chamber as a direct measure of carbonate dissolution.

C:N:P stoichiometry

The ratios of carbon:nitrogen:phosphorous fluxes from the sediments of Port Phillip Bay were investigated considering that marine phytoplankton was the main source of organic matter to the sediments (Figure 20).

Sediments with lower rates of C_{OX} return to the water column a proportionally lower fraction of the total N predicted, relative to the stations undergoing greater rates of carbon oxidation (ie the lowest denitrification efficiencies). It is clear from our work that the efficiency of N recycling is enhanced at sites of greater carbon oxidation. These also represent the sites with the greatest rates of sulfate reduction. In an attempt to recover the 'missing N' we measured DON fluxes within the chambers. Even when DON fluxes are added to nitrite, nitrate and ammonia fluxes, the predicted N:C ratio in the flux chamber is never observed. However, the DON fluxes show so much variability, it has not been determined to our satisfaction that DON values from the flux chambers are entirely free of sampling artefacts, and we advise against considering DON as a component of the N budget.

The authors of this report are aware of the considerable importance the results depicted in Figure 20 (top panel) bring to bear on the modelling efforts underway within the larger Port Phillip Bay project. We have confidence, indicated by the error bars, in these results and note that they confirm the 1994 results. We wish to make a point in this report, that the results depicted in Figure 20 (top panel) are quite dissimilar to results obtained by the senior author in his studies of comparable coastal systems in other parts of the world.

The efflux of phosphate in the stoichiometrically predicted proportion to C_{OX} (1:106) is observed for some sites (Figure 20, lower panel). In fact, phosphate flux relative to C_{OX} shows a pattern whereby P is preferentially retained in sediments undergoing low rates of carbon oxidation, and excess P is returned to the overlying water at sites undergoing high rates of C_{OX}. This pattern has also been observed within California coastal environments (Berelson, unpub. data). The P:C flux ratio at Site 16, which shows an excess of P efflux over that supplied by C_{OX}, must be due to the release of adsorbed or iron-bound P in addition to P associated with organic matter.

A budget for N

The difference between the observed and predicted N fluxes (Figure 20) is hypothesised to result from net denitrification and conversion of ammonia via nitrate to N_2. In Table 4 we have summarised the total N flux budgets and describe predicted N and missing N fluxes. Predicted N fluxes amount to the C_{OX} flux /(C:N) of organic matter. We have assumed C:N follows Redfield stoichiometry (approximately 6.6). This N flux may appear as nitrate, nitrite, ammonium or N_2 (not measured routinely). The missing N flux is the difference between the predicted and the observed. If the missing N flux is attributable to denitrification and the production of N_2, we can predict the expected N_2 fluxes and compare these values to measured fluxes. A discussion of N_2 measurements is given in the following section of this report. Below, we discuss several problems with closing the nitrogen balance:

1. The contribution of DON to the total N inventory is large, however, estimation of fluxes was complicated by large and unexplained variations in the measurements. We consider that the DON flux is likely to be small in PPB and have not considered it in the N budget.
2. The predicted total N flux is based on Redfield stoichiometry and the sulfate reduction scenario as the best estimate for C_{OX}. Uncertainty in the value of C_{OX} does not affect the predicted N fluxes by more than 20% whereas the N deficit approaches 80%.
3. The missing N flux is based on the difference between the predicted and measured values. A small difference is likely to be associated with a large uncertainty.
4. The N_2 flux calculations did not include the same draw samples as the nutrient flux calculations because of the limited supply of 6-port valves. As a result, the N_2 flux calculations are often based on draws 5 and 6 that occur late in the incubation period. Flux estimates based on samples from draws 5 and 6 are likely to underestimate the true flux, especially at sites where the chamber concentration is strongly non-linear with time.

Nitrate spike experiments

One chamber deployed at Site 6* and one at 37* were spiked with a solution of $K^{15}NO_3$. By enriching the chamber water with nitrate we provided an additional potential electron acceptor to be utilised in the process of carbon oxidation.

Both chambers that were enriched in nitrate showed significantly greater fluxes of NO_2 (nitrite) out of the sediments, much greater fluxes than had been observed in the unspiked deployments at these sites (Table 2). This is indirect evidence that denitrification is indeed occurring in these sediments since nitrite is an intermediary product of denitrification.

Although some of the nitrate injected to these chambers is utilised in carbon oxidation, diffusion and advection into the sediments account for most of the observed uptake of the NO_3 spike. These transport processes are discussed further in another section of this report. The consumption of the spike nitrate has not been quantified, hence we are not sure how much N_2 to expect from the sediments underlying the spiked chambers. Because the CO_2 effluxes to these chambers are not significantly higher than the fluxes to other, unspiked chambers, we conclude that little of the introduced nitrate had the opportunity to undergo denitrification reactions. The N_2 measurements confirm this conclusion. However, the enhanced nitrite flux

does indicate that the denitrification reaction was slightly stimulated by the presence of high nitrate concentrations. Also, isotopic abundances of the ^{15}N in N_2 chamber samples from this single experiment (A. Herczeg pers. comm.) indicate that the exogenous NO_3 was not utilised during denitrification (at least over the time period of this experiment).

Chamber artefacts?

Benthic chambers are forever criticised for their modification and alteration of the 'natural' environment. Perturbation is unavoidable. However, many tests and experiments have been made to prove that the data from these chamber experiments are very close representations of the natural fluxes. Some of these experiments and measurements are discussed below.

The effect of paddle stir rate

At Site 8 we modified the Yellow chamber paddle stir rate so that it only turned at 2 rpm, all other chamber paddles, including Site 8-Blue, turned at 6 rpm. The similarity in fluxes between 8-Yellow and 8-Blue is evidence that diffusive boundary layer (DBL) thickness does not play an important role in the control of benthic fluxes in this environment. We reached the same conclusion based on a similar comparison of fluxes conducted during the 1994 field season. Dr W. Berelson has conducted these comparisons in many environments with similar results.

These DBL results have bearing on the interpretation and understanding of solute transport processes. The difference in boundary layer thickness that accompanies a 3-fold decrease in stir rate is about an increase by a factor of 2 (Berelson et al., 1990). The flux data (Tables 1 and 2) show no tendency for the slower stirred chamber to have systematically lower fluxes. This means that the zone of reaction and transport within Port Phillip Bay sediments is >> the thickness of the DBL. Transport by irrigation is a plausible reason for this result. Deep reaction sites and a diffusive path length >> the thickness for the DBL is another; (see C. Burke 1995, as his studies pertain to the penetration depth of oxygen in Bay sediments). The conclusion of the work conducted with the benthic chambers is entirely consistent with the oxygen electrode studies; chamber hydrodynamics is not a primary factor controlling benthic fluxes in Port Phillip Bay.

Tidal pumping

The oxygen electrode data provides a continuous record (every 6 minutes) of oxygen concentration outside and within the benthic chambers. Ambient electrodes show very clearly the changes in oxygen concentration within Port Phillip Bay water that must accompany tidal flow. Nowhere in the oxygen record of electrodes mounted inside the chambers is there a coincidence between shifts in oxygen in the ambient water and shifts in oxygen in the chamber water. If tidal pumping were occurring, there would be a correlation between these records.

Interpretation of the Cs, deuterium and nitrate spike injections

The loss of Cs from the chamber, in all cases, follows a monotonic decrease with incubation time (Figs. 3-12). These data have been re-plotted in Figure 21a and fitted to an exponential function. The purpose of this is to demonstrate that Cs loss from the chamber is not driven by concentration gradients (i.e. not controlled by the boundary layer thickness) and it is not due to loss of Cs by dilution with ambient water. Within sediments of the same general composition (fraction of fine particles), Cs loss from the chamber indicates the rate of chamber water-pore water exchange and thereby the rate of pore water irrigation.

The rate of Cs uptake has been modelled using the fitting equation:

$$Cs = Cs_0 \exp(bt)$$

where Cs is Cs concentration in the chamber at time=t, Cs_0 is the Cs concentration in the chamber immediately after injection and b is a fitting parameter with units hr^{-1}.

The results of fitting the Port Phillip Bay 1994 and 1995 data indicates a general consistency in the removal rate constant for regions within the bay (Table 5). For example, the Yarra River and Werribee regions have generally larger removal rate constants than other regions; the central Bay site 37 has generally the lowest rates. This difference implies significant differences in bioirrigation which may be due to burrow densities or to different taxa. Further, the 1995 Yarra site had an extraordinary rate of tracer loss, nearly 2 times greater than the rate measured at any other site. The overall range in removal rate constants spans an order of magnitude, identifying a wide variety in bio-irrigation bay-wide.

Although the greatest rate of Cs loss from a chamber occurs at Site 16, the greatest initial Cs_0 occurs in chamber 37-Blue. Thus, if Cs loss were diffusion controlled, 37-Blue should have the largest value of b. It has a value 4 times lower than the value of b for Site 16. This is evidence that tracer loss is not primarily a diffusive process.

If the loss of Cs from the chamber is due to leakage and dilution with ambient water, the chambers with greater values of b should have lower oxygen, silica and other nutrient fluxes. Just the opposite is true. During the early portion of chamber incubation at Site 16 the rate of loss of Cs is very high and the uptake of oxygen is also very high. This is not the result expected if chamber leakage is the cause of tracer loss.

In Figure 22 we have shown the relationship between the Cs fitting parameter and radon fluxes. This figure demonstrates the positive relationship between Cs uptake rate and radon flux. For chambers deployed at a single station, the chamber with the largest value of "b" also had the largest radon flux. These data emphasise the importance of irrigation as a mechanism of transporting solutes between the water column and the sediment pore waters.

Within the network of burrows that underlie a benthic chamber it is conceivable that some may intersect the sediment surface at sites away from the chamber enclosure. If this were the case, it would seem likely that the chamber incubation water would not be a closed system with respect to the ambient water column and the nutrient and radon fluxes would not show a good correlation to Cs loss. However, it has been shown that the correlation is very good and

is positive. We designed an experiment to test of the effect of deep burrow networks below the chamber walls. With the deployment of chamber 37*-Blue, we extended the depth of chamber penetration by an additional 10 cm. This would effectively cut off more of the burrows. The fluxes of the nutrients, and radon-222, as summarised in Tables 1-2, do not indicate a significant difference in fluxes to the chamber with extended penetration. Hence, the use of chambers with a greater depth of penetration does not significantly change the benthic fluxes measured. We conclude that the network of burrows beneath a benthic chamber does not create pathways for chamber leakage.

Cesium may not be a completely conservative tracer for use in benthic chambers because it has been shown that some adsorptive uptake on marine sediments can occur (Buchholtz and Brink, 1987). The same spike that introduced the Cs to each chamber also carried deuterium labelled H_2O (D_2O). Hence, modeling this totally conservative tracer should indicate if the Cs uptake rates are indicative of advection versus adsorption. The data for changes in D_2O within each chamber are presented in Figure 21b and Cs fitting parameters are compared to deuterium fitting parameters in Table 5. There is very good agreement between the shapes of the concentration versus time data for these two tracers.

We note that the uptake rate parameter "b", defined from the Cs fit is consistently, although only slightly greater than "b" defined by the D_2O data. If loss of tracer were due to leakage, it would be expected that the rate constants for the tracers would be identical. If exchange of chamber water and tracer were controlled by irrigation transport and diffusion into the surrounding pore fluids, the removal rate constant for the more diffusively mobile D_2O tracer should be greater than for Cs. That this is not the observed condition suggests the enhanced loss of Cs is by adsorptive removal. The effective loss term for Cs removal includes diffusion and adsorption.

Nitrate was also introduced to two chambers as a spike injection. The loss of nitrate from these incubations is shown in Figure 21c. For this tracer, the uptake loss parameter "b" is even larger than the same parameter fit to the Cs data. This data indicates loss of nitrate due to advective transport and reaction. Reaction is assumed to represent reduction to nitrite. Again it is noted that if chamber leakage were the process by which tracer concentration were reduced, we would not see differences in the loss rate terms. Differences between the rate loss parameters for different tracers is firm evidence that these chambers did not leak.

Radon fluxes and physical transport processes

As described earlier, radon is not associated with organic matter diagenesis, and will only indicate the source strength of the sediment with respect to radon production and the transport mechanism between pore water and chamber water. We can make the assumption that the radium-226 concentration of Bay mud is fairly homogeneous, based on the 1994 and 1995 measurements (summarised in Table 6), and that the diffusive flux of radon-222 supported by the radium-226 within the sediments is approximately 40 atoms/m^2/sec.

Site 8 is sandy compared to the other muddy sites and the radon flux from this area may be uncharacteristically low relative to the other sites. The deuterium spike data at this station indicate a low rate of chamber water-pore water exchange and the radon budget suggests that

exchange could be controlled by diffusion. The observed radon fluxes from the other sites (Table 1) exceed the diffusive flux by 5-15 times. This is certainly evidence of non-diffusive transport between the pore water and overlying water. A more thorough study of radon emanation from the sediments of Port Phillip Bay is recommended as is a study of the distribution of radon deficiencies down-core. The latter measure is a method of establishing the depth of bio-irrigation.

Dissolved silica and radon fluxes are positively correlated (Figure 23) and show the same trend for 1995 as established in 1994. However, the two Hobsons Bay stations 14 and 16 deviate from this trend. The dissolution of opaline silica is much greater in Hobsons Bay and Yarra River in 1995 compared to 1994. This may be due to a combination of factors: a) the recent input of readily dissolvable silica, such as a diatom bloom event, b) a significant change in the rate or depth of benthic irrigation.

Conclusions from summer (February) 1995 USC chamber deployments

We deployed ten benthic chambers at sites throughout Port Phillip Bay in order to further define the extent and rates of sea floor overlying water solute exchange. The important conclusions are summarised as follows:

1. The general pattern in nutrient fluxes observed in 1994 is repeated in the 1995 data. Nutrient fluxes show a general pattern whereby fluxes at Station 16>14>6>8>37. The pattern of nutrient fluxes generally mimics the pattern of radon fluxes.
2. Organic carbon oxidation rates can be modelled after two scenarios, one where carbonate dissolution dominates the alkalinity flux, another where sulfate reduction is responsible. Although the sulfate reduction model is favoured, it is likely that some carbonate dissolution also occurs and in either case, carbon oxidation (C_{OX}) rates are known to ±20%.
3. The measured N:C flux ratio is always less than the predicted value and we conclude that the missing N is due to denitrification, the sequential conversion of organic N to N_2. Measurements of N_2 fluxes generally support this conclusion.
4. The extent of denitrification in 1995 is similar to the extent present in 1994. Sites undergoing the lowest rates of carbon regeneration are most efficient at converting fixed N to N_2, and sites undergoing greater rates of C_{OX}, which are sites with greater rates of sulfate reduction and generally greater rates of bio-irrigation, recycle a greater proportion of organic N as ammonium.
5. Chambers spiked with nitrate show significantly higher efflux rates of nitrite from the incubated sediments as compared to unspiked chambers. This is clear evidence of active denitrifying bacteria.
6. P release from sediments of Port Phillip Bay are not governed by the Redfield ratio and the rate of carbon oxidation but is a function of P retention, perhaps by co-precipitation with iron-oxyhydroxides under oxygenated conditions, and P release from adsorbed or precipitated forms under low oxygen conditions.
7. The nutrient flux data show no sensitivity toward paddle stir rate and hence are insensitive to diffusive boundary layer thickness over a scale factor of two.
8. The rate of Cs loss from chamber water is indicative of the rate of chamber water-pore water exchange and not indicative of chamber leakage. However, deuterium is shown to be

a better indicator of chamber water-pore water exchange because it undergoes no adsorption reactions with the sediments.

9. Radon fluxes are indicative of irrigation rates and show a correlation with many nutrient fluxes. The very high silicate fluxes observed in Hobsons Bay/Yarra River in 1995 may be due to the recent delivery of biogenic silica by diatomaceous phytoplankton to this region of the bay.

Acknowledgments

We wish to thank the staff of the Victoria Marine Science Laboratories and V.F.R.I. (now Marine and Freshwater Resources Institute) for the extensive logistical support required to carry out this work, particularly Andy Longmore and the staff of the Nutrient Task Group of the Port Phillip Bay study. Andy Longmore and Geoff Nicholson provided massive laboratory, logistical and field support throughout the program. Geoff Nicholson, Arnie Jahncke, and Rhonda Flint dived and surveyed the seafloor of the sites chosen for chamber deployments. Andy Longmore and Rob Cowdell conducted nutrient and alkalinity analyses. Gus Fabris conducted cesium analyses. Philip Ford suggested the deuterium tracer experiments and kindly supplied the analyses. We wish to thank the master, Tony Sheehan, and mate, Ian Duckworth of the FRV *Melita* for their considerable assistance and support during the field work program.

Figure 1: Study Area. This map shows all the 1994, 1995 and 1996 sites; the 1995-96 sites are highlighted with stars.

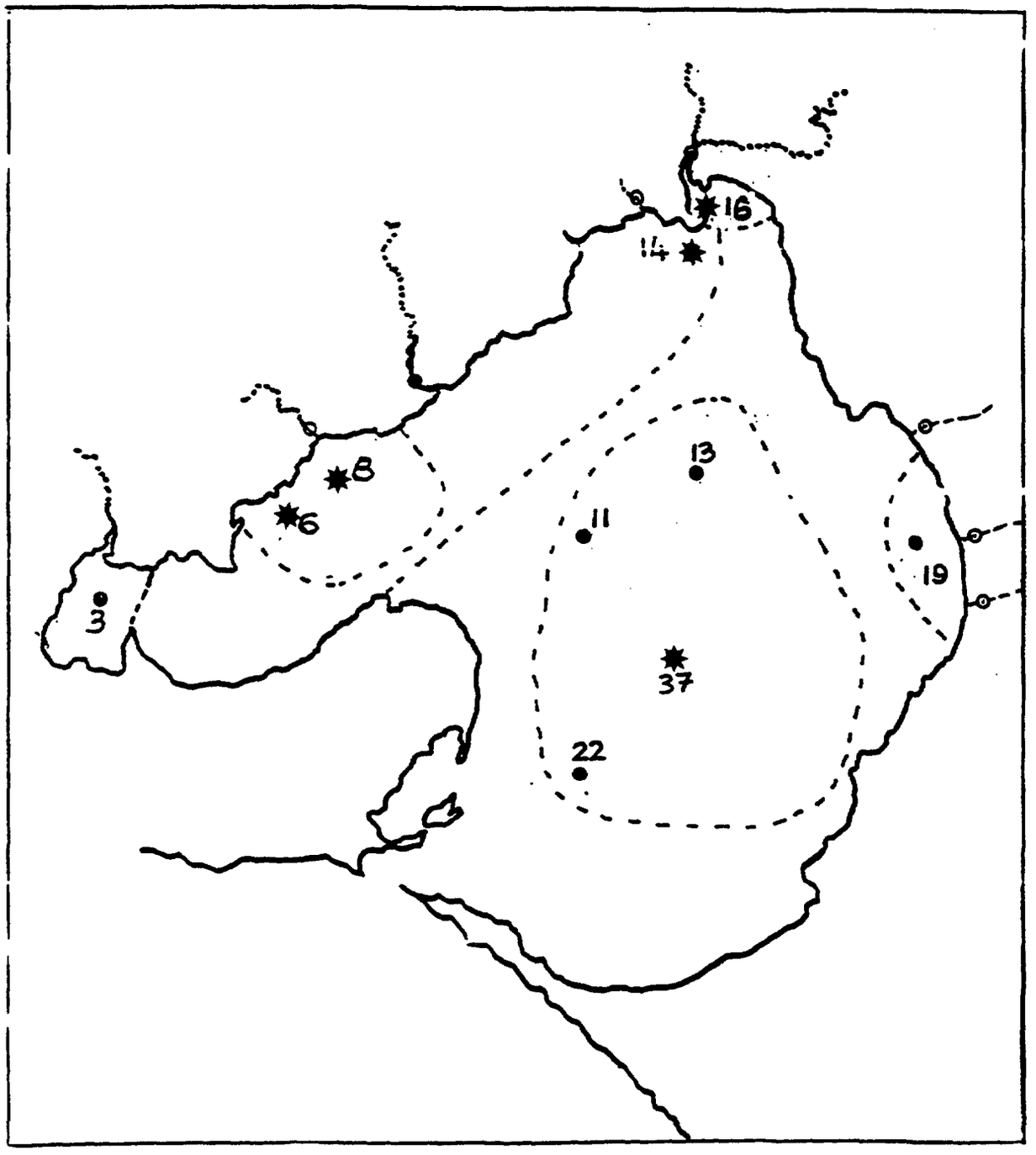

Figure 2: Benthic Chamber Schematic. The unit consists of a PVC chamber (a), supported by an alluminium frame (o) that is approximately 1.2m x 0.5m x 0.5m. Other components include: chamber stirring paddle (b), hinged lid to top of chamber (c), pressure case with magnet-turning motor (d), pressure case with micro-processor (e) and batteries (f) with burn wire leads (g), bulb that draws 300 mL samples (h), sample tubes (k,j,i) and tubing leading out of chamber (l).

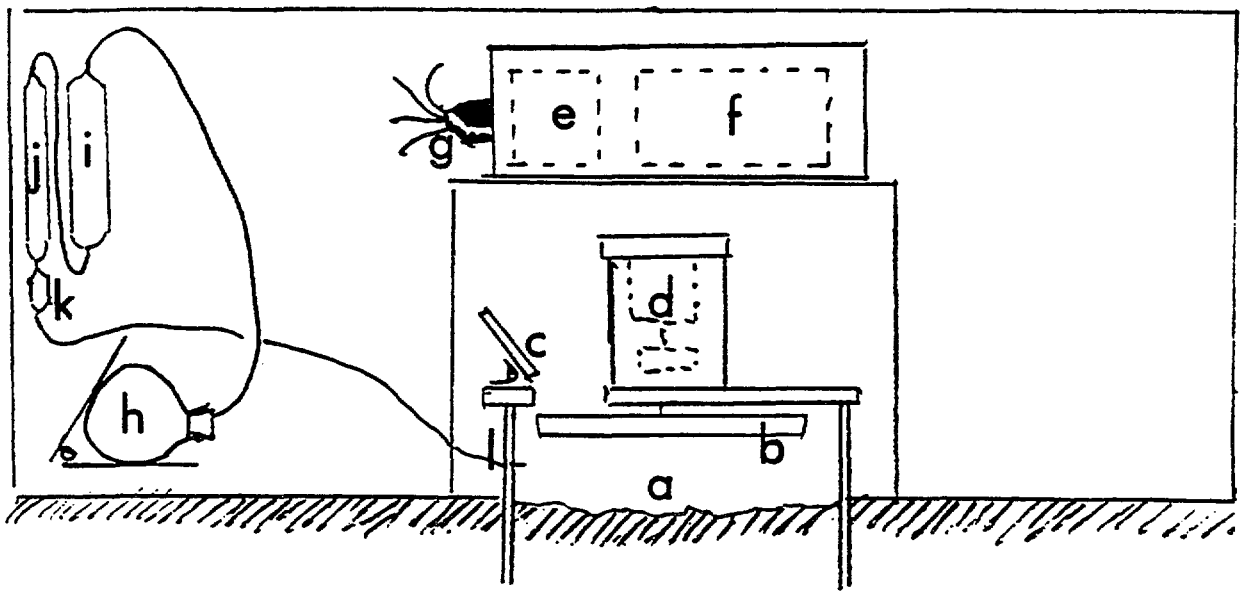

Figure 3: Analyte versus time plots for all the chambers deployed. Concentration is µM except alkalinity (µeq/L) and Cs (ppm). Values plotted are corrected for the dilution which takes place during successive sampling. Analytical uncertainties are found in Tables 1 - 10. Points plotted on the Y-axis are bottom water values measured from Niskin samples.

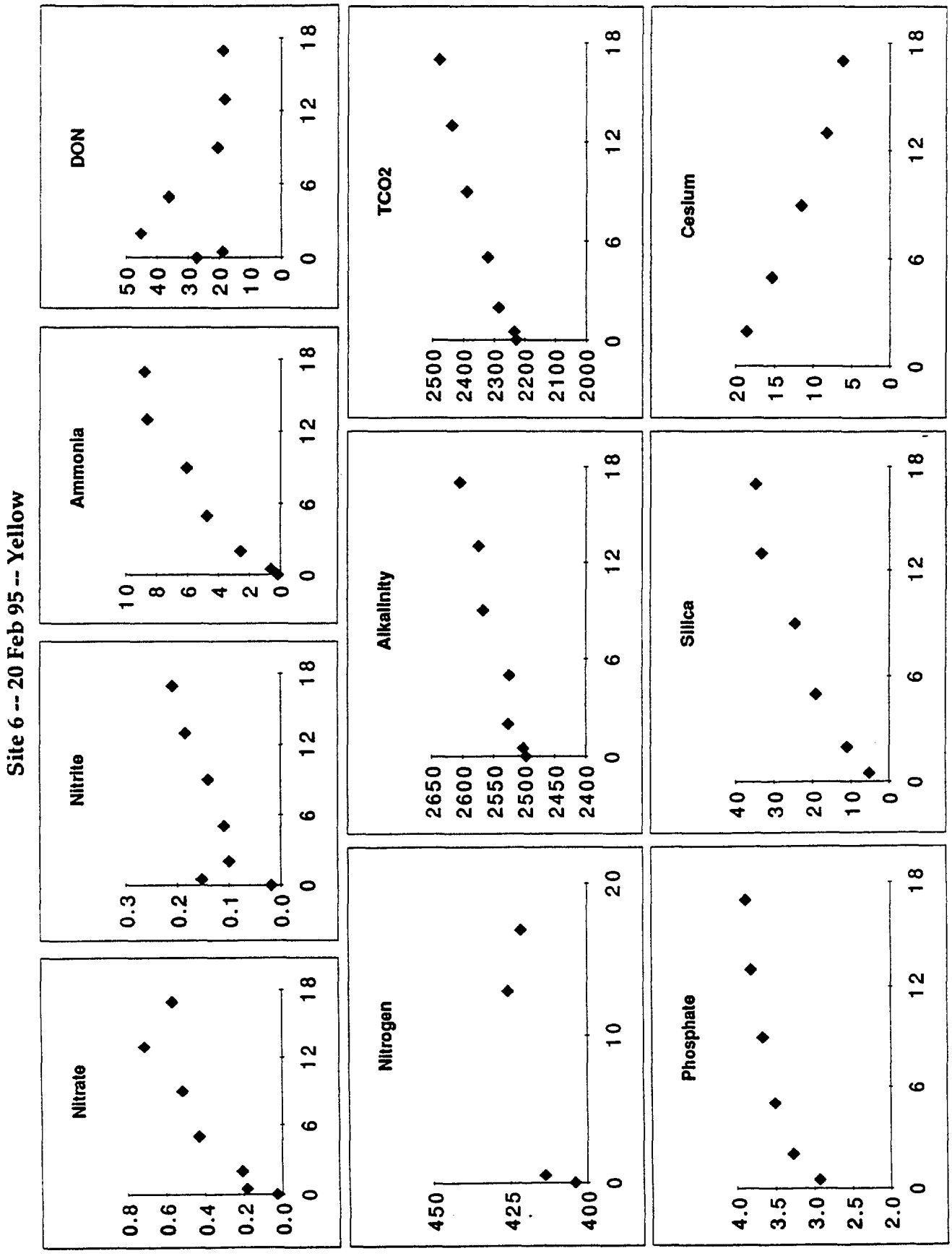

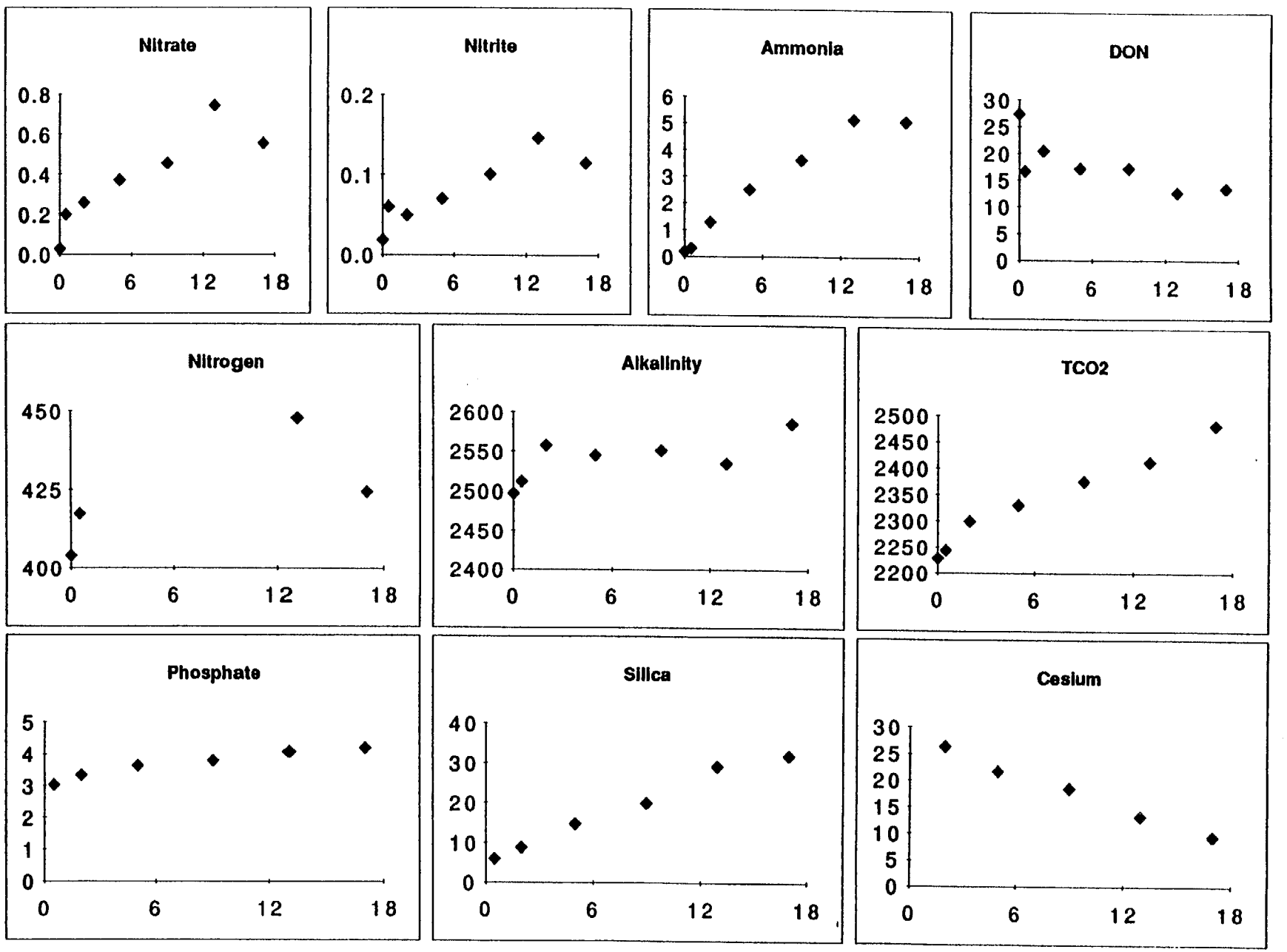
Site 6 -- 20 Feb 95 -- Blue
Nitrate
0.8
0.6
0.4
0.2
0.0
0 6 12 18
Nitrite
0.2
0.1
0.0
0 6 12 18
Ammonia
6
5
4
3
2
1
0
0 6 12 18
DON
30
25
20
15
10
5
0
0 6 12 18
Nitrogen
450
425
400
0 6 12 18
Alkalinity
2600
2550
2500
2450
2400
0 6 12 18
TCO2
2500
2450
2400
2350
2300
2250
2200
0 6 12 18
Phosphate
5
4
3
2
1
0
0 6 12 18
Silica
40
30
20
10
0
0 6 12 18
Cesium
30
25
20
15
10
5
0
0 6 12 18

Figure 4.

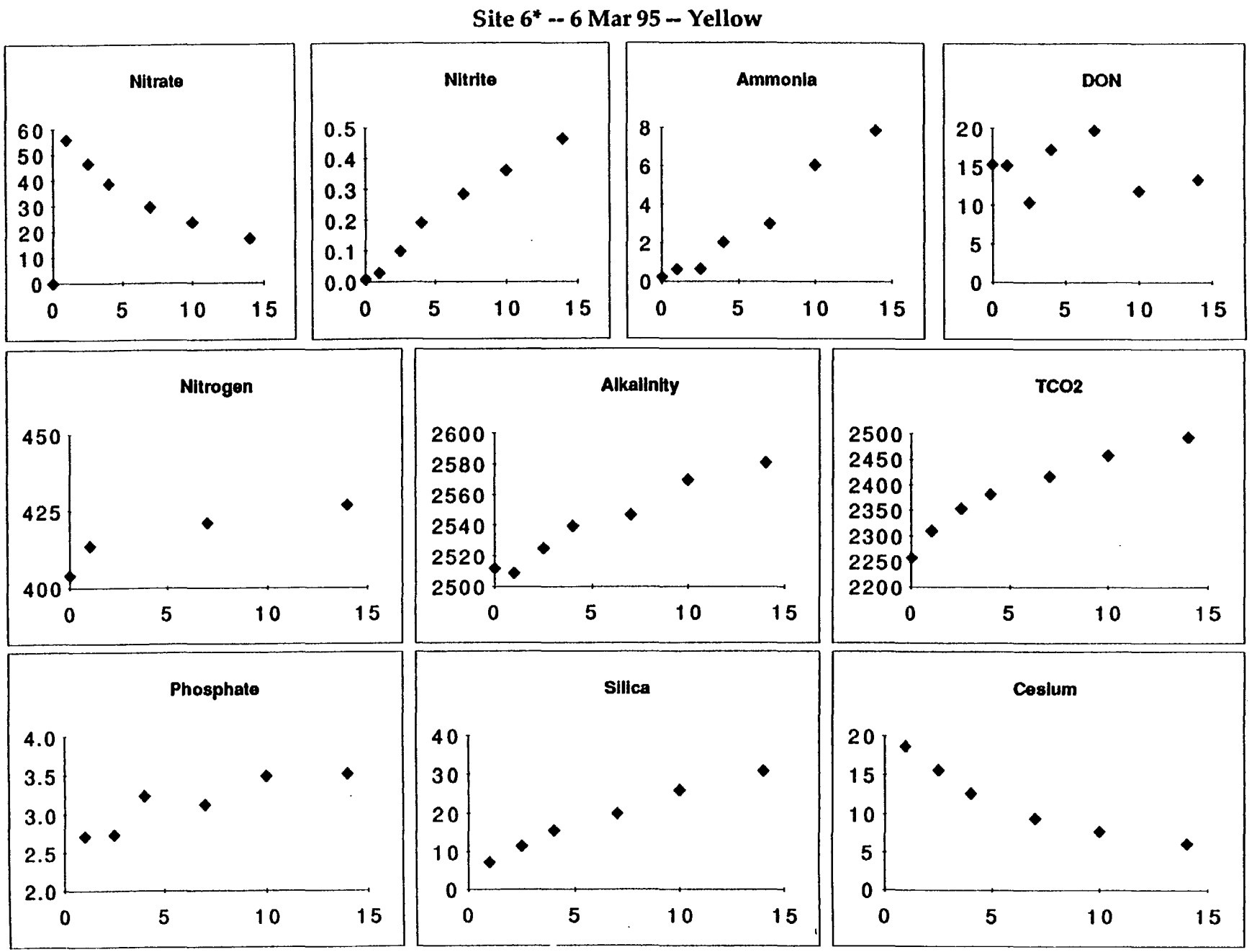
Site 6* -- 6 Mar 95 -- Yellow
Nitrate
Nitrite
Ammonia
DON
Nitrogen
Alkalinity
TCO2
Phosphate
Silica
Cesium

Figure 5.

Site 8 -- 27 Feb 95 -- Yellow

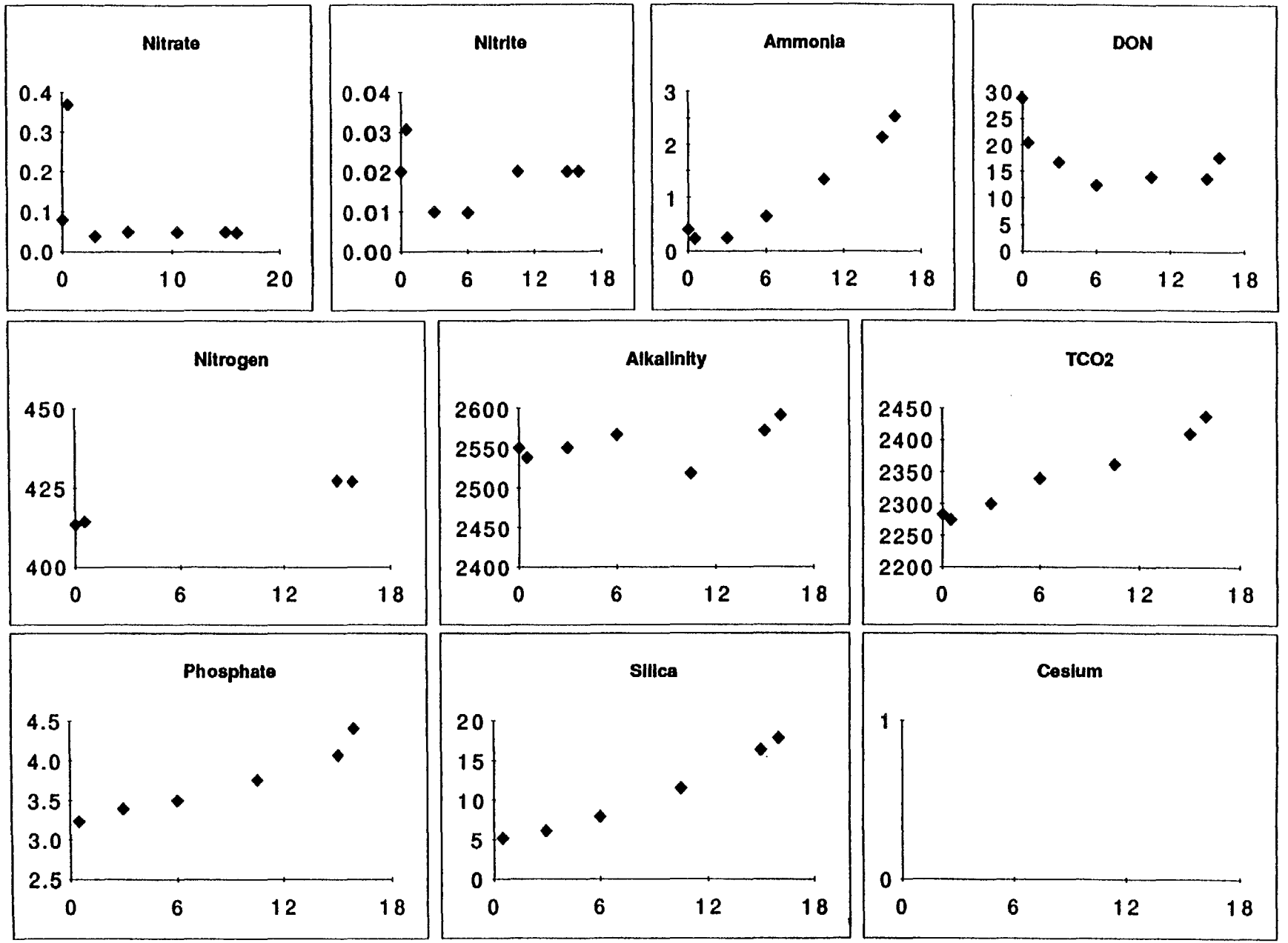

Figure 6.

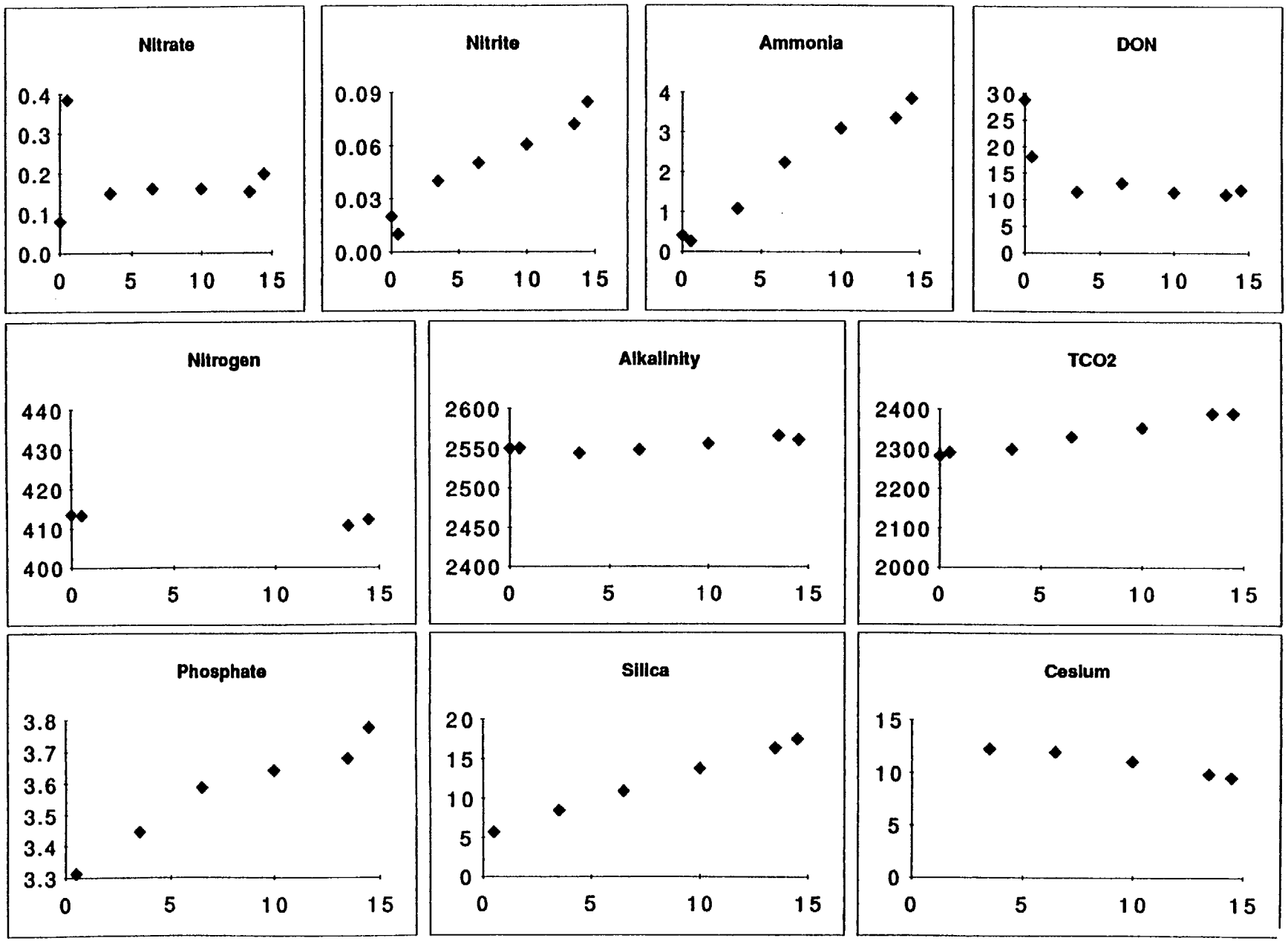
Site 8 -- 27 Feb 95 -- Blue
Nitrate
0.4
0.3
0.2
0.1
0.0
0 5 10 15
Nitrite
0.09
0.06
0.03
0.00
0 5 10 15
Ammonia
4
3
2
1
0
0 5 10 15
DON
30
25
20
15
10
5
0
0 5 10 15
Nitrogen
440
430
420
410
400
0 5 10 15
Alkalinity
2600
2550
2500
2450
2400
0 5 10 15
TCO2
2400
2300
2200
2100
2000
0 5 10 15
Phosphate
3.8
3.7
3.6
3.5
3.4
3.3
0 5 10 15
Silica
20
15
10
5
0
0 5 10 15
Cesium
15
10
5
0
0 5 10 15

Figure 7.

Site 37 -- 23 Feb 95 -- Yellow

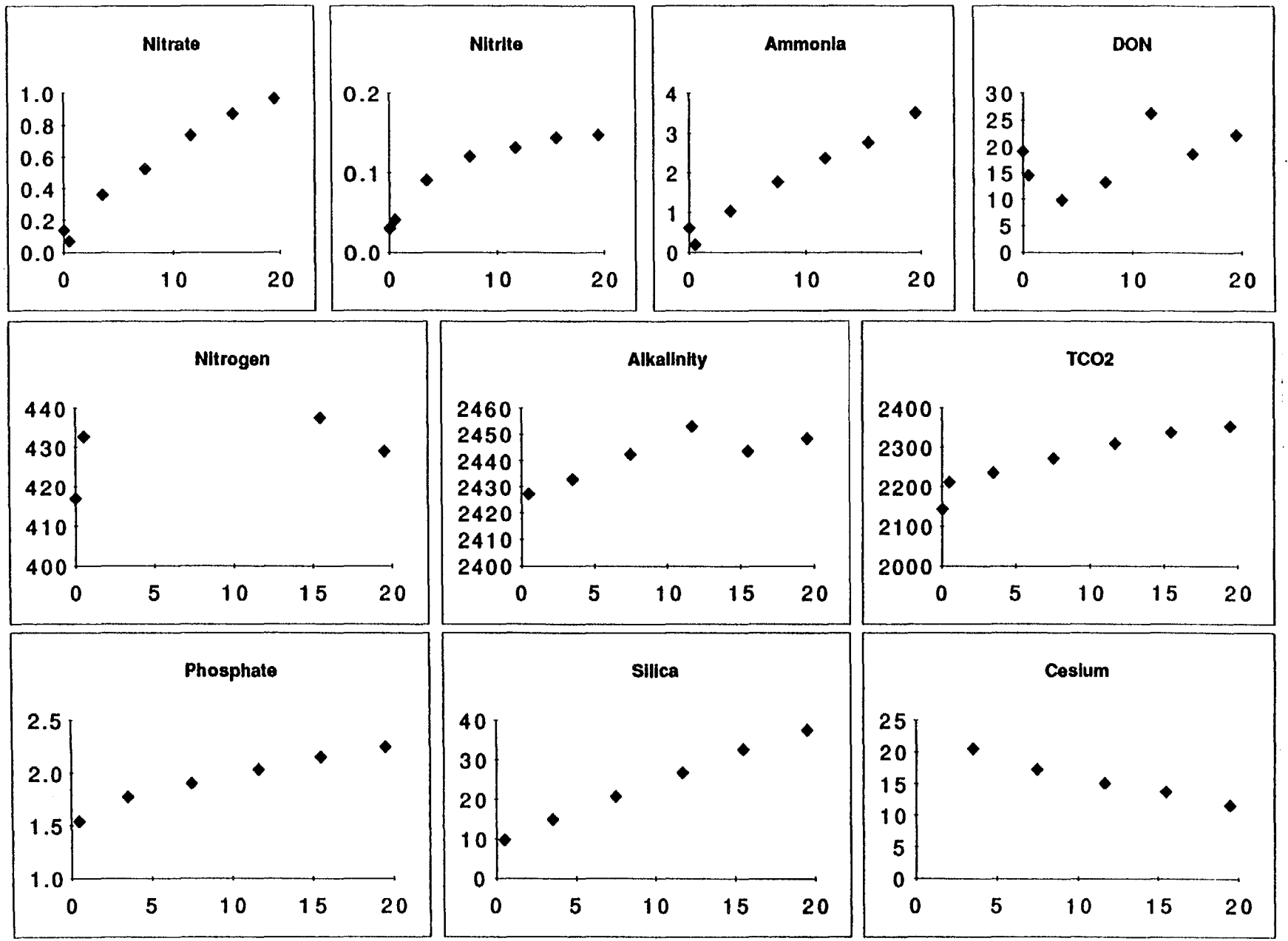

Figure 8.

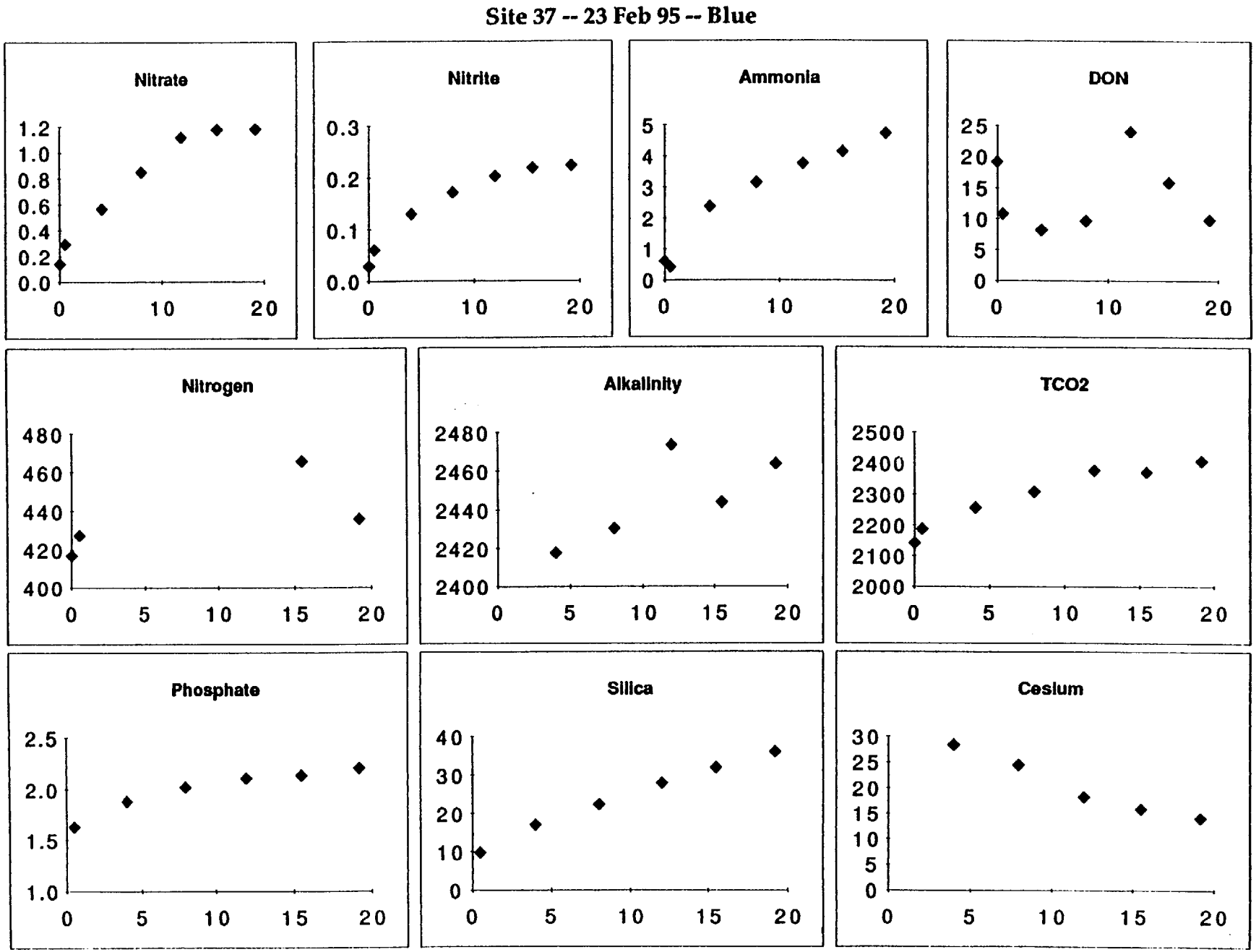
Site 37 -- 23 Feb 95 -- Blue
Nitrate
1.2
1.0
0.8
0.6
0.4
0.2
0.0
0
10
20
Nitrite
0.3
0.2
0.1
0.0
0
10
20
Ammonia
5
4
3
2
1
0
0
10
20
DON
25
20
15
10
5
0
0
10
20
Nitrogen
480
460
440
420
400
0
5
10
15
20
Alkalinity
2480
2460
2440
2420
2400
0
5
10
15
20
TCO2
2500
2400
2300
2200
2100
2000
0
5
10
15
20
Phosphate
2.5
2.0
1.5
1.0
0
5
10
15
20
Silica
40
30
20
10
0
0
5
10
15
20
Ceslum
30
25
20
15
10
5
0
0
5
10
15
20

Figure 9.

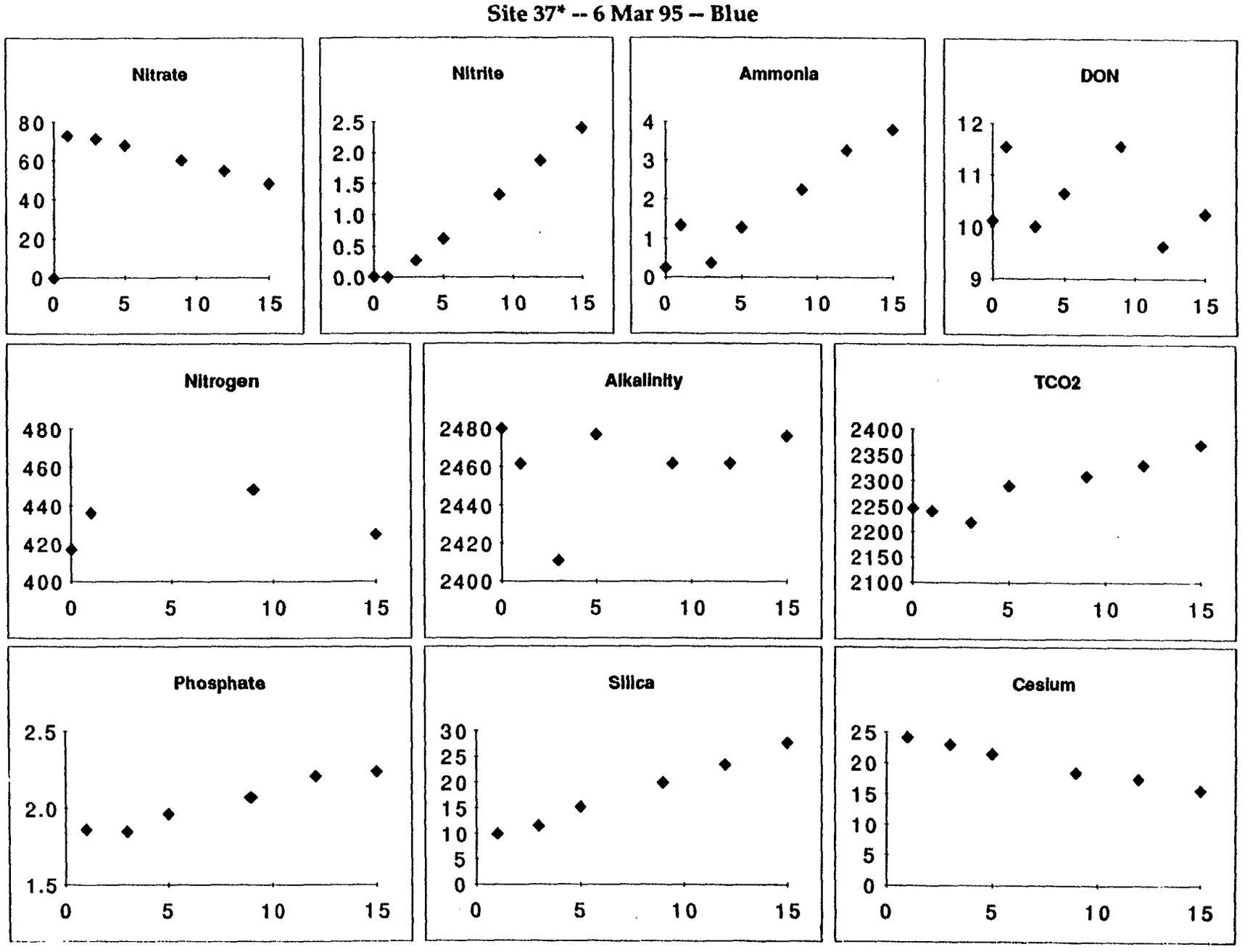
Site 37* -- 6 Mar 95 -- Blue
Nitrate
80
60
40
20
0
0 5 10 15
Nitrite
2.5
2.0
1.5
1.0
0.5
0.0
0 5 10 15
Ammonia
4
3
2
1
0
0 5 10 15
DON
12
11
10
9
0 5 10 15
Nitrogen
480
460
440
420
400
0 5 10 15
Alkalinity
2480
2460
2440
2420
2400
0 5 10 15
TCO2
2400
2350
2300
2250
2200
2150
2100
0 5 10 15
Phosphate
2.5
2.0
1.5
0 5 10 15
Silica
30
25
20
15
10
5
0
0 5 10 15
Cesium
25
20
15
10
5
0
0 5 10 15

Figure 10.

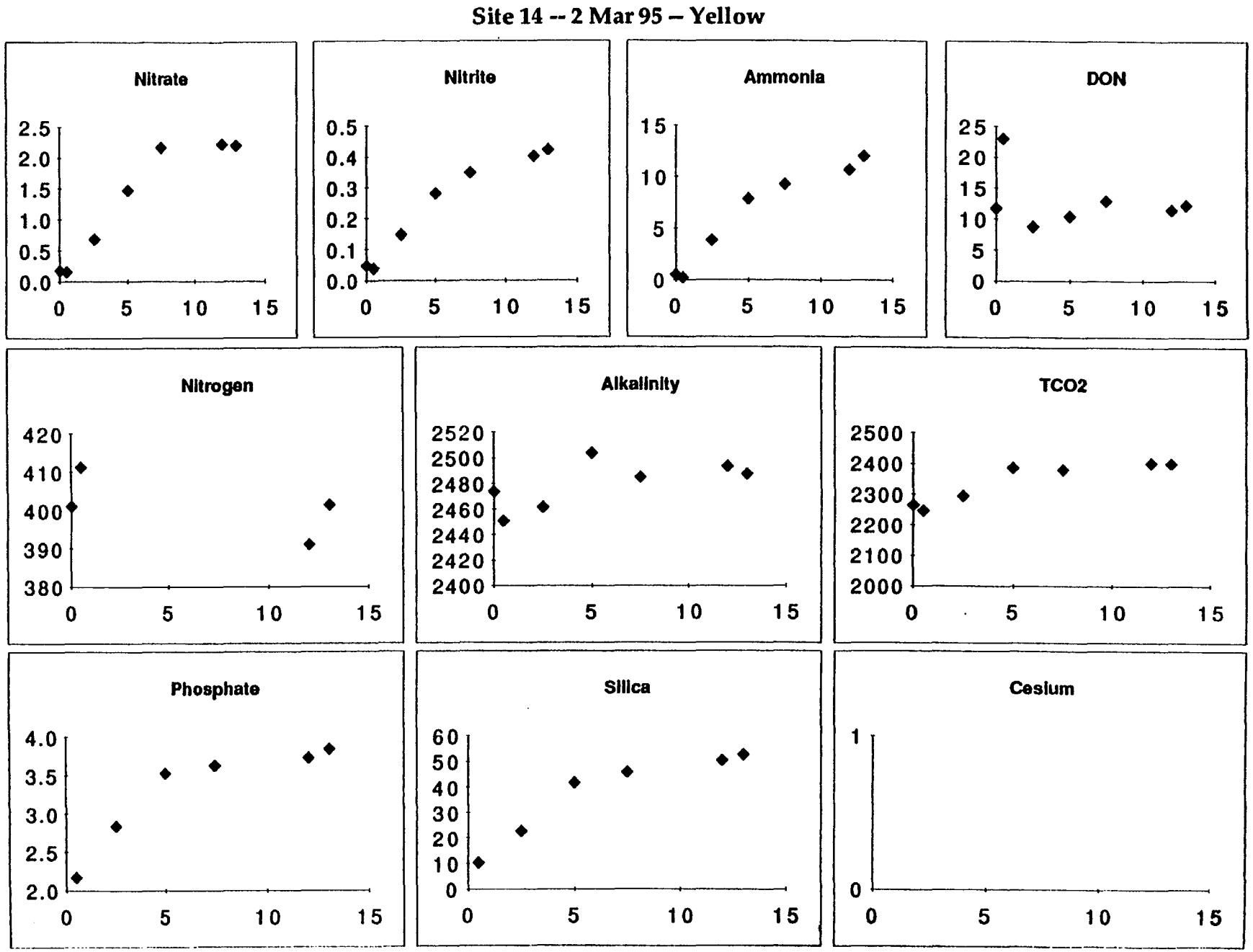
Site 14 -- 2 Mar 95 – Yellow
Nitrate
2.5
2.0
1.5
1.0
0.5
0.0
0 5 10 15
Nitrite
0.5
0.4
0.3
0.2
0.1
0.0
0 5 10 15
Ammonia
15
10
5
0
0 5 10 15
DON
25
20
15
10
5
0
0 5 10 15
Nitrogen
420
410
400
390
380
0 5 10 15
Alkalinity
2520
2500
2480
2460
2440
2420
2400
0 5 10 15
TCO2
2500
2400
2300
2200
2100
2000
0 5 10 15
Phosphate
4.0
3.5
3.0
2.5
2.0
0 5 10 15
Silica
60
50
40
30
20
10
0
0 5 10 15
Cesium
1
0
0 5 10 15

Figure 11.

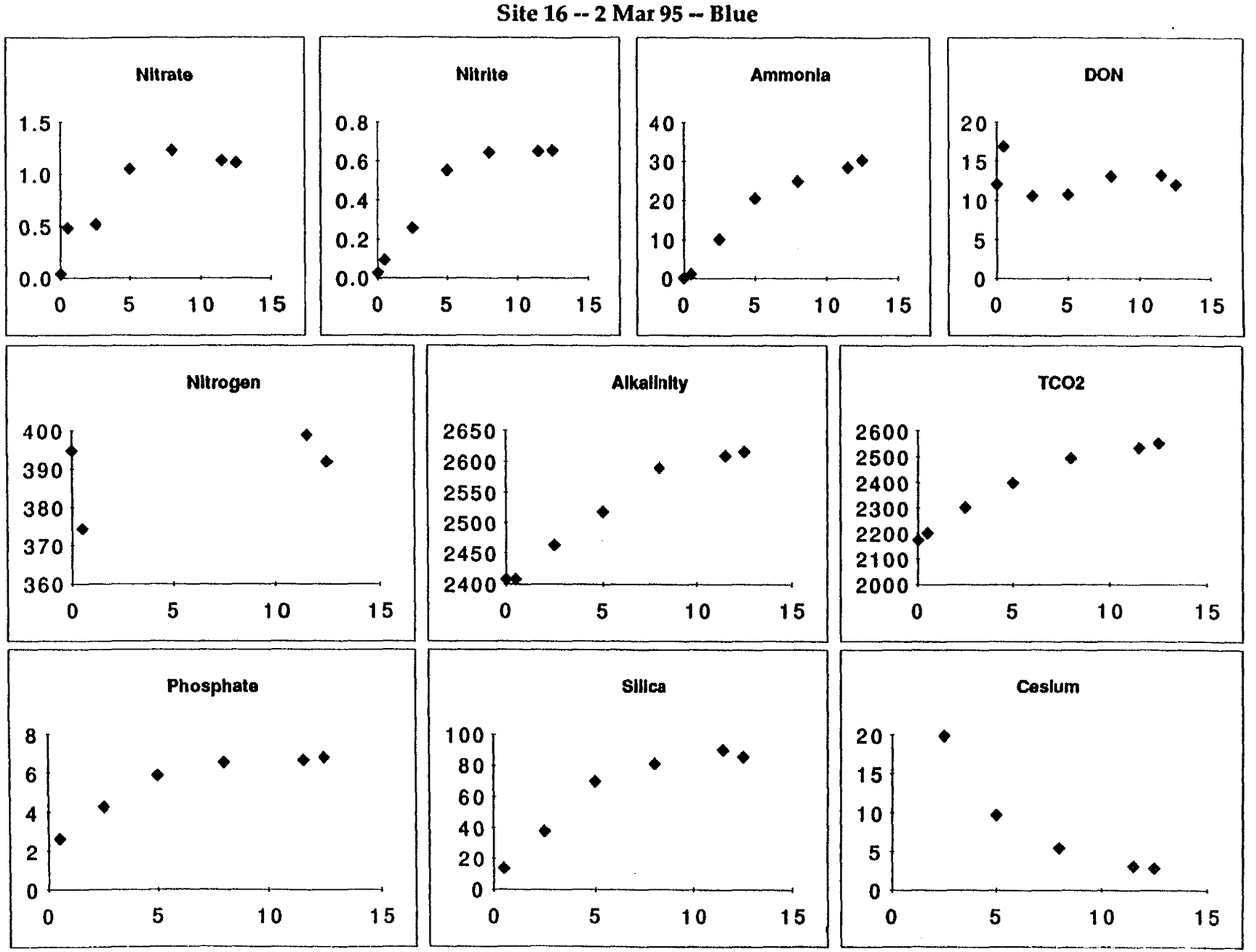
Site 16 -- 2 Mar 95 -- Blue
Nitrate
1.5
1.0
0.5
0.0
0 5 10 15
Nitrite
0.8
0.6
0.4
0.2
0.0
0 5 10 15
Ammonia
40
30
20
10
0
0 5 10 15
DON
20
15
10
5
0
0 5 10 15
Nitrogen
400
390
380
370
360
0 5 10 15
Alkalinity
2650
2600
2550
2500
2450
2400
0 5 10 15
TCO2
2600
2500
2400
2300
2200
2100
2000
0 5 10 15
Phosphate
8
6
4
2
0
0 5 10 15
Silica
100
80
60
40
20
0
0 5 10 15
Cesium
20
15
10
5
0
0 5 10 15

Figure 12.

Figures 13 & 14: Oxygen electrode output. Electrode readings are made every six minutes. The plateau in output prior to time = 0 suggests equilibration with the ambient bottom water. Ambient bottom water oxygen values were determined by Winkler titration on Niskin samples. The ambient oxygen electrode only operated successfully during 4 deployment, but the chamber-electrode operated well in all deployments. The vertical tic-marks denote the timing of sample draws; six in total. The horizontal dashed line denotes the portion of the incubation deemed representative of a constant condition. The arrows against the X-axis denote local time, at 6-hour intervals.

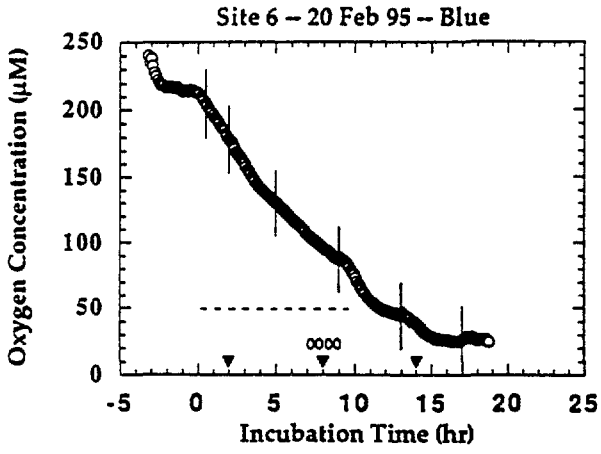

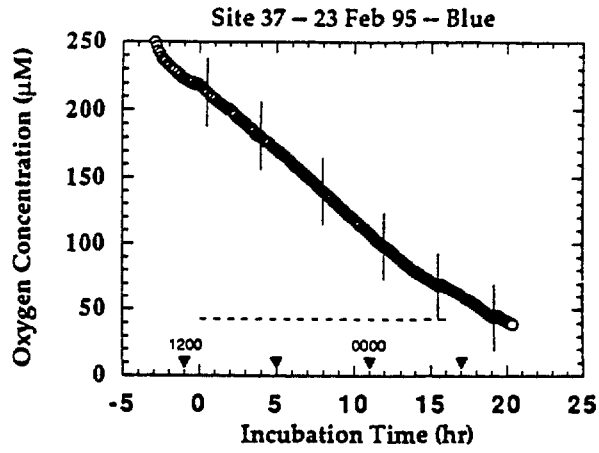

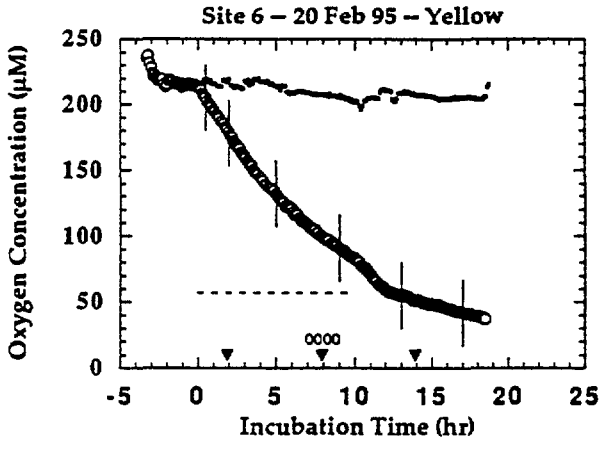

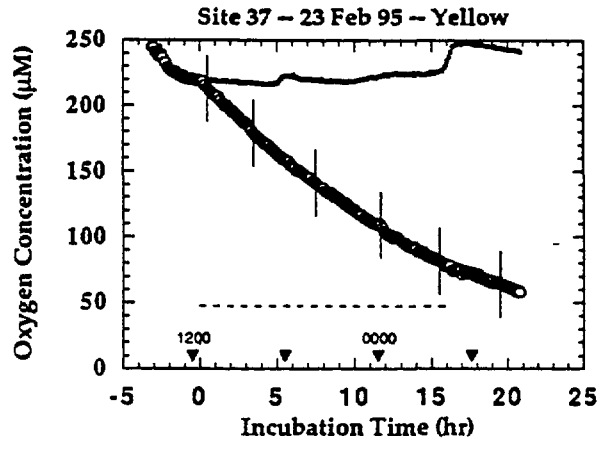

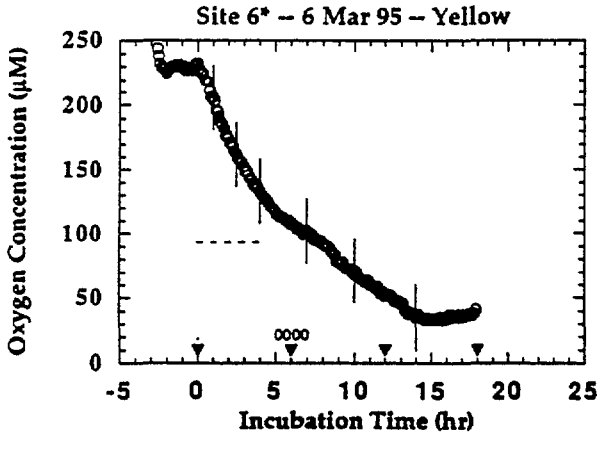

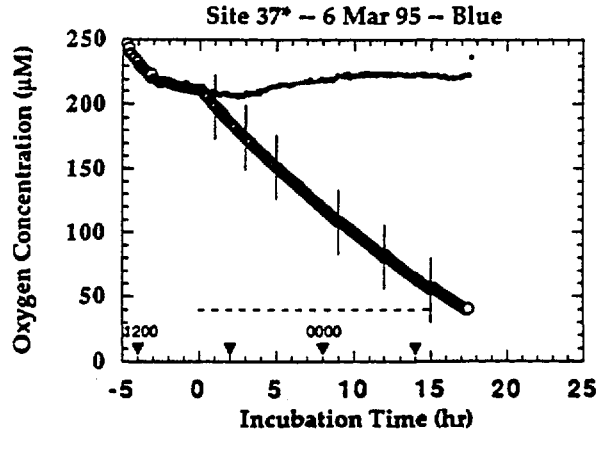

Figure 14.

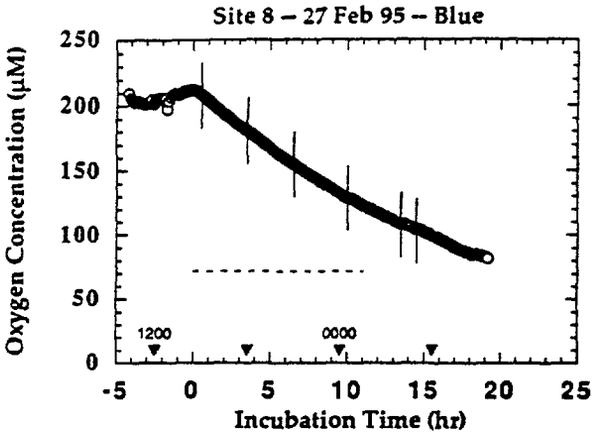
Site 8 – 27 Feb 95 – Blue
Oxygen Concentration (µM)
250
200
150
100
50
0
1200
0000
-5
0
5
10
15
20
25
Incubation Time (hr)

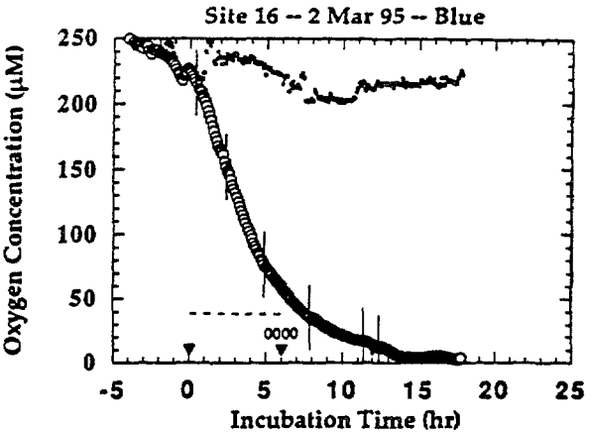
Site 16 – 2 Mar 95 – Blue
Oxygen Concentration (µM)
250
200
150
100
50
0
0000
-5
0
5
10
15
20
25
Incubation Time (hr)

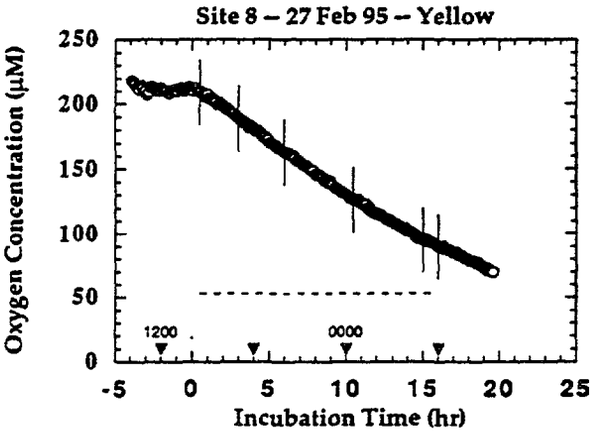
Site 8 – 27 Feb 95 – Yellow
Oxygen Concentration (µM)
250
200
150
100
50
0
1200
0000
-5
0
5
10
15
20
25
Incubation Time (hr)

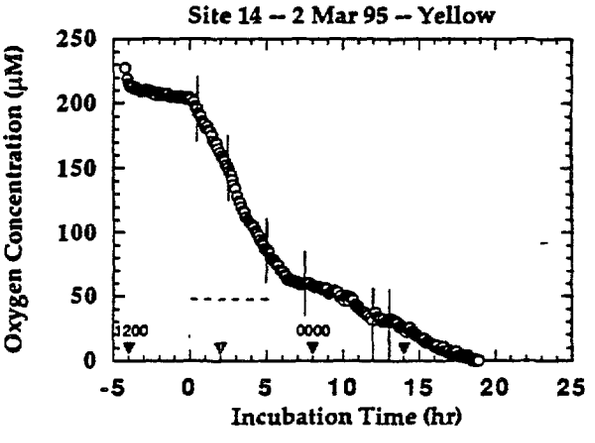
Site 14 – 2 Mar 95 – Yellow
Oxygen Concentration (µM)
250
200
150
100
50
0
1200
0000
-5
0
5
10
15
20
25
Incubation Time (hr)

Figures 15 & 16: Radon-222 versus inclubation time plots. Data from measurem,ents of the last three samples drawn. The lines through the data define the flux of radon from bay sediments as a function of input and decay.

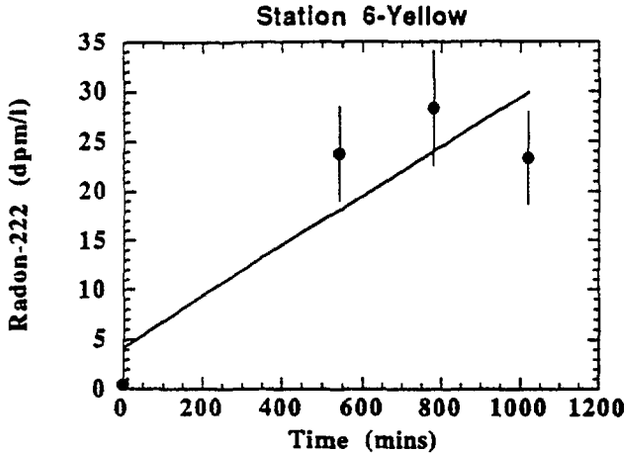

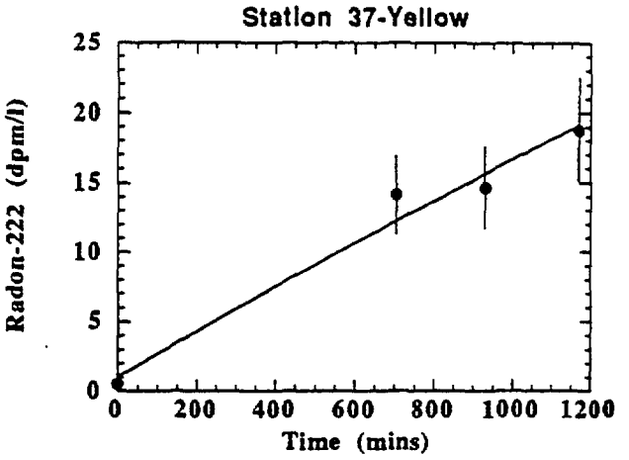

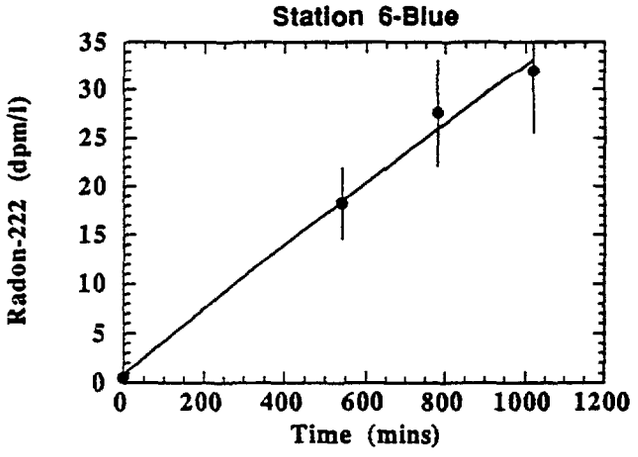

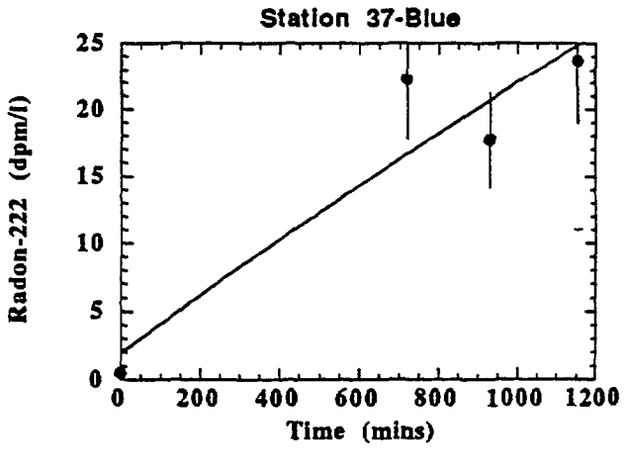

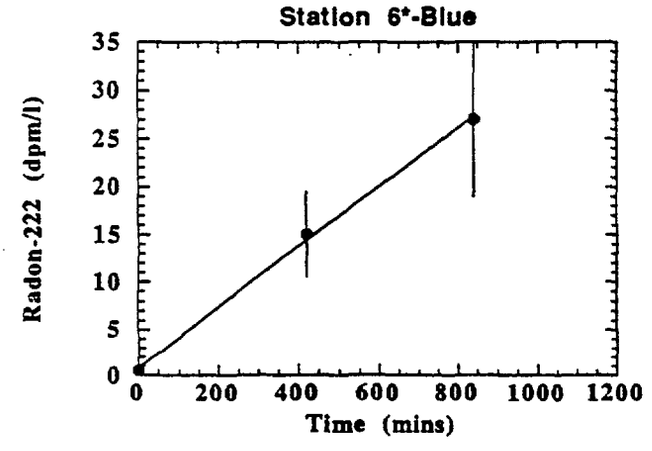

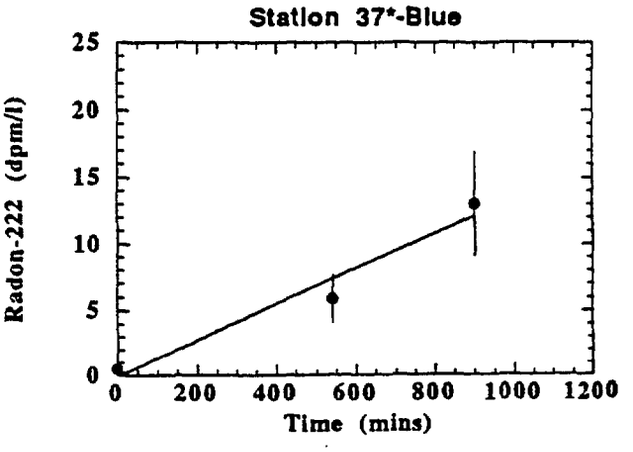

Figure 16.

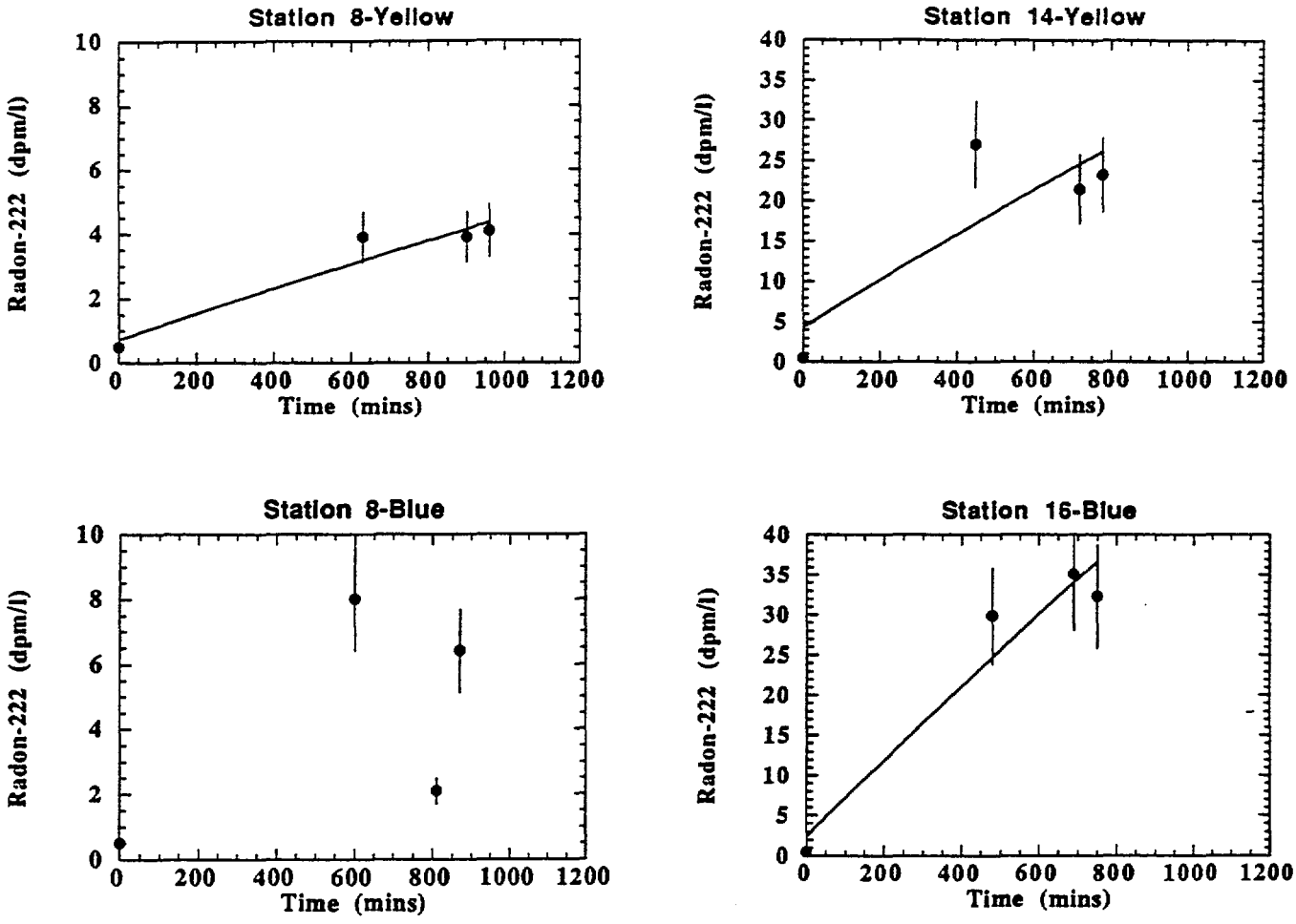
Station 8-Yellow
Radon-222 (dpm/l)
Time (mins)
Station 14-Yellow
Radon-222 (dpm/l)
Time (mins)
Station 8-Blue
Radon-222 (dpm/l)
Time (mins)
Station 16-Blue
Radon-222 (dpm/l)
Time (mins)

Figures 17 & 18: A comparison of benthic fluxes from Port Phillip Bay. Measurements made with the USC benthic chambers in January 1994 and February 1995. The data represent averages of chambers deployed at a given station (excluding the nitrate spiked experiments), or single chamber flux determinations. Uncertainties are S.D. of the averages of s.d. of the flux.

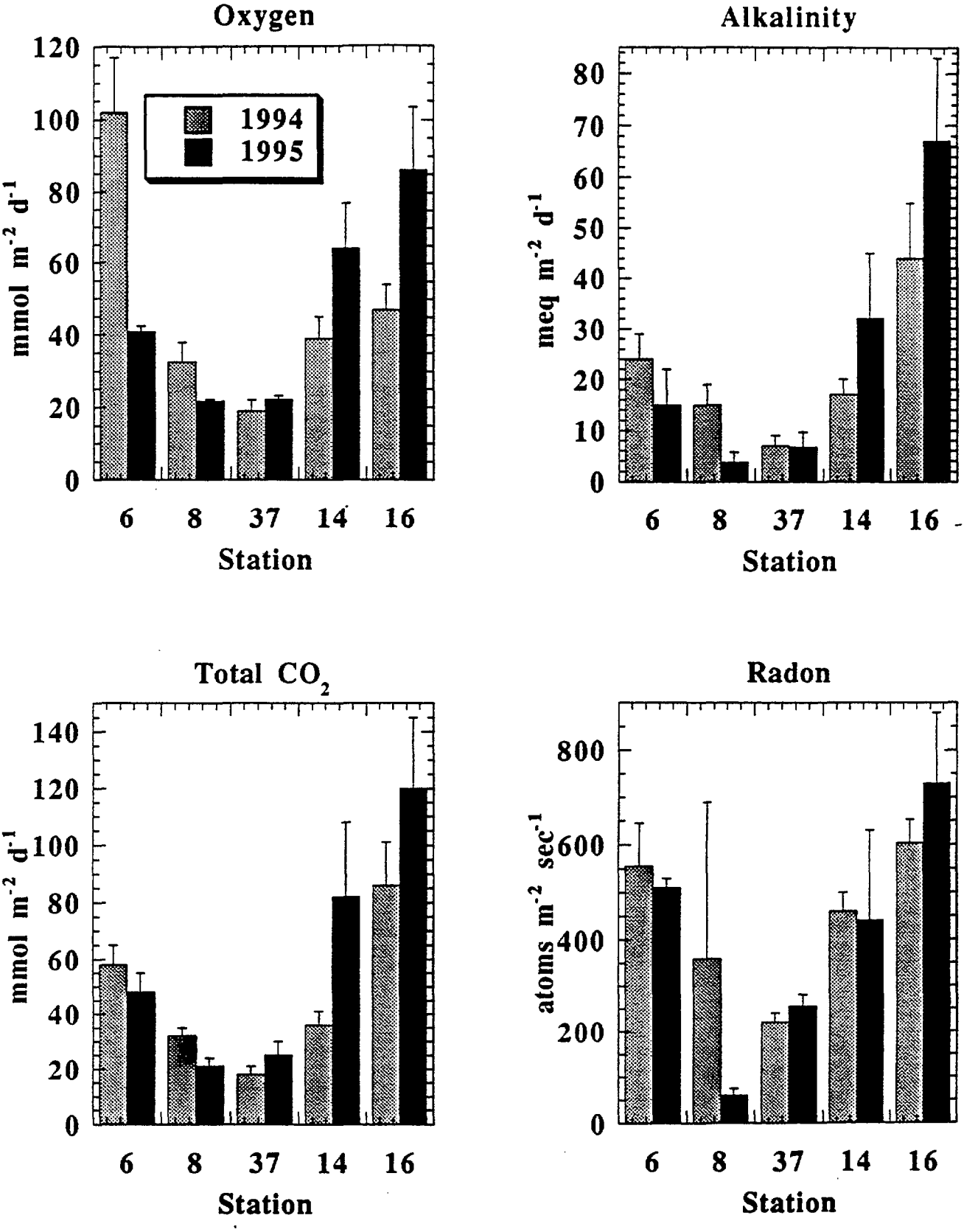

Figure 18.

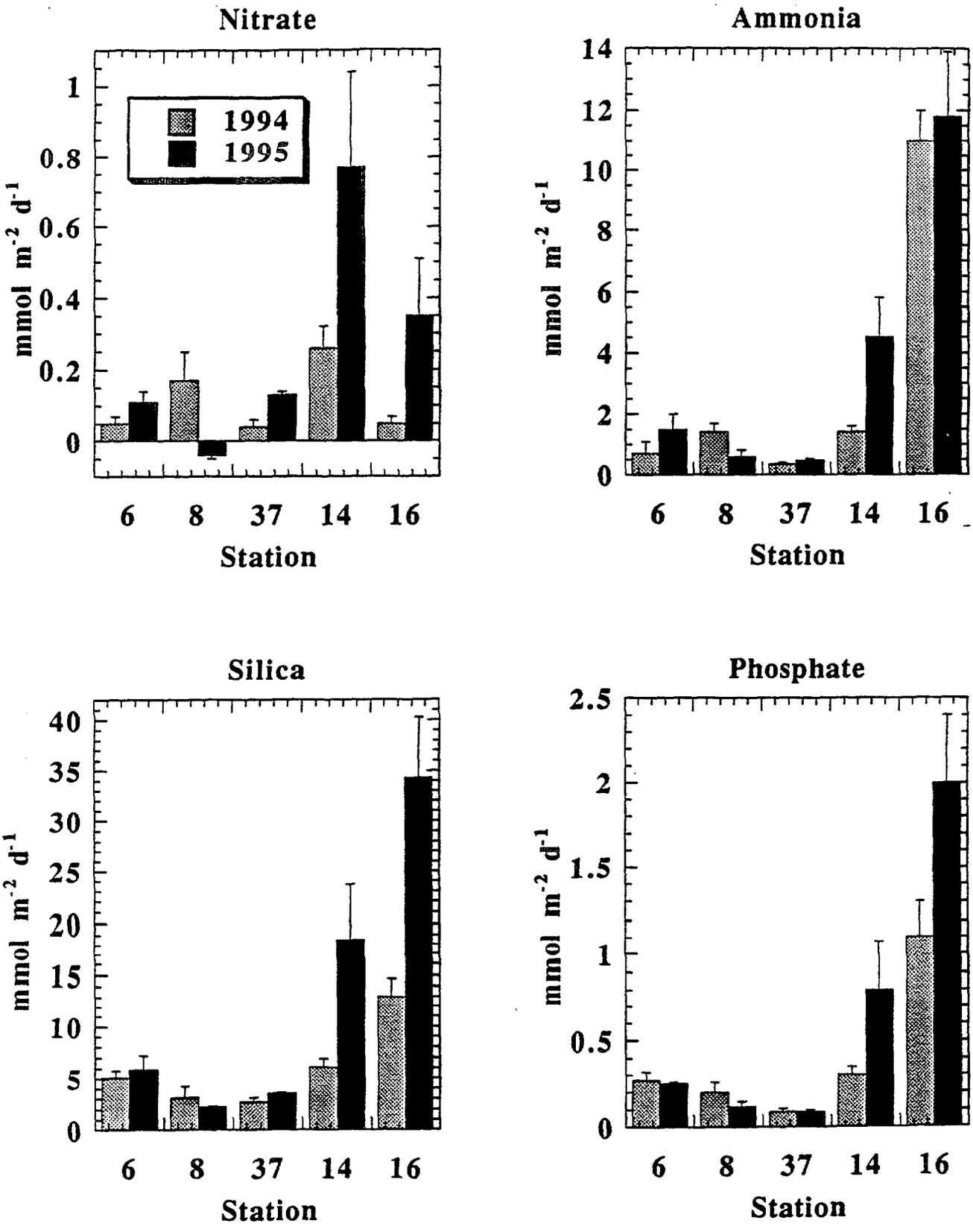
Nitrate
1994
1995
mmol m-2 d-1
0
0.2
0.4
0.6
0.8
1
6
8
37
14
16
Station
Ammonia
mmol m-2 d-1
0
2
4
6
8
10
12
14
6
8
37
14
16
Station
Silica
mmol m-2 d-1
0
5
10
15
20
25
30
35
40
6
8
37
14
16
Station
Phosphate
mmol m-2 d-1
0
0.5
1
1.5
2
2.5
6
8
37
14
16
Station

Figure 19: Oxygen uptake versus organic carbon oxidised, for two scenarios decribed in the text. The dashed lines labeled 1.0 and 1.3 define the O_2/C_{ox} flux ratios.

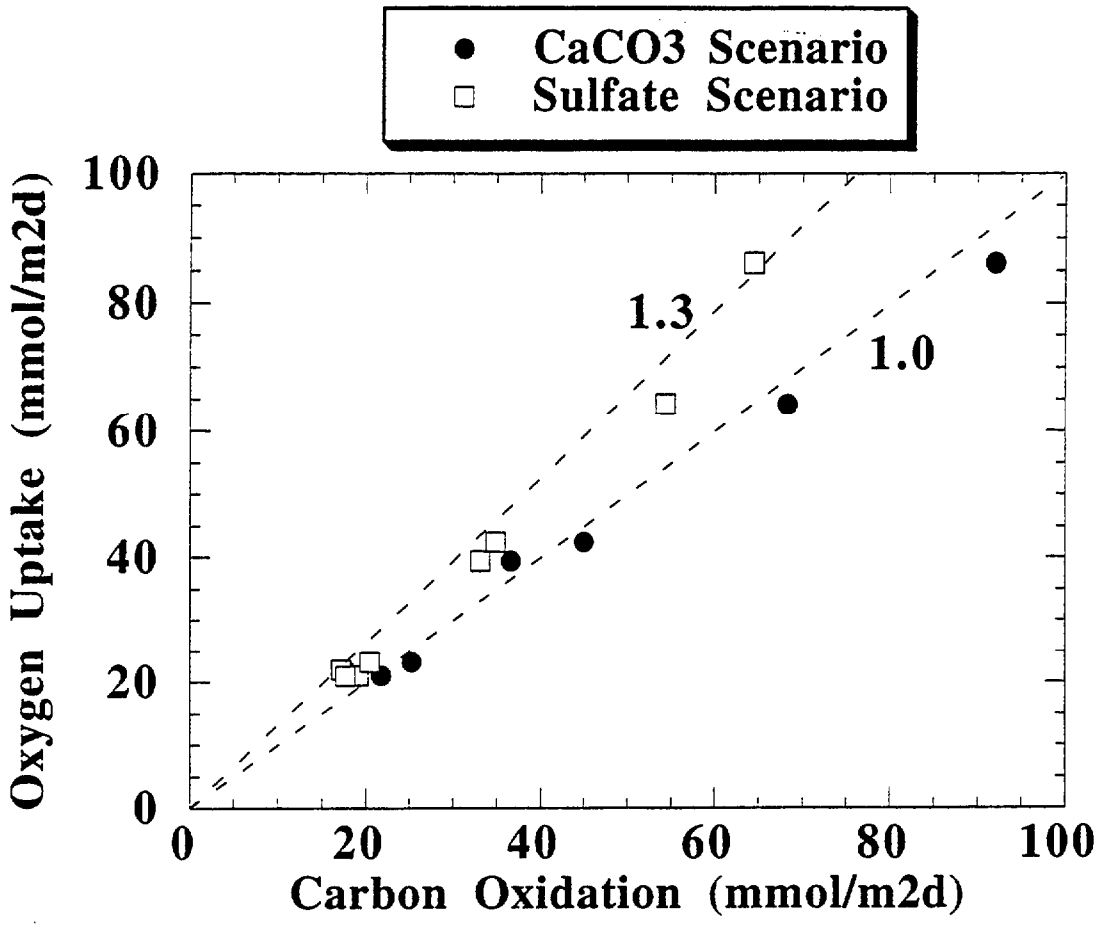

Figure 20: Plots of nitrogen and phosphate fluxes versus total carbon oxidised. The top two panels include a line that defines the expected flux of N for a given flux of CO_2. The top panel includes the sum of nitrate, nitrate and ammonia fluxes, the middle panel adds DON to the three other N fluxes. The bottom panel shows the phosphate flux versus the TCO_2 flux and the line denotes the expected relationship of the organic matter oxidised is typical marine phytoplankton.

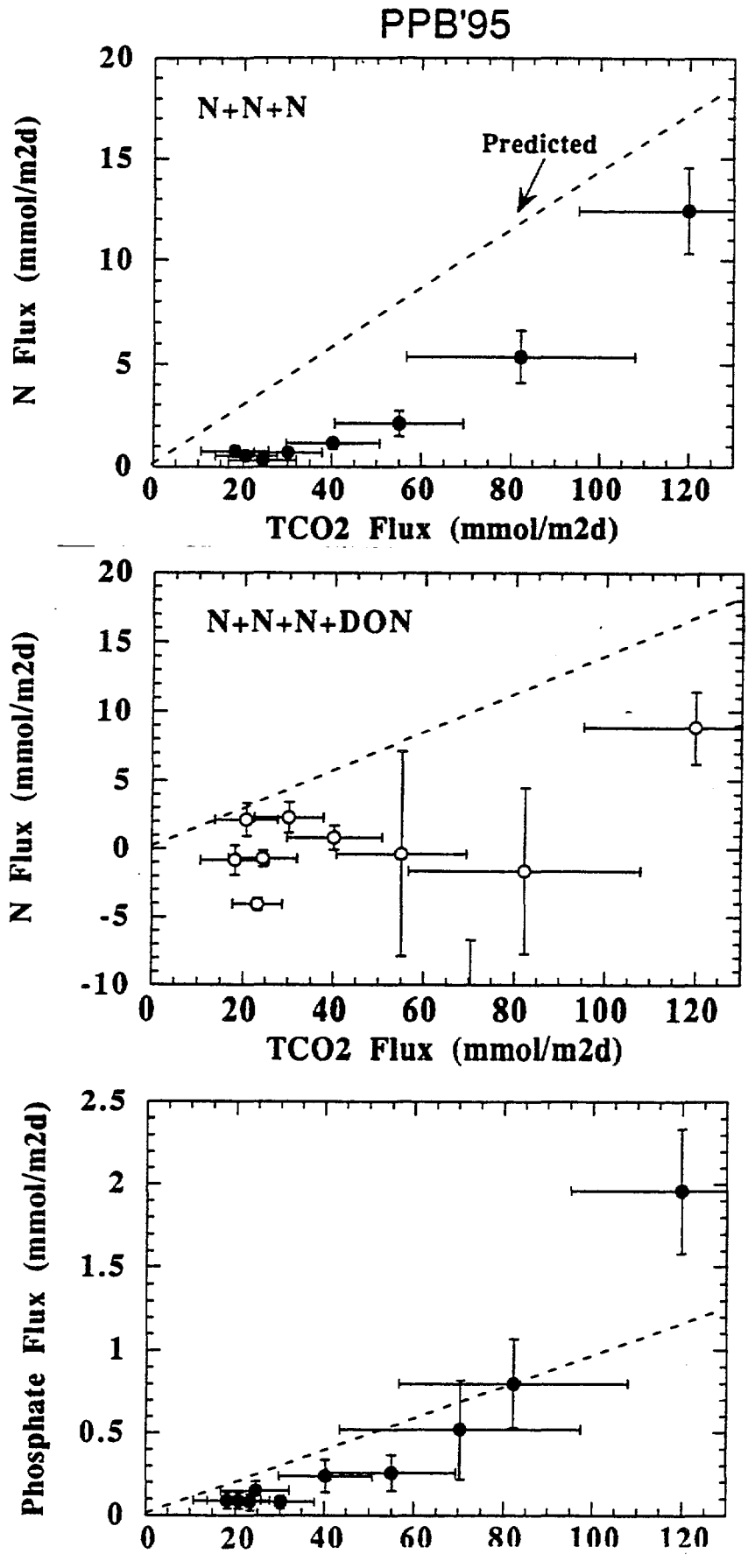

Figure 21 a) - c): Cs concentration versus time after injection. The fit to these data are an exponential function and the fitting parameter, b, given on each plot, defines the curvature in each plot. b) Plots of delta deuterium versus time after injection. The fitting function is the same as a) and the fitting parameter, b, is given for each station. c) Plots of spike added nitrate versus time in two chambers. Fitting function same as for previous figures.

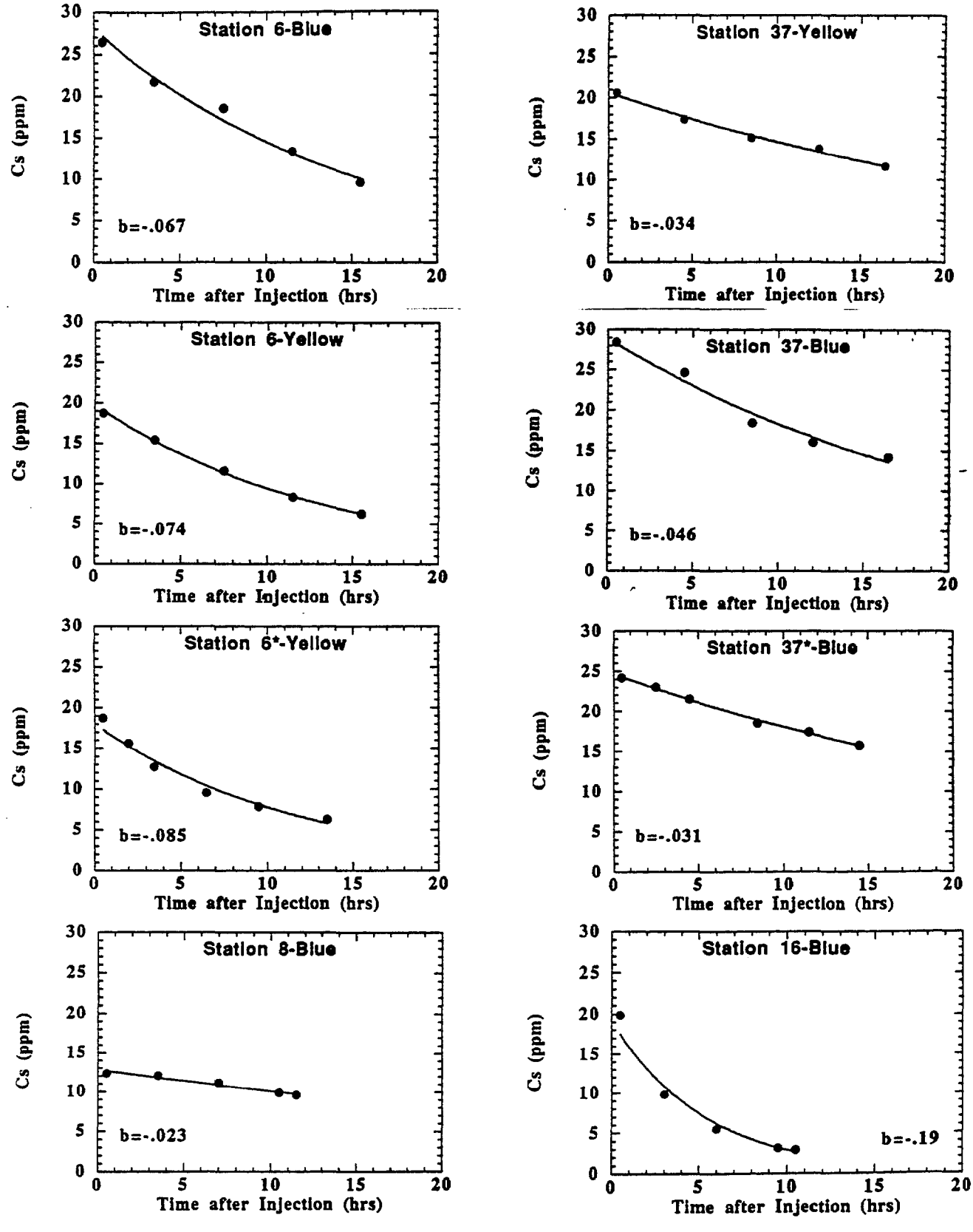

Figure 21 b)

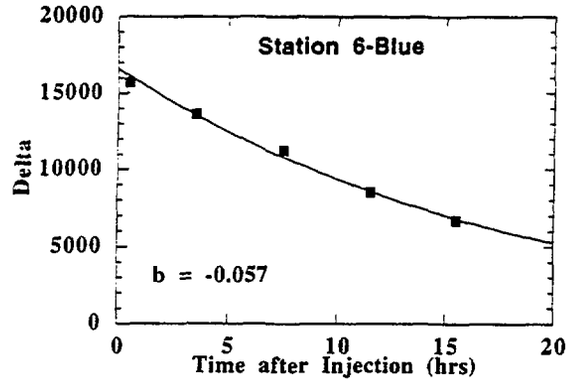
Station 6-Blue
Delta
20000
15000
10000
5000
0
b = -0.057
0
5
10
15
20
Time after Injection (hrs)

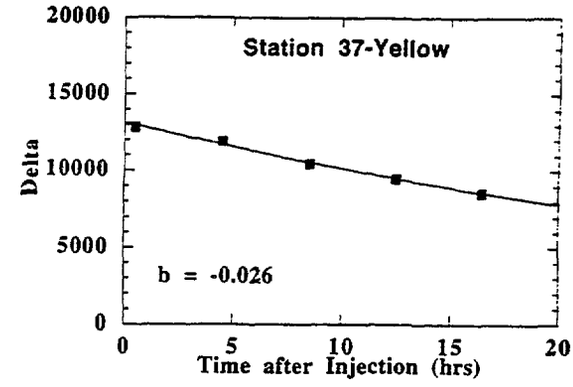
Station 37-Yellow
Delta
20000
15000
10000
5000
0
b = -0.026
0
5
10
15
20
Time after Injection (hrs)

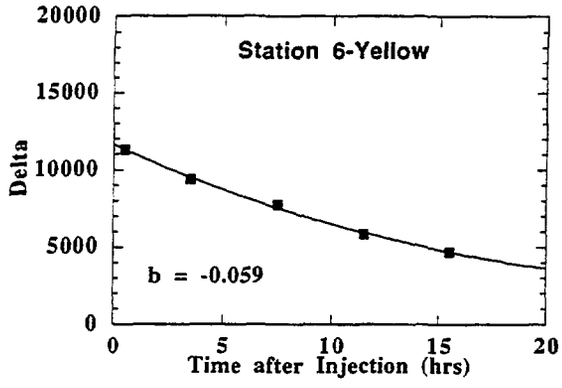
Station 6-Yellow
Delta
20000
15000
10000
5000
0
b = -0.059
0
5
10
15
20
Time after Injection (hrs)

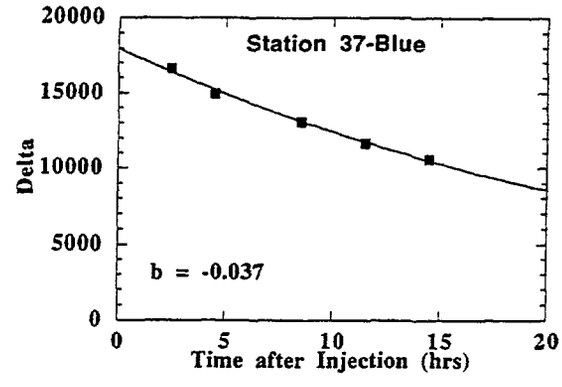
Station 37-Blue
Delta
20000
15000
10000
5000
0
b = -0.037
0
5
10
15
20
Time after Injection (hrs)

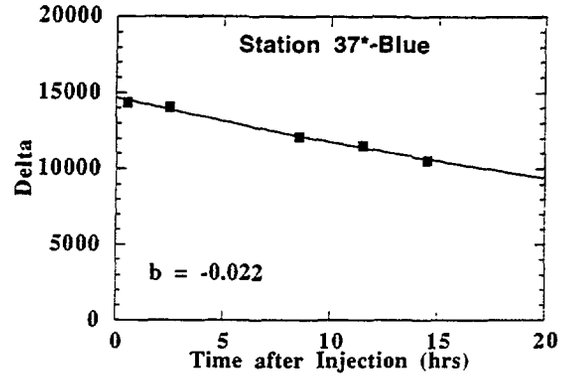
Station 37*-Blue
Delta
20000
15000
10000
5000
0
b = -0.022
0
5
10
15
20
Time after Injection (hrs)

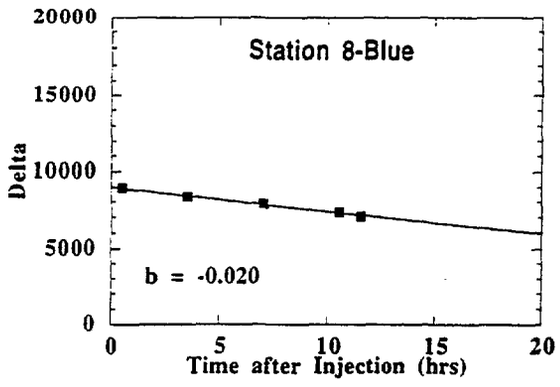
Station 8-Blue
Delta
20000
15000
10000
5000
0
b = -0.020
0
5
10
15
20
Time after Injection (hrs)

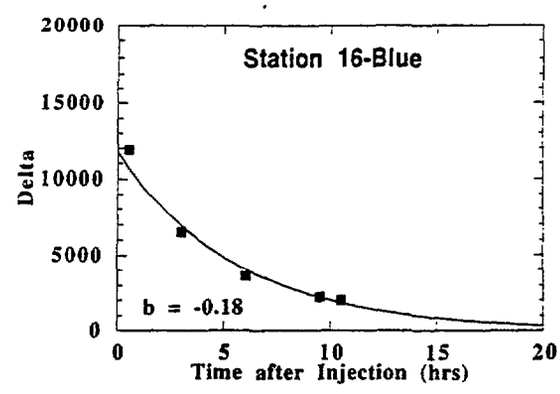
Station 16-Blue
Delta
20000
15000
10000
5000
0
b = -0.18
0
5
10
15
20
Time after Injection (hrs)

Figure 21 c)

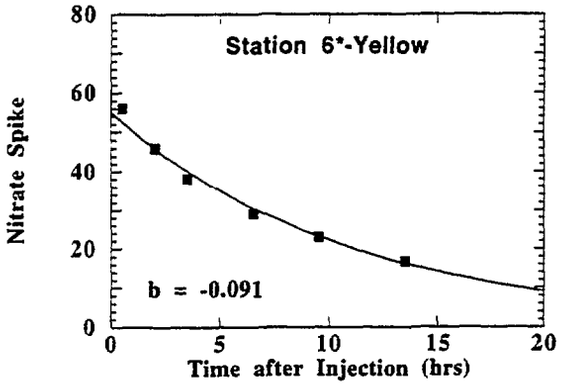
Station 6*-Yellow
Nitrate Spike
b = -0.091
Time after Injection (hrs)
0
20
40
60
80
0
5
10
15
20

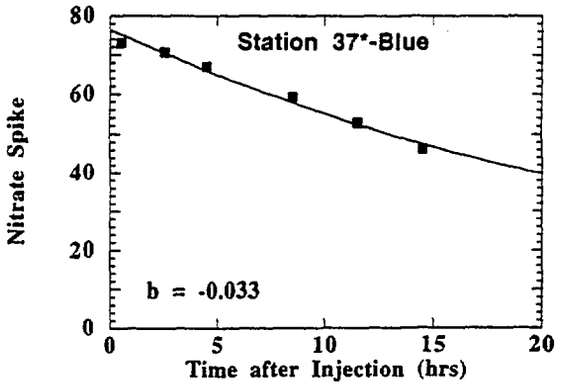
Station 37*-Blue
Nitrate Spike
b = -0.033
Time after Injection (hrs)
0
20
40
60
80
0
5
10
15
20

Figure 22: The Cs parameter, b, versus the measured radon flux. The rate of Cs loss from the chamber correlates positively with the magnitude of radon emanation from the sediments. Two sets of three points clustered together represent stations 6 and 37.

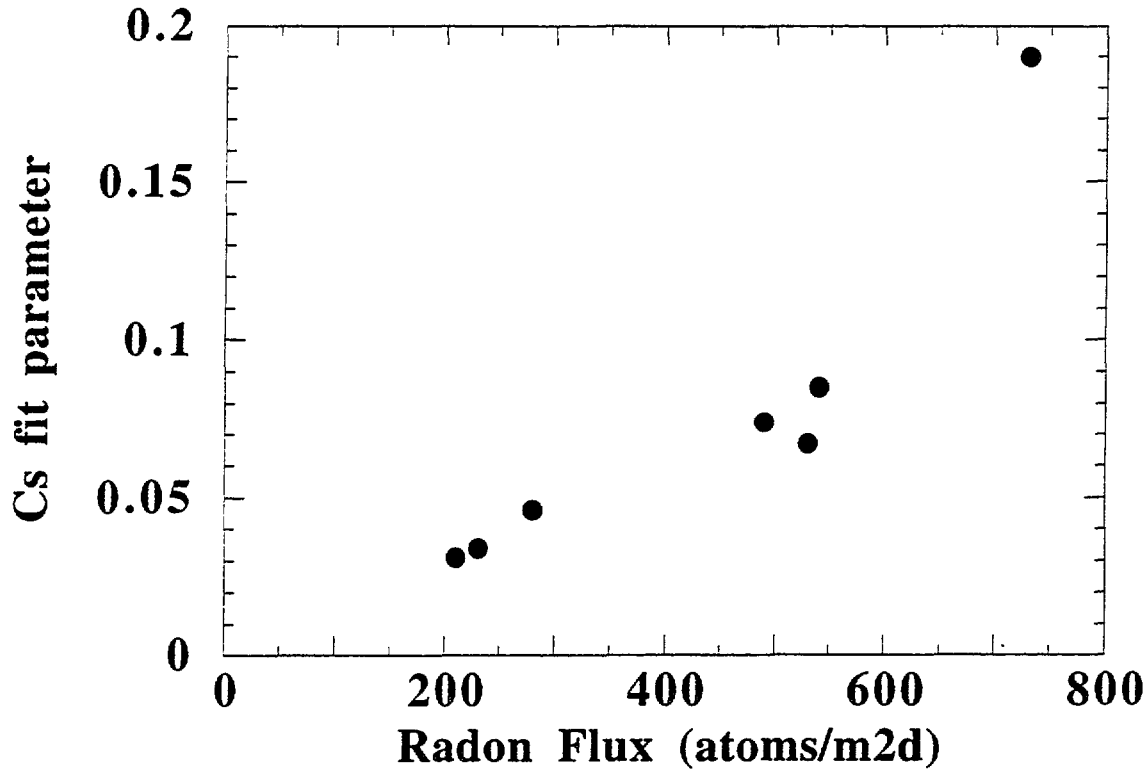

Figure 23: Dissolved silica flux versus radon flux. Data from 1994 and 1995 are included on this plot. The relationship between these parameters is systematic and positive although two points with very large silicate fluxes fall off the trend. These two points are from Hobsons Bay and indicate very high rates of biogenic silica in 1995 compared to 1994.

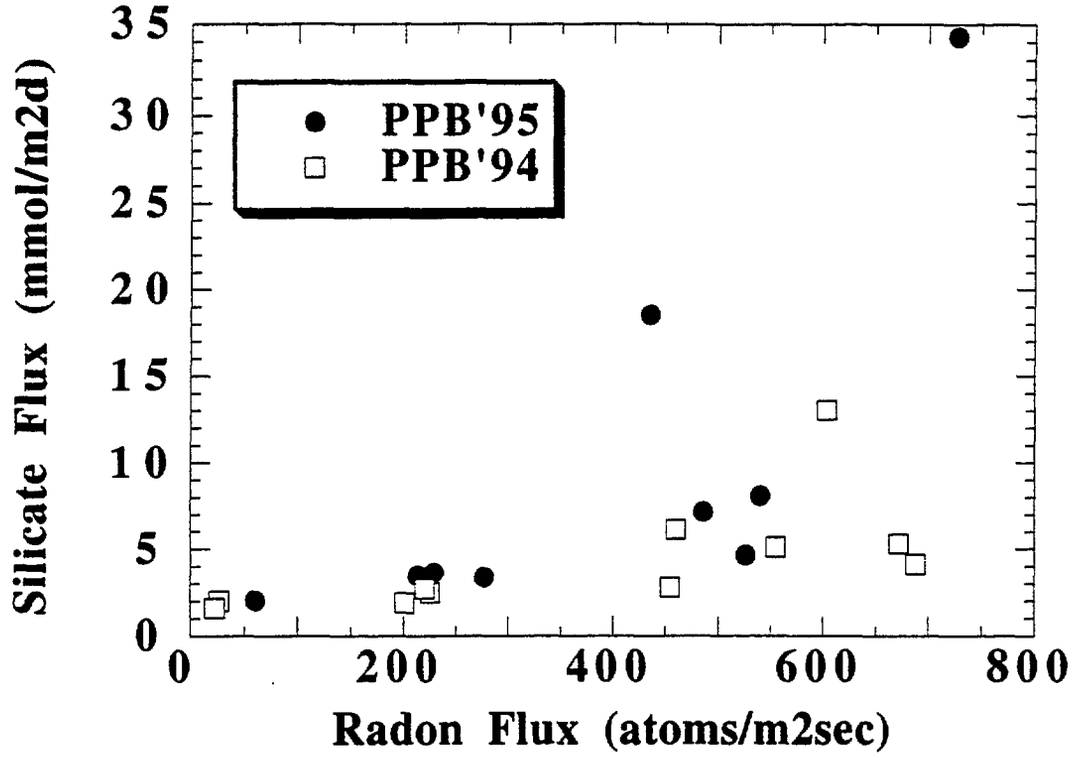

Table 1: Summary of oxygen, alkalinity, total CO_2 and radon fluxes. Uncertainties are +/- 1s.d. Negative fluxes indicate uptake by the sediments.

Site-ID	Oxygen (mmol/m2d)	Alkalinity (meq/m2d)	Total CO2 (mmol/m2d)	Radon-222 (atoms/m2sec)
6-Yellow	−42.4±8.5	21.9±7.7	55.0±14.4	490±170
6-Blue	−39.4±7.9	8.1±9.2	40.2±10.5	530±70
6*-Yellow	−73.3±14.7	29.7±18.1	70.4±27.0	540±140
8-Yellow	−21.1±4.2	5.6±3.3	24.4±7.6	60±15
8-Blue	−22.0±4.4	1.9±4.5	18.2±7.5	—
37-Yellow	−21.0±4.2	3.3±2.6	20.7±6.9	230±50
37-Blue	−23.2±4.6	10.0±4.2	30.1±7.7	280±70
37*-Blue	−27.8±5.6	1.0±2.9	23.2±5.5	210±50
14-Yellow	−64.2±12.8	31.5±13.1	82.2±25.6	440±190
16-Blue	−86.2±17.2	66.8±15.6	119.8±24.7	730±150

Table 2: Summary of phosphate, ammonia, nltrite, nitrate, DON, N_2 and silicate fluxes. Uncertainties are +/- 1s.d. Negative fluxes indicate uptake by the sediments. The chambers that had spike additions of KNO_3, those indicated by a star, have nitrate fluxes that are influenced by advection of pore water, hence are reported parenthetically.

Site-ID	Phosphate (mmol/m2d)	Ammonia (mmol/m2d)	Nitrite (mmol/m2d)	Nitrate (mmol/m2d)	DON (mmol/m2d)	N2 (mmol/m2d)	Silicate (mmol/m2d)
6-Yellow	0.26±0.11	1.97±0.59	0±.03	0.14±0.10	−2.5±7.5	1.88±1.90	7.2±1.9
6-Blue	0.24±0.10	1.06±0.25	0.02±0.02	0.08±0.05	−0.33±0.90	2.53±4.57	4.6±0.9
6*-Yellow	0.52±0.30	1.37±0.82	0.16±0.08	(−16.7±5.0)	2.0±6.5	2.94±2.34	8.1±2.1
8-Yellow	0.15±0.06	0.36±0.14	0.0±0.0	−0.04±0.03	−1.0±0.6	2.24±1.63	2.1±0.6
8-Blue	0.09±0.05	0.81±0.27	0.01±0.01	−0.05±0.04	−1.6±1.1	−0.34±1.68	2.2±0.6
37-Yellow	0.09±0.05	0.40±0.15	0.02±0.01	0.12±0.05	1.6±1.2	−0.13±1.19	3.6±1.1
37-Blue	0.08±0.04	0.54±0.16	0.02±0.02	0.14±.05	1.6±1.1	2.46±4.11	3.4±0.7
37*-Blue	0.08±0.05	0.53±0.14	0.47±0.10	(−4.9±1.1)	−0.17±0.45	−1.87±4.14	3.5±0.6
14-Yellow	0.80±0.27	4.46±1.26	0.14±0.09	0.77±0.27	−7.0±6.1	−3.15±2.36	18.5±5.2
16-Blue	1.96±0.38	11.8±2.1	0.28±0.07	0.35±0.16	−3.6±2.6	4.87±2.21	34.3±6.0

Table 3: Carbon oxidised and carbonate dissolved.

	CaCO3 Dissolution Scenario				*Sulfate Reduction Scenario*		
Site-ID	Carbonate Dissolved (mmol/m2d)	Total Carbon Oxidized (mmol/m2d)	Measured O2 Flux (mmol/m2d)	Measured TCO2 Flux (mmol/m2d)	Cox by Sulfate (mmol/m2d)	Cox by Oxygen (mmol/m2d)	% Cox by Sulfate
6-Yellow	10.0	45.0	42.4	55.0	20.1	34.9	37
6-Blue	3.6	36.6	39.4	40.2	7.1	33.1	18
8-Yellow	2.6	21.8	21.1	24.4	5.2	19.2	21
8-Blue	0.5	17.7	22.0	18.2	1.0	17.2	5
37-Yellow	1.5	19.2	21.0	20.7	3.0	17.7	14
37-Blue	4.8	25.3	23.2	30.1	9.6	20.5	32
14-Yellow	13.9	68.3	64.2	82.2	27.8	54.4	34
16-Blue	27.7	92.1	86.2	119.8	55.3	64.5	46

Table 4: Nitrogen budget (does not include DON). All units mmol/m^2d. The chambers spiked with KNO_3 are included but the NO_3 uptake rate is not determined.

Site-ID	Nitrate Flux	Nitrite Flux	Ammonia Flux	Total N Flux	Carbon Oxidized	Predicted Total N Flux	Missing N Flux	Expected N2 Flux	Measured N2 Flux
6-Yellow	0.14	0	1.97	2.11	55	8.2	6.1	3.0	1.88
6-Blue	0.08	0.02	1.06	1.16	40.2	6.0	4.8	2.4	2.53
6*-Yellow		0.16	1.37		70.4	10.5			2.94
8-Yellow	-0.04	0	0.36	0.32	24.4	3.6	3.3	1.7	2.24
8-Blue	-0.05	0.01	0.81	0.77	18.2	2.7	1.9	1.0	-0.34
37-Yellow	0.12	0.02	0.4	0.54	20.7	3.1	2.5	1.3	-0.13
37-Blue	0.14	0.02	0.54	0.7	30.1	4.5	3.8	1.9	2.46
37*-Blue		0.47	0.53		23.2	3.5			-1.87
14-Yellow	0.77	0.14	4.46	5.37	82.2	12.3	6.9	3.4	-3.15
16-Blue	0.35	0.28	11.8	12.43	119.8	17.9	5.5	2.7	4.87

Table 5: The fitting parameter, b (units 1/hour) fit to the various injected tracers. The last column contains the ratio of b values for Cs and deuterium.

Site-ID	D2O	Cesium	Nitrate	Cs/D2O
6B	-0.057	-0.067		1.18
6Y	-0.059	-0.074		1.25
6*Y	–	-0.085	-0.091	-
8B	-0.02	-0.023		1.15
37Y	-0.026	-0.034		1.31
37B	-0.037	-0.046		1.24
37*B	-0.022	-0.031	-0.033	1.41
16B	-0.18	-0.19		1.06

Table 6: Diffusive fluxes of radon from Port Phillip Bay sediments based on sediment radium measurements. Fluxes in atoms/m^2/sec.

Site-ID	Diffusive flux from Sediments 1994	Diffusive flux from Sediments 1995
6	27	38
8	39	–
37	–	–
14	–	56
16	49	–

Appendix: Table 1

Station 6 (Yellow)

Cruise: PPB 95 **Station:** 6 **Lander:** Yellow

Time of Lid Drop	20-Feb 16:05
Height of Blue Chamber (cm)	13.4
± uncertainty	±3.0
Chamber Area (m^2)	0.073

	Clock Time	Elapsed Time
Draw 1	20-Feb 16:35	0.50
Draw 2	20-Feb 18:05	2.00
Draw 3	20-Feb 21:05	5.00
Draw 4	21-Feb 1:05	9.00
Draw 5	21-Feb 5:05	13.00
Draw 6	21-Feb 9:05	17.00

Original Data

Sample	Volume mL	Nitrate µM	Nitrite µM	Ammonia µM	DON µM	Nitrogen µM	Alkalinity µeq/L	Calculated TCO2 µM	Phosphate µM	Silica µM	pH
Blue-1	130	0.18	0.15	0.66	19.0	414	2502	2236	2.93	5.3	8.11
Blue-2	130	0.21	0.10	2.59	45.2		2527	2287	3.27	11.1	8.06
Blue-3	130	0.43	0.11	4.72	36.1		2525	2322	3.51	19.1	7.99
Blue-4	300	0.51	0.14	6.01	20.8		2567	2389	3.67	24.4	7.93
Blue-5	300	~~0.69~~	~~0.18~~	~~8.41~~	~~18.6~~	425	~~2573~~	~~2431~~	~~3.81~~	~~32.7~~	7.85
Blue-6	300	~~0.54~~	~~0.20~~	~~8.43~~	~~19.3~~	421	~~2601~~	~~2468~~	~~3.86~~	~~33.5~~	7.83
Niskin		0.03	0.02	0.20	27.4	404	2497	2230	3.07	4.5	8.11
Uncertainty		±0.02	±0.02	±0.05	±2.0	±7	±12	±15	±0.03	±0.1	
Bottom Water		0.03	0.02	0.20	27.4	404	2497	2230	3.07	4.5	
										Integrity	
y-Intercept		**0.2**	**0.1**	**1.00**	**33.5**	**415**	**2502**	**2239**	**3.0**	**5.9**	
Source		Fit	Fit	Fit	Fit	Analysis	Analysis	Analysis	Fit	Fit	
Error in Slope		0.0081	0.0047	0.1200	2.3134	0.5751	1.8475	2.3094	0.0208	0.3412	
Flux (unit/1000/m2/day)		**0.135**	**0.001**	**1.970**	**-2.492**	**1.876**	**21.91**	**55.00**	**0.26**	**7.15**	
Error in Flux		**±0.040**	**±0.015**	**±0.586**	**±7.461**	**±1.897**	**±7.705**	**±14.38**	**±0.09**	**±1.94**	

Station 6 (Blue)

Cruise: PPB 95 **Station:** 6 **Lander:** Blue

Time of Lid Drop	20-Feb 16:00
Height of Blue Chamber (cm)	11.7
± uncertainty	±2.0
Chamber Area (m^2)	0.073

	Clock Time	Elapsed Time
Draw 1	20-Feb 16:30	0.50
Draw 2	20-Feb 18:00	2.00
Draw 3	20-Feb 21:00	5.00
Draw 4	21-Feb 1:00	9.00
Draw 5	21-Feb 5:00	13.00
Draw 6	21-Feb 9:00	17.00

Original Data

Sample	Volume mL	Nitrate µM	Nitrite µM	Ammonia µM	DON µM	Nitrogen µM	Alkalinity µeq/L	Calculated TCO2 µM	Phosphate µM	Silica µM	pH
Blue-1	130	0.20	0.06	0.33	16.6	418	2513	2244	3.05	6.0	8.11
Blue-2	130	0.26	0.05	1.28	20.5		2558	2300	3.35	8.9	8.09
Blue-3	130	0.37	0.07	2.49	17.3		2545	2330	3.65	14.8	8.01
Blue-4	300	0.45	0.10	3.58	17.3		2551	2375	3.81	19.8	7.93
Blue-5	300	~~0.72~~	~~0.14~~	~~4.97~~	~~13.1~~	447	~~2534~~	~~2407~~	~~4.06~~	~~28.5~~	7.82
Blue-6	300	~~0.53~~	~~0.11~~	~~4.85~~	~~14.1~~	424	~~2582~~	~~2471~~	~~4.16~~	~~30.6~~	7.78
Niskin		0.03	0.02	0.20	27.4	404	2497	2230	3.07	4.5	8.11
Uncertainty		±0.02	±0.02	±0.05	±2.0	±7	±12	±15	±0.03	±0.1	
Bottom Water		0.03	0.02	0.20	27.4	404	2497	2230	3.07	4.5	

Integrity

y-Intercept	**0.2**	**0.0**	**0.38**	**18.4**	**421**	**2530**	**2254**	**3.1**	**5.6**
Source	Fit	Analysis	Fit	Fit	Fit	Fit	Fit	Fit	Fit
Error in Slope	0.0033	0.0031	0.0435	0.3209	1.6184	3.2297	2.8141	0.0200	0.1294
Flux (unit/1000/m2/day)	**0.084**	**0.015**	**1.060**	**-0.332**	**2.529**	**8.145**	**40.20**	**0.24**	**4.64**
Error in Flux	**±0.017**	**±0.009**	**±0.219**	**±0.903**	**±4.565**	**±9.175**	**±10.47**	**±0.07**	**±0.87**

Station 6* (Yellow)

Cruise: PPB 95 **Station:** 6* **Lander:** Yellow

Time of Lid Drop	6-Mar 18:00
Height of Blue Chamber (cm)	12.2
± uncertainty	±3.0
Chamber Area (m^2)	0.073

	Clock Time	Elapsed Time
Draw 1	6-Mar 19:00	1.00
Draw 2	6-Mar 20:30	2.50
Draw 3	6-Mar 22:00	4.00
Draw 4	7-Mar 1:00	7.00
Draw 5	7-Mar 4:00	10.00
Draw 6	7-Mar 8:00	14.00

Original Data

Sample	Volume mL	Nitrate µM	Nitrite µM	Ammonia µM	DON µM	Nitrogen µM	Alkalinity µeq/L	TCO2 µM	Phosphate µM	Silica µM	pH
Blue-1	300	55.9	0.03	0.64	15.2	414	2509	2311	2.72	7.2	7.98
Blue-2	130	46.0	0.10	0.67	10.5		2525	2353	2.74	11.3	7.92
Blue-3	130	38.1	0.19	2.01	17.2		2539	2381	3.24	15.3	7.89
Blue-4	300	~~29.2~~	~~0.28~~	~~2.96~~	~~19.7~~	421	~~2546~~	~~2414~~	~~3.13~~	~~19.6~~	7.83
Blue-5	130	~~22.9~~	~~0.35~~	~~5.86~~	~~12.0~~		~~2568~~	~~2453~~	~~3.47~~	~~25.0~~	7.79
Blue-6	300	~~16.8~~	~~0.45~~	~~7.61~~	~~13.4~~	426	~~2579~~	~~2486~~	~~3.50~~	~~29.9~~	7.73
Niskin		0.0	0.01	0.24	15.3	404	2512	2258	2.73	4.5	8.09
Uncertainty		±0.02	±0.02	±0.05	±2.0	±7	±12	±15	±0.03	±0.1	
Bottom Water		0.0	0.01	0.24	15.3	404	2512	2258	2.73	4.5	

Integrity

y-Intercept	**61.4**	**0.0**	**-0.05**	**12.6**	**413**	**2499**	**2289**	**2.5**	**4.5**
Source	Fit	Analysis	Fit	Fit	Analysis	Analysis	Analysis	Fit	Analysis
Error in Slope	0.2756	0.0094	0.2559	2.2266	0.7607	5.6569	7.0711	0.0940	0.0471
Flux (unit/1000/m2/day)	**-16.721**	**0.160**	**1.367**	**1.993**	**2.938**	**29.74**	**70.42**	**0.52**	**8.09**
Error in Flux	**±4.190**	**±0.048**	**±0.821**	**±6.538**	**±2.342**	**±18.106**	**±26.99**	**±0.30**	**±1.99**

Station 8 (Yellow)

Cruise: PPB 95 **Station:** 8 **Lander:** Yellow

			Clock Time	Elapsed Time
Time of Lid Drop	27-Feb 14:00	Draw 1	27-Feb 14:30	0.50
Height of Blue Chamber (cm)	11.0	Draw 2	27-Feb 17:00	3.00
± uncertainty	±3.0	Draw 3	27-Feb 20:00	6.00
Chamber Area (m^2)	0.073	Draw 4	28-Feb 0:30	10.50
		Draw 5	28-Feb 5:00	15.00
		Draw 6	28-Feb 6:00	16.00

Original Data

Sample	Volume mL	Nitrate µM	Nitrite µM	Ammonia µM	DON µM	Nitrogen µM	Alkalinity µeq/L	TCO2 µM	Phosphate µM	Silica µM	pH
Blue-1	130	0.37	0.03	0.25	20.5	415	2538	2275	3.24	5.2	8.10
Blue-2	130	0.04	0.01	0.25	16.8		2551	2301	3.40	6.2	8.07
Blue-3	130	0.05	0.01	0.66	12.6		2567	2340	3.51	7.9	8.03
Blue-4	300	0.05	0.02	1.33	14.3		~~2519~~	~~2361~~	3.76	11.4	7.97
Blue-5	300	0.05	0.02	2.09	14.4	427	2571	2406	4.06	16.0	7.90
Blue-6	300	~~0.05~~	~~0.02~~	~~2.40~~	~~18.5~~	426	~~2589~~	~~2429~~	~~4.34~~	~~17.0~~	7.89
Niskin		0.08	0.02	0.41	28.9	414	2550	2284	3.37	5.2	8.10
Uncertainty		±0.02	±0.0	±0.05	±2.0	±7	±12	±15	±0.03	±0.1	
Bottom Water		0.08	0.02	0.41	28.9	414	2550	2284	3.37	5.2	
											Integrity
y-Intercept		**0.2**	**0.0**	**-0.03**	**18.2**	**414**	**2544**	**2275**	**3.2**	**4.0**	
Source		Fit	Analysis	Fit	Fit	Analysis	Analysis	Analysis	Fit	Fit	
Error in Slope		0.0114	0.0017	0.0155	0.2210	0.5706	1.0946	1.3682	0.0032	0.0730	
Flux (unit/1000/m2/day)		**-0.040**	**0.000**	**0.364**	**-1.021**	**2.242**	**5.634**	**24.44**	**0.15**	**2.05**	
Error in Flux		**±0.032**	**±0.005**	**±0.107**	**±0.646**	**±1.626**	**±3.273**	**±7.58**	**±0.04**	**±0.59**	

Station 8 (Blue)

Cruise: PPB 95 **Station:** 8 **Lander:** Blue

Time of Lid Drop	27-Feb 14:30
Height of Blue Chamber (cm)	11.0
± uncertainty	±3.0
Chamber Area (m^2)	0.073

	Clock Time	Elapsed Time
Draw 1	27-Feb 15:00	0.50
Draw 2	27-Feb 18:00	3.50
Draw 3	27-Feb 21:00	6.50
Draw 4	28-Feb 0:30	10.00
Draw 5	28-Feb 4:00	13.50
Draw 6	28-Feb 5:00	14.50

Original Data

Sample	Volume mL	Nitrate µM	Nitrite µM	Ammonia µM	DON µM	Nitrogen µM	Alkalinity µeq/L	TCO2 µM	Phosphate µM	Silica µM	pH
Blue-1	130	0.39	0.01	0.27	18.2	413	2551	2293	3.31	5.7	8.09
Blue-2	130	0.15	0.04	1.08	11.6		2544	2301	3.45	8.5	8.06
Blue-3	130	0.16	0.05	2.23	13.3		2549	2331	3.59	10.9	8.01
Blue-4	300	0.16	0.06	3.07	11.7		2556	2354	3.64	13.6	7.98
Blue-5	300	~~0.15~~	~~0.07~~	~~3.27~~	~~11.8~~	411	~~2566~~	~~2387~~	~~3.67~~	~~16.1~~	7.93
Blue-6	300	~~0.19~~	~~0.08~~	~~3.63~~	~~13.1~~	412	~~2561~~	~~2384~~	~~3.75~~	~~16.7~~	7.93
Niskin		0.08	0.02	0.41	28.9	414	2550	2284	3.37	5.2	8.10
Uncertainty		±0.02	±0.02	±0.05	±2.0	±7	±12	±15	±0.03	±0.1	
Bottom Water		0.08	0.02	0.41	28.9	414	2550	2284	3.37	5.2	
											Integrity
y-Intercept		**0.3**	**0.0**	**0.11**	**16.6**	**413**	**2546**	**2285**	**3.3**	**5.4**	
Source		Fit	Analysis	Fit	Fit	Analysis	Analysis	Analysis	Fit	Fit	
Error in Slope		0.0135	0.0028	0.0192	0.3629	0.6338	1.7024	2.1280	0.0056	0.0228	
Flux (unit/1000/m2/day)		**-0.054**	**0.013**	**0.809**	**-1.553**	**-0.344**	**1.855**	**18.23**	**0.09**	**2.23**	
Error in Flux		**±0.039**	**±0.008**	**±0.227**	**±1.047**	**±1.676**	**±4.523**	**±7.50**	**±0.03**	**±0.61**	

Station 37 (Yellow)

Cruise: PPB 95 **Station:** 37 **Lander:** Yellow

Time of Lid Drop	23-Feb 12:30
Height of Blue Chamber (cm)	10.0
± uncertainty	±3.0
Chamber Area (m^2)	0.073

	Clock Time	Elapsed Time
Draw 1	23-Feb 13:00	0.50
Draw 2	23-Feb 16:00	3.50
Draw 3	23-Feb 20:00	7.50
Draw 4	24-Feb 0:12	11.70
Draw 5	24-Feb 4:00	15.50
Draw 6	24-Feb 8:00	19.50

Original Data

Sample	Volume mL	Nitrate µM	Nitrite µM	Ammonia µM	DON µM	Nitrogen µM	Alkalinity µeq/L	Calculated TCO2 µM	Phosphate µM	Silica µM	pH
Blue-1	130	0.07	0.04	0.20	14.6	433	2427	2213	1.54	9.8	8.02
Blue-2	130	0.36	0.09	1.05	9.9		2433	2236	1.78	14.9	7.98
Blue-3	130	0.52	0.12	1.77	13.3		2442	2273	1.90	20.7	7.93
Blue-4	300	0.73	0.13	2.36	26.3		2452	2308	2.03	26.6	7.87
Blue-5	300	0.84	0.14	2.68	18.7	437	2441	2332	2.14	31.6	7.78
Blue-6	300	~~0.91~~	~~0.14~~	~~3.34~~	~~22.2~~	428	~~2444~~	~~2341~~	~~2.22~~	~~35.7~~	7.77
Niskin		0.14	0.03	0.63	19.2	417	2381	2144	1.79	7.7	8.07
Uncertainty		±0.02	±0.02	±0.05	±2.0	±7	±12	±15	±0.03	±0.1	
Bottom Water		0.14	0.03	0.63	19.2	417	2381	2144	1.79	7.7	

Integrity

y-Intercept	**0.1**	**0.1**	**0.34**	**11.3**	**434**	**2429**	**2208**	**1.6**	**9.4**
Source	Fit	Analysis	Fit	Fit	Analysis	Analysis	Analysis	Fit	Fit
Error in Slope	0.0052	0.0017	0.0175	0.4654	0.4942	0.9919	1.2399	0.0045	0.0211
Flux (unit/1000/m2/day)	**0.123**	**0.015**	**0.404**	**1.631**	**-0.133**	**3.292**	**20.72**	**0.09**	**3.62**
Error in Flux	**±0.039**	**±0.006**	**±0.128**	**±1.219**	**±1.187**	**±2.577**	**±6.89**	**±0.03**	**±1.09**

Station 37 (Blue)

Cruise: PPB 95 **Station:** 37 **Lander:** Blue

Time of Lid Drop	23-Feb 13:00
Height of Blue Chamber (cm)	9.7
± uncertainty	±2.0
Chamber Area (m^2)	0.073

	Clock Time	Elapsed Time
Draw 1	23-Feb 13:30	0.50
Draw 2	23-Feb 17:00	4.00
Draw 3	23-Feb 21:00	8.00
Draw 4	24-Feb 1:00	12.00
Draw 5	24-Feb 4:30	15.50
Draw 6	24-Feb 8:12	19.20

Original Data

Sample	Volume mL	Nitrate µM	Nitrite µM	Ammonia µM	DON µM	Nitrogen µM	Alkalinity µeq/L	Calculated TCO2 µM	Phosphate µM	Silica µM	pH
Blue-1	130	0.29	0.06	0.44	10.8	428	2391	2189	1.63	9.9	8.00
Blue-2	130	0.57	0.13	2.39	8.2		2418	2258	1.88	17.1	7.91
Blue-3	130	0.84	0.17	3.14	9.8		2430	2307	2.02	22.3	7.82
Blue-4	300	1.10	0.20	3.72	24.0		2472	2375	2.10	27.8	7.75
Blue-5	300	1.14	0.21	4.00	16.0	464	2441	2363	2.12	30.9	7.70
Blue-6	300	~~1.12~~	~~0.21~~	~~4.46~~	~~10.5~~	435	~~2458~~	~~2391~~	~~2.18~~	~~34.1~~	7.67
Niskin		0.14	0.03	0.63	19.2	417	2381	2144	1.79	7.7	8.07
Uncertainty		±0.02	±0.02	±0.05	±2.0	±7	±12	±15	±0.03	±0.1	
Bottom Water		0.14	0.03	0.63	19.2	417	2381	2144	1.79	7.7	
											Integrity
y-Intercept		**0.3**	**0.1**	**0.93**	**8.1**	**431**	**2397**	**2198**	**1.7**	**10.3**	
Source		Fit	Analysis	Fit	Fit	Fit	Fit	Fit	Fit	Fit	
Error in Slope		0.0062	0.0017	0.0466	0.4690	1.7385	1.5886	1.9632	0.0065	0.0915	
Flux (unit/1000/m2/day)		**0.143**	**0.024**	**0.539**	**1.634**	**2.464**	**10.03**	**30.11**	**0.08**	**3.38**	
Error in Flux		**±0.033**	**±0.006**	**±0.155**	**±1.143**	**±4.079**	**±4.237**	**±7.71**	**±0.02**	**±0.73**	

Station 37* (Blue)

Cruise: PPB 95 **Station:** 37* **Lander:** Blue

Time of Lid Drop	6-Mar 16:00
Height of Blue Chamber (cm)	11.3
± uncertainty	±2.0
Chamber Area (m^2)	0.073

	Clock Time	Elapsed Time
Draw 1	6-Mar 17:00	1.00
Draw 2	6-Mar 19:00	3.00
Draw 3	6-Mar 21:00	5.00
Draw 4	7-Mar 1:00	9.00
Draw 5	7-Mar 4:00	12.00
Draw 6	7-Mar 7:00	15.00

Original Data

Sample	Volume mL	Nitrate µM	Nitrite µM	Ammonia µM	DON µM	Nitrogen µM	Alkalinity µeq/L	TCO2 µM	Phosphate µM	Silica µM	pH
Blue-1	300	73.0	0.00	1.33	11.5	437	2462	2242	1.86	10.0	8.03
Blue-2	130	70.7	0.27	~~0.37~~	10.0		~~2412~~	~~2219~~	1.84	11.6	7.98
Blue-3	130	66.9	0.61	1.26	10.6		2477	2290	1.95	15.1	7.96
Blue-4	300	59.2	1.30	2.21	11.5	448	2462	2310	2.06	19.8	7.88
Blue-5	130	52.8	1.79	3.14	9.7		2463	2328	2.17	22.8	7.84
Blue-6	300	46.2	2.30	3.66	10.3	425	2476	2366	2.20	26.9	7.78
Niskin		0.1	0.02	0.26	10.1	417	2480	2247	1.36	5.5	8.05
Uncertainty		±0.02	±0.02	±0.05	±2.0	±7	±12	±15	±0.03	±0.1	
Bottom Water		0.1	0.02	0.26	10.1	417	2480	2247	1.36	5.5	
											Integrity
y-Intercept		**76.3**	**-0.2**	**0.75**	**11.1**	**442**	**2465**	**2238**	**1.8**	**8.5**	
Source		Fit	Fit	Fit	Analysis	Fit	Analysis	Analysis	Fit	Fit	
Error in Slope		0.0836	0.0029	0.0354	0.1647	1.5217	1.0811	1.3514	0.0029	0.0357	
Flux (unit/1000/m2/day)		**-4.905**	**0.471**	**0.529**	**-0.167**	**-1.869**	**0.980**	**23.15**	**0.08**	**3.48**	
Error in Flux		**±0.897**	**±0.084**	**±0.134**	**±0.448**	**±4.140**	**±2.937**	**±5.50**	**±0.02**	**±0.62**	

Station 14 (Yellow)

Cruise: PPB 95 **Station:** 14 **Lander:** Yellow

Time of Lid Drop	2-Mar 16:00
Height of Blue Chamber (cm)	11.0
± uncertainty	±3.0
Chamber Area (m^2)	0.073

	Clock Time	Elapsed Time
Draw 1	2-Mar 16:30	0.50
Draw 2	2-Mar 18:30	2.50
Draw 3	2-Mar 21:00	5.00
Draw 4	2-Mar 23:30	7.50
Draw 5	3-Mar 4:00	12.00
Draw 6	3-Mar 5:00	13.00

Original Data

Sample	Volume mL	Nitrate µM	Nitrite µM	Ammonia µM	DON µM	Nitrogen µM	Alkalinity µeq/L	TCO2 µM	Phosphate µM	Silica µM	pH
Blue-1	130	0.16	0.04	0.25	23.1	411	2452	2248	2.17	10.4	8.00
Blue-2	130	0.69	0.15	3.89	8.9		2462	2296	2.84	22.7	7.92
Blue-3	130	1.46	0.28	7.80	10.5		2504	2386	3.52	41.5	7.80
Blue-4	300	~~2.14~~	~~0.34~~	~~9.11~~	~~12.8~~		2485	~~2379~~	~~3.62~~	~~45.4~~	7.77
Blue-5	300	~~2.16~~	~~0.39~~	~~10.43~~	~~11.6~~	392	2493	2399	~~3.69~~	~~49.1~~	7.74
Blue-6	300	~~2.07~~	~~0.40~~	~~11.35~~	~~12.2~~	402	~~2487~~	~~2393~~	~~3.75~~	~~50.0~~	7.74
Niskin		0.18	0.05	0.59	11.7	401	2474	2267	2.30	8.3	8.00
Uncertainty		±0.02	±0.02	±0.05	±2.0	±7	±12	±15	±0.03	±0.1	
Bottom Water		0.18	0.05	0.59	11.7	401	2474	2267	2.30	8.3	
											Integrity
y-Intercept		**0.0**	**0.0**	**-0.49**	**21.2**	**412**	**2441**	**2227**	**2.0**	**6.3**	
Source		Fit	Analysis	Fit	Fit	Fit	Analysis	Analysis	Fit	Fit	
Error in Slope		0.0125	0.0063	0.0670	2.1885	0.8336	3.7635	4.7044	0.0167	0.4143	
Flux (unit/1000/m2/day)		**0.774**	**0.141**	**4.457**	**-6.995**	**-3.152**	**31.53**	**82.23**	**0.80**	**18.50**	
Error in Flux		**±0.214**	**±0.042**	**±1.228**	**±6.084**	**±2.363**	**±13.139**	**±25.64**	**±0.22**	**±5.16**	

Station 16 (Blue)

Cruise: PPB 95 **Station:** 16 **Lander:** Blue

Time of Lid Drop	2-Mar 18:00
Height of Blue Chamber (cm)	11.4
± uncertainty	±2.0
Chamber Area (m^2)	0.073

	Clock Time	Elapsed Time
Draw 1	2-Mar 18:30	0.50
Draw 2	2-Mar 20:30	2.50
Draw 3	2-Mar 23:00	5.00
Draw 4	3-Mar 2:00	8.00
Draw 5	3-Mar 5:30	11.50
Draw 6	3-Mar 6:30	12.50

Original Data

Sample	Volume mL	Nitrate µM	Nitrite µM	Ammonia µM	DON µM	Nitrogen µM	Alkalinity µeq/L	TCO2 µM	Phosphate µM	Silica µM	pH
Blue-1	130	0.49	0.09	1.13	17.0	374	2409	2202	2.65	13.8	8.01
Blue-2	130	0.52	0.26	10.10	10.6		2464	2303	4.30	38.0	7.91
Blue-3	130	1.04	0.55	20.44	10.8		2518	2398	5.86	69.5	7.80
Blue-4	300	~~1.22~~	~~0.64~~	~~24.52~~	~~13.1~~		~~2588~~	~~2492~~	~~6.52~~	~~80.1~~	7.74
Blue-5	300	~~1.10~~	~~0.63~~	~~27.39~~	~~13.3~~	399	~~2603~~	~~2525~~	~~6.56~~	~~87.5~~	7.69
Blue-6	300	~~1.05~~	~~0.62~~	~~28.44~~	~~12.1~~	392	~~2604~~	~~2532~~	~~6.55~~	~~80.8~~	7.68
Niskin		0.04	0.03	0.19	12.1	395	2409	2174	2.52	9.4	8.06
Uncertainty		±0.02	±0.02	±0.05	±2.0	±7	±12	±15	±0.03	±0.1	
Bottom Water		0.04	0.03	0.19	12.1	395	2409	2174	2.52	9.4	
											Integrity
y-Intercept		**0.3**	**0.0**	**-0.91**	**16.3**	**374**	**2399**	**2185**	**2.4**	**7.2**	
Source		Fit	Fit	Fit	Fit	Analysis	Analysis	Analysis	Fit	Fit	
Error in Slope		0.0556	0.0096	0.0851	0.9273	0.7434	3.7635	4.7044	0.0547	0.1822	
Flux (unit/1000/m2/day)		**0.352**	**0.281**	**11.840**	**-3.594**	**4.868**	**66.77**	**119.84**	**1.96**	**34.29**	
Error in Flux		**±0.164**	**±0.056**	**±2.090**	**±2.614**	**±2.206**	**±15.596**	**±24.65**	**±0.38**	**±6.04**	

DIRECT MEASUREMENTS OF DENITRIFICATION IN SEDIMENTS

Introduction

The first part of this section describes the direct determination of biogenically-formed nitrogen gas in benthic chamber deployments conducted in Port Phillip Bay from February 1995 to January 1996. These measurements were undertaken to test the hypothesis that denitrification in the sediments, proposed from stoichiometric considerations and a simple model of organic matter degradation (Berelson et al. 1994) is a major control on water and sediment quality in Port Phillip Bay.

Early measurements of biogenic N_2 were made by gas chromatographic methods (see below), but the precision of these methods appeared only marginally adequate to properly assess the presence or absence of active denitrification. Subsequent N_2 measurements were made by mass spectrometry, and these were carried out at the University of Rhode IS Graduate School of Oceanography. These measurements had significantly better precision than the GC methods and the mass spectrometric results are reported here first, as they do prove the presence of denitrification in the sediments. Furthermore, the mass spectrometric measurements validated the complementary GC N_2 measurements on the same sub-samples of chamber waters collected during February 1996. This intercomparison improved our confidence in the interpretation of the GC data obtained from the February 1995 to January 1996 deployments.

The second part of the section describes the seasonal variations in denitrification fluxes conducted in February 1995, June 1995, August/September 1995 and January 1996; these analyses were conducted by gas chromatography (Table 7).

Table 7: Sites and periods of benthic chamber deployments with N_2 measurements

Site	Period	Temperature
6 Werribee	February/March 1995	20-24 C
6 Werribee	June 1995	11 C
16 Yarra Estuary	February/March 1995	20-24 C
16 Yarra Estuary	August/September 1995	12.3 C
16 Yarra Estuary	January 1996	19 C
37 Central Basin	February/March 1995	20-24 C
37 Central Basin	August/September 1995	12.3 C
37 Central Basin	January 1996	19 C

Methods for estimating denitrification rates with direct N_2 measurements

Benthic chambers, sampling, GC analyses and data processing

The USC benthic chambers were modified to carry six 1-ml sample loops attached to Altech GC sampling valves for the February/March 1995 investigation. The GC valves were connected in series with the sample-draw mechanism and seawater samples for gas analysis were drawn through the loop/valve assembly at the first sampling period (0.5 hrs) and at the 5th and 6th sampling periods following 15 and 20 hours incubation. The seawater samples from these chambers were collected automatically in calibrated sample loops (ca 1 ml) attached to a six-port gas valve. This method preserved the gaseous components of the sample during detachment from the chamber, transport to the laboratory and transfer to the gas line of the chromatograph. The samples were kept under water at in situ temperatures until analysis. These data are discussed in the first section of this report; only those site data relevant for inclusion in the time-series data will be discussed here.

For subsequent sampling periods (June 1995 through January/February 1996) we used the MAFRI benthic chambers. Water samples for these investigations were collected in gas-tight glass 50ml syringes by divers, stored under seawater at a temperature below in-situ, and returned to Canberra by air, for analysis in the AGSO laboratories.

N_2 was measured with a Thermal Conductivity Detector (TCD) installed into a Gas Chromatograph in the AGSO Canberra laboratory. Because the Ar and O_2 peaks have the same retention times, the dissolved oxygen was stripped from the sample by rapid mixing with a concentrated solution of reduced methyl viologen and sparging with high purity helium. The methyl viologen was reduced with activated mercury/zinc and the solution was stripped with helium before introduction into the stripping tower of the gas lines. Sample volumes of 1-ml were used.

GC analyses and data processing

The feasibility of direct measurements of N_2 (expected to increase in the benthic chambers as a result of denitrification) was predicated on the precision and sensitivity of the methodology and on the assumption that water in Port Phillip Bay would be equilibrated with air and that the concentrations of argon would be constant in surface seawater and porewaters, subject only to the effects of temperature and salinity. Because absolute measurements of N_2 concentrations with the resolution required for this work are difficult, reliance for measuring increases (or decreases) in the N_2 concentrations of the water samples was based on accurate measurements of N_2/Ar ratios.

For the February 1995 investigation, around 50 seawater samples were collected in 50ml syringes at the station locations and these were used as reference controls. A similar strategy was adopted for the remainder of the 1995 and 1996 investigations. During the course of analysis the response of the TCD detector exhibited drift. Accordingly, the N_2/Ar of all water samples were normalised with respect the N_2/Ar of the seawater samples which were analysed in sequence with the same data set (ie each sample of chamber water was bracketed by a

sample of the internal seawater standard maintained at a constant temperature). There was a fairly consistent trend for the averaged values of the N_2/Ar for the 6th draw to be less than those of the 5th draw in the February 1995 deployments. All January/February 1995 data are summarised in Tables 8 a) & b). Also, in the Site 6 seasonal data-set, a mid-incubation N_2 concentration was lower than the final point value (Table 8). Because the rates of CO_2 production and O_2 uptake were estimated from the steepest slope of the O_2 uptake data, the N_2 production rates were estimated from the 5th draw data for the February 1995 investigation.

Biogenic N_2 data (by GC analysis), from the other investigation periods, are summarised in Table 9.

Benthic chambers, sampling and mass spectrometry.

For the January/February 1996 deployments, N_2 was also measured by mass spectrometry. Seawater samples were collected from the benthic chambers in 100ml glass syringes which were promptly and carefully loaded into specially designed evacuated containers which had a small amount of mercuric chloride added to them to prevent microbial activity. These samples were returned by air to the Graduate School of Oceanography at the University of Rhode Island where a mass spectrometer was used to measure the absolute amounts of argon, nitrogen and oxygen in the samples, by measuring the 28/40, 32/40 mass abundance ratios. These complemented the GC and nutrient flux measurements for the Yarra Estuary and Central Basin sites in Port Phillip Bay. Concentrations of N_2 were calculated by assuming that Port Phillip Bay water N_2 and Ar contents are in equilibrium with the atmosphere at the in-situ measured temperature and salinity. The N_2 in each samples was calculated from the relationship:
$[N_2] = N_2/Ar * [Ar]$ at in-situ temperature and salinity.

Biogenic N_2 Results

A test of the denitrification hypothesis

The high precision mass spectrometric measurements were used to test the denitrification hypothesis. We noted that early measurements of the GC data were precise at about +/- 2% (which was found to be marginal to uniquely identify biogenic N_2 production), although this precision improved with subsequent analyses. The precision of the mass spectrometry January/February 1996 data were better than 1%.

The N_2 gas results (by both gas chromatography and mass spectrometry) from chamber deployments during January/February 1996 are summarised in Table 10. The N_2 data are plotted in Figure 24 a), for Site 37 in the central Port Phillip Bay and in Figure 24 b), for Site 16 in the Yarra estuary. Also shown in these plots are the GC data for comparison (see text below). Note that in these figures, one mass spectrometric measurement from one chamber at the end of the deployment is bracketed and we consider this sample was contaminated with air. Two of the GC measurements are bracketed and we consider also that these were also contaminated. Designation of these as contaminated samples is based upon the prediction of a

maximum denitrification rate which could not increase the total nitrogen inventory by more than 10%; each of these measurements are in excess of 10% of the total N_2 inventory.

The data from Site 37 (Figure 24 a), indicate increases in N_2 concentrations in the three chambers deployed. The bottom water N_2 (19°C, 35 psu) concentrations are plotted at zero time, and these are in good agreement with the expected N_2 concentrations in equilibrium with the atmosphere at the in-situ temperature and salinity. Because this Site is relatively deep in central Port Phillip Bay (23 m), only two samples could be collected from each chamber over a 24 hour period; these included the first 'draw' approximately 15 mins after the chambers were seated on the seafloor, and the other at the end of the deployment (approximately 24 hrs). The first sample 'draw' shows measured N_2 somewhat higher than bottom water and the Weiss equilibrium value and this may result from a disturbance of the sediments when the chambers were deployed with the release of some N_2 from the sediments. All three chambers showed consistent small elevations in the first 'draw' above bottom waters. At 24 hours, all three chambers show significant increases in N_2 above the first draw and the Weiss equilibrium value, with concentrations varying between 450 and 455 µM.

The data from Site 16 are shown in Figure 24 b. As noted for the Site 37 chambers, the first 'draw' on all three deployments at Site 16 were somewhat higher than the measured bottom water and the Weiss equilibrium concentration. This deployment is over a significantly shorter period of about 5 hours compared to the 24 hr deployment at Site 37. The reason for the shorter deployment period at Site 16 is because the chambers become anoxic if incubated for longer periods. Oxygen in all three chambers is nearly depleted at Site 16 (see Nicholson et al. 1996) but there is comparably smaller N_2 production, with concentrations at the end of the deployment <450 µM. This is an important observation because, despite the higher oxygen fluxes at Site 16, comparably smaller proportions of N are liberated as N_2 (via denitrification) than at Site 37, where oxygen fluxes are only about half of those at Site 16 (see discussion below).

We examined the N balance for each chamber to test the denitrification hypothesis. The model assumes that the degradation of organic matter in the sediments takes place in accordance with Redfield stoichiometry. First, the amount of N_2 predicted to be released to the chamber from the underlying sediments was calculated from the CO_2 released to the chamber waters. This is metabolic CO_2 and is calculated from the measured alkalinity and pH (corrected for NH_3 alkalinity) and assuming there is no significant calcium carbonate dissolution on the seafloor. This predicted N is shown on the following plots as N expected. Secondly, the measured N liberated during the deployment is shown as the moles of N_2 gas and also as total N formed [total N = 2 x moles of N_2 + moles of (ammonia + nitrate+ nitrite)] during the deployment. These data are summarised in Figures 25 & 26. The mass spectrometric data are shown in Figure 25, and the discussion below refers to this figure, although the same general conclusion can be drawn from the gas chromatograph data.

Figure 25 shows integrated chamber N inventories versus time. The integrated chamber inventory is N concentration * chamber volume and is given in µmole N. The data for Site 37, chamber 4 show a small enrichment of N_2-N in the first 'draw' above bottom water. The N measured at the end of the incubation period (corrected for the initial increase observed during the first 'sample-draw) is generally in good agreement with the predicted N value. We conclude that Redfield stoichiometry is proved; namely that the primary source of organic

matter undergoing degradation is phytoplankton and that denitrification is active in the sediments.

These plots reveal further important information. When the relative proportions of N released, because of denitrification, are compared to the total N (N_2+ ammonia + nitrate +nitrite) released, denitrification is noted to account for about 90 % of the N recycled in the sediments. Similar comments can be made about chambers 5 and 6 deployed at Site 37.

Plots of the integrated chamber N inventories for Site 16 are also shown in Figure 25. Data for chamber 4 also show a small elevation in the first 'draw' above bottom waters for N_2-N, and N_2-N inventories increase systematically throughout the deployment and prove the release of biogenic N_2. The agreement between the measured N increase (corrected for the first draw) and the predicted N increase again demonstrates that Redfield stoichiometry is an appropriate model to describe the degradation of organic matter at these Sites in Port Phillip Bay. A comparison of the proportions of N liberated as N_2 and as DIN (dissolved inorganic nitrogen ammonia + nitrate + nitrite), indicate that about 60% of the total N liberated at Site 16 is released as N_2-N. Similar observations can be made for the results for chamber 5, but the data from chamber 6 show a significant contamination of the last sample. From the data collected at the mid-point of the experiment most of the N liberated appears as DIN. These observations also prove denitrification is occurring at Site 16, but the relative proportion of N_2-N released is significantly less than that released at Site 37, despite the fact that significantly higher fluxes of all metabolites were measured at Site 16. This observation is revealed more clearly in Figure 27, which shows the carbon dioxide flux from the seafloor versus the N released from the seafloor. For Sites 16 and 37, the measured and predicted N flux from the sediments are similar and show Redfield stoichiometry. This plot also shows the amounts of N liberated as N_2 and as DIN for each of the chambers from Sites 16 and 37.

Denitrification efficiencies, Summer 1996

We define denitrification efficiency as the proportion of nitrogen liberated as N_2 compared to the total N liberated during metabolism. Percent denitrification efficiency = [moles of N as N_2]/[moles of N as N_2 + moles of dissolved inorganic nitrogen as ammonia + nitrate + nitrite]. Figures 25, 26 and 27 show that most N at Site 37 is released as N_2 via denitrification, but in contrast, a higher proportion of N is released as ammonia at Site 16. These data are summarised in Figure 28, which plots % denitrification efficiency versus CO_2 flux (or the flux of organic matter metabolised in the sediments); the data indicate that denitrification efficiency decreases as the metabolisable carbon flux to the sediments increases. Also shown in this plot are data from a chamber at Site 16 collected in March 1995 (at comparable temperatures to the January/February 1996 data), which had a considerably higher CO_2 flux from the sediments. This is an important observation because it has significant implications for water and sediment quality in Port Phillip Bay. The result suggests that with increased organic carbon loads to the sediments the denitrification pathway in the sediments is short-circuited, perhaps by more rapid rates of burial of organic matter, and more of the N flux into the sediments is returned to the overlying waters as ammonia (produced during sulphate reduction), and not as N_2. Nitrogen returned to bottom-waters as NH_3 is available for phytoplankton growth, and such a recycling scenario provides a positive feedback to external loads of metabolisable N. Although irrigation is patchy, as observed during both the 1994 and 1995 USC chamber deployments, irrigation did not appear higher at Site 16 than at Site 37,

implying that at comparable irrigation rates and higher organic matter rain rates, less N is recycled through the denitrification pathway than at sites of lower organic matter fluxes.

From the seasonal data collected at Sites 16 & 37, the % denitrification efficiencies were calculated at various times of the year and these are summarised in Figure 28 b. These data confirm the trend established from the summer 1996 data (see discussion below).

Comparison of mass spectrometer (MS) and gas chromatography (GC) N_2 measurements

The integrated N data from the GC and MS N_2 measurements which were made on separate but samples drawn almost simultaneously are given in Table 10 and shown graphically for Sites 16 and 37 in Figure 26. The same DIN values were used in Figure 26 as those for the mass spectrometric N_2 data in Figure 25. The two data sets have been compared statistically, and the overall agreement between the MS and GC measurements for Site 37 was excellent (r^2=0.9 and the slope=0.9; n=12). The complementary GC and MS N_2 measurements for Site 16 did not exhibit a similar correlation but the chamber incubation time was short (5 hours) and the increases in biogenic N_2 were small. These analyses indicate that the GC measurements were reliable when N_2 enrichment was greater than 1% of the bottom water concentration (ie around 4 μM N_2).

Seasonal variations in denitrification fluxes

Seasonal variations in denitrification fluxes and denitrification efficiency may be interpreted from the data presented in Table 11 and Figure 30. The following observations are made:

1. The range of CO_2 fluxes (or the flux of organic matter metabolised in the sediments at Site 37) varied by only a factor of two between eight chamber deployments over a 12 month period. The February 1995 CO_2 flux data are somewhat higher (average is approximately 25 mmol/m^2/day) than the August 1995 (winter), and the January/February (summer 1996) data, with average CO_2 fluxes of < 20 mmol/m^2/day.

2. At Site 37, the proportion of N released as N_2 was very high (> 70%) during summer and winter periods.

3. There was significant seasonal variation in CO_2 fluxes at Site 16. The summer 1995 rate was 120 mmol/m^2/day, the August (winter) 1995 rate was less than 20 mmol/m^2/day and the summer (January/February 1996) rate was greater than 50 mmol/m^2/day; seasonal variation factors of 2-5 were characteristic of this Site. This is in marked contrast to the lower variability (< factor 2) at Site 37 in the central Bay.

4. There was seasonal variability of the denitrification efficiency at Site 16. There is clearly an inverse relationship between the CO_2 flux and the denitrification efficiency, with higher denitrification efficiencies at lower CO_2 fluxes. At Site 16, the highest denitrification efficiencies were measured during the winter months when the CO_2 fluxes were lowest. Conversely, denitrification efficiencies were lower at higher CO_2 fluxes; a result that indicates more N is released as NH_3 via sulfate reduction, than is cycled through the denitrification loop at higher CO_2 fluxes (see discussion above).

N_2/Ar measurements in sediments

During the summer of 1995 some measurements of the N_2/Ar ratios in sediment porewaters were made to complement those made on seawater samples collected from the USC benthic chambers. Sediment samples were collected by divers. The 'syringe' cores were collected in such a way that approximtely 10 - 20 ml of overlying 'bottom-water' was trapped in the syringe, between the syringe-nipple (sealed with a three-way stopcock) and approximately 10 - 20 ml of sediment. A 25mm glass fibre filter was inserted into the syringe prior to field sampling to prevent sediment from being extruded into the sample loop during processing in the laboratory. The syringe, loaded with sediment and overlying water, was stored vertically under seawater at in situ temperatures, and returned to the laboratory for analysis, on the same day as collection. In the laboratory the overlying water and sediment was carefully extruded from the syringe in small (mm) increments. Approximately 1-ml samples of overlying water were loaded into the 1-ml sample loops, stripped and the N_2/Ar ratios measured. Similarly, approximately 2 mm of sediment was 'squeezed' and the interstitial waters extruded into the nylon 1-ml samples coils, stripped with He and the N_2/Ar ratio measured in the interstitial waters. Because of the difficulties experienced during this process, mostly as a result of the 'flocculent' nature of the interfacial sediments, many measurements could not be made because of the fine sediment which escaped the filter paper and 'blocked' the glass frit in the gas stripper. However several measurements were made successfully and these results are summarised in Figures 31a & b.

Data from Sites 6 and 8 (offshore the WTC) are shown in Figure 31a. The N_2/Ar ratios in the overlying water captured in the 'syringe'core and in the interstitial waters are compared to the N_2/Ar ratios of surface seawater. Because Port Phillip Bay is 'well mixed', the measured ratios in overlying water from the syringe (which represent mini incubations of sediment) and those in the sediments, if enriched compared to surface seawater are indicative of nitrogen in excess of its equilibrium concentration, indicating denitrification in the sediments. Eleven of the seventeen measurements made of N_2/Ar ratios in overlying waters and sediments (39 - 53) exceeded the N_2/Ar of surface seawater by 1 - 25%. Six of the seventeen measurements made of these ratios were lower than the N_2/Ar ratios of surface seawater, although 5 of these were within about 2% the surface seawater value and one was below by about 5%. It is not easy to explain a decrease in the N_2/Ar ratio in the sediments below the overlying bottom water values, but CO_2 bubble formation in the sediments accompanied by migration could strip dissolved gases and distort the equilibrium ratio. On balance we consider that these data are also indicative of excess nitrogen (above equilibrium concentrations) gas in the sediments, indicating denitrification at Sites 6 and 8.

Figure 31b summaries the data collected from Sites 14 (Hobson Bay), 16 (the Yarra estuary) and 37 (Central Port Phillip Bay). Of the twelve meaurements of N_2/Ar ratios made in overlying waters and sediments, all were equal to or exceeeded the N_2/Ar in the control or surface seawater sample, indicating excess nitrogen and inferring denitrification in the sediments.

Summary of biogenic N_2 measurements: the denitrification scenario revisited

1. The mass spectrometric measurements of N_2 made on seawater samples collected from the benthic chamber deployments at Sites 37 and 16 during January 1996 have proved that denitrification occurs in the sediments of Port Phillip Bay. There was significant increase

of the N_2 inventory in the chambers, at both sites, for the duration of the deployments which varied between 5 hours (Site 16) and 24 hours (Site 37).

2. The gas chromatographic and mass spectrometric data from Site 37 (January 1996) were highly correlated indicating that when the N_2 biogenically produced increases by at least 1% over the total N inventory in the bottom water, reliable GC measurements can be made provided all samples are measured relative to an internal standard to account for very small amounts of GC detector drift.
3. A comparison of the measured amounts of N released to the chambers agreed (within about 20%) with the predicted amounts of N released, calculated from the amount of metabolic CO_2 released and the stoichiometric ratio of N/C (assuming the metabolisable organic matter has N and C in Redfield proportions). The results suggest that the metabolisable organic matter undergoing degradation is primarily phytoplankton with Redfield stoichiometry.
4. The relative amounts of N liberated as N_2 into the chambers at Site 37 compared to the total N was about 90% at Site 37. In contrast N liberated as N_2 compared to total N released at Site 16 is approximately 60%. This was an important observation because it indicated that higher denitrification efficiencies at Site 37 correlate with low organic loads to the sediment.
5. A seasonal effect on denitrification was reflected in denitrification efficiency with the highest occurring in the summer months for Site 16 (Yarra Estuary). Seasonal effects on both rates and efficiencies of denitrification at Site 37 (Central) were marginal.
6. The N_2/Ar ratios of bottom and sediment porewaters from several sites, were higher than the ratio for bottom waters and indicated N_2 enrichment, considered to result from in situ denitrification.
7. The direct measurements of denitrification in the sediments of Port Phillip Bay have now shown beyond doubt that the denitrifying bacteria are active and that they play an important role in preventing the sediments and waters of the Bay from becoming an N sink.

Acknowledgments

We wish to thank the MAFRI staff, Andy Longmore, Geoff Nicholson, Annie Jahncke and Rhonda Flint for their logistics support, diving and other assistance during the field sampling phases of this work. Drewe Hampton (AGSO) did the GC analyses. Joe Orchardo from the University of Rhode Island did the mass spectrometric analyses. Colin Tindall (AGSO) assisted with all facets of the field work, including sampling and the field-based GC analyses. Andrew Herczeg, CSIRO Division of Water Resources, Adelaide, did the N isotope measurements on the chamber samples from the 'spiked' experiments. We sincerely thank these colleagues for their contribution to the success of the study.

TABLE 8a: Measurements of N_2 and Ar in samples from benthic chambers and seawater at Sites 6, 8, 14, 16 and 37, February 1995.

Site	Sample Draw	Time (hrs)	Ar µM	Mean Ar	std dev	N_2 µM	Mean N_2	std dev	N_2/Ar	Mean N_2/Ar	std dev
SITE 6	SSW	0		10.709			404.4		37.77		
SITE 6(spk)	Y 4B	1	11.6	11.544	0.084	448.2	442.9	5.36	38.55	38.36	0.19
SITE 6(spk)	Y 4A	1	11.5			437.5			38.18		
SITE 6(spk)	Y 5A	7	11.6	11.204	0.388	454.9	437.1	17.83	39.24	39.00	0.24
SITE 6(spk)	Y 5B	7	10.8			419.3			38.76		
SITE 6(spk)	Y 6A	14	11.4	11.228	0.145	450.7	443.6	7.16	39.63	39.50	0.13
SITE 6(spk)	Y 6B	14	11.1			436.4			39.37		
SITE 6	B(1A)L	0.50	12.0	11.514	0.519	463.8	445.3	18.50	38.55	38.69	0.14
SITE 6	B(1B)C	0.50	11.0			426.8			38.82		
SITE 6	B(5A)M	13.00	10.6			436.8			41.21	41.21	
SITE 6	B(6A)K	17.00	10.8	10.828	0.028	422.2	425.0	2.73	39.10	39.25	0.15
SITE 6	B(6B)D	17.00	10.9			427.7			39.40		
SITE 6	Y (1A)	0.50	12.8	11.401	1.443	439.8	429.1	10.71	34.24	38.13	3.89
SITE 6	Y (1B)	0.50	10.0			418.4			42.02		
SITE 6	YELL(5A)B	13.00	11.0	11.000		433.6	433.6		39.42	39.42	
SITE 6	YELL(6B)A	17.00	11.3	11.757	0.438	444.4	458.4	14.01	39.26	38.99	0.26
SITE 6	YELL(6B)F	17.00	12.2			472.4			38.73		
SITE 37	SSW	0		11.220	0.103		417.0	7.06		37.16	0.33
SITE 37(spk)	B 4A	1	11.6	11.681	0.125	469.1	454.2	14.92	40.60	38.90	1.69
SITE 37(spk)	B 4B	1	11.8			439.3			37.21		
SITE 37(spk)	B 5A	9	12.2	11.907	0.312	494.6	475.6	19.01	40.48	39.93	0.55
SITE 37(spk)	B 5B	9	11.6			456.6			39.38		
SITE 37(spk)	B 6A	15	11.8	11.603	0.223	447.5	439.2	8.24	37.84	37.86	0.02
SITE 37(spk)	B 6B	15	11.4			431.0			37.87		
SITE 37	B 1A	0.5	7.1	9.318	2.221	274.2	353.9	79.72	38.63	38.11	0.53
SITE 37	B 1B	0.5	11.5			433.7			37.58		
SITE 37	B 5A	15.5	11.2	9.346	1.807	460.9	452.5	8.47	41.33	50.11	8.78
SITE 37	B 5B	15.5	7.5			444.0			58.90		
SITE 37	B 6A	19.2	12.1	11.808	0.283	465.4	457.4	8.00	38.50	38.75	0.25
SITE 37	B 6B	19.2	11.5			449.4			39.00		
SITE 37	Y 1A	0.5	11.2	10.945	0.254	420.3	421.9	1.62	37.53	38.57	1.04
SITE 37	Y 1B	0.5	10.7			423.5			39.62		
SITE 37	Y 5A	15.5	12.0	11.576	0.408	472.5	450.8	21.64	39.42	38.93	0.50
SITE 37	Y 5B	15.5	11.2			429.2			38.43		
SITE 37	Y 6A										
SITE 37	Y 6B	19.5	11.2			426.1			38.17		
SITE 8	SSW			10.755	0.330		413.6	9.56		38.47	0.72
SITE 8	B 1B	0.5	11.4	11.663	0.239	438.9	448.1	9.23	38.42	38.42	0.00
SITE 8	B 1A	0.5	11.9			457.4			38.43		
SITE 8	B 5A	13.5	11.3	11.298	0.025	439.9	431.4	8.46	38.85	38.19	0.67
SITE 8	B 5B	13.5	11.3			423.0			37.52		
SITE 8	B 6A	14.5	11.9	11.409	0.444	450.3	437.2	13.15	37.99	38.33	0.34
SITE 8	B 6B	14.5	11.0			424.0			38.67		
SITE 8	Y 1B	0.5	10.7	10.929	0.237	405.6	421.3	15.64	37.94	38.53	0.59
SITE 8	Y 1A	0.5	11.2			436.9			39.13		

SITE 8	Y 5A	15	11.6	11.039	0.532	458.0	438.1	19.82	39.58	39.69	0.12
SITE 8	Y 5B	15	10.5			418.3			39.81		
SITE 8	Y 6A										
SITE 8	Y 6B	16	11.1			439.8			39.62		
SITE 16	SSW	0		10.587	0.222		394.9	6.34		37.31	0.51
SITE 16	B 1A	0.5	14.3	12.898	1.354	462.9	451.0	11.86	32.48	35.26	2.78
SITE 16	B 1B	0.5	11.5			439.2			38.04		
SITE 16	B 5A	11.5	12.0	11.792	0.214	441.7	442.7	0.99	36.79	37.55	0.76
SITE 16	B 5B	11.5	11.6			443.7			38.32		
SITE 16	B 6A	12.5	12.4	11.878	0.494	446.6	438.3	8.27	36.09	36.93	0.84
SITE 16	B 6B	12.5	11.4			430.0			37.77		
SITE 14	SSW	0		10.619	0.415		401.1	10.99		37.79	0.71
SITE 14	Y 1A	0.5	11.7	11.444	0.231	440.1	443.1	3.04	37.69	38.74	1.05
SITE 14	Y 1B	0.5	11.2			446.1			39.79		
SITE 14	Y 5B	12	11.5	11.508	0.036	425.6	429.7	4.04	36.87	37.34	0.47
SITE 14	Y 6B	13	11.5			433.7			37.81		

TABLE 8b: N_2 concentrations in chamber samples at Sites 6, 8, 14, 16 and 37, February 1995

Site	Temp. (C)	Ar µM	N_2 µM	Measured N_2/Ar	hours	N_2/Ar^*Ar_c	Average of N_2/Ar^*Ar_c
6 blue	21.6	12.03	464	38.55	0.5	416	417
		10.99	427	38.82	0.5	419	
		10.60	437	41.21	13	445	445
		10.80	422	39.10	17	422	423
		10.86	428	39.40	17	425	
		10.79	404	37.46	0	404	404
6 yellow	21.6	12.84	440	34.24	0.5	369	411
		9.96	418	42.02	0.5	453	
		11.00	434	39.42	13	425	425
		11.32	444	39.26	17	424	421
		12.20	472	38.74	17	418	
		10.79	404	37.46	0	404	404
6 (spike)	21.6	11.63	448	38.55	1	416	414
		11.46	437	38.18	1	412	
		11.59	455	39.24	7	423	421
		10.82	419	38.76	7	418	
		11.37	451	39.63	14	428	426
		11.08	436	39.37	14	425	
		10.79	404	37.46	0	404	404
8 blue	21.6	11.42	439	38.42	0.5	413	413
		11.90	457	38.43	0.5	413	
		11.32	440	38.85	13.5	418	411
		11.27	423	37.52	13.5	404	
		11.85	450	37.99	14.5	409	412
		10.97	424	38.67	14.5	416	
		10.76	414	38.44	0	414	414
14 yellow	20.9	11.67	440	37.69	0.5	400	411
		11.21	446	39.79	0.5	423	
		11.54	426	36.87	12	392	392
		11.47	434	37.81	13	402	402
		10.62	401	37.77	0	401	401
16 blue	24.2	14.25	463	32.48	0.5	345	374
		11.54	439	38.04	0.5	404	
		12.01	442	36.79	11.5	391	399
		11.58	444	38.32	11.5	407	
		12.37	447	36.09	12.5	383	392
		11.38	430	37.77	12.5	401	401
		10.62	395	37.18	0	395	
37 blue	20.4	7.10	274	38.63	1	433	428
		11.54	434	37.58	1	422	
		11.15	461	41.33	9	464	464
		7.54	444	58.90	9	*661*	
		12.09	465	38.50	15	432	435
		11.52	449	39.00	15	438	
		11.22	417	37.17	0	417	417
37 yellow	20.4	11.20	420	37.53	0.5	421	433
		10.69	424	39.62	0.5	445	
		11.98	472	39.42	15.5	442	437
		11.17	429	38.43	15.5	431	
		11.16	426	38.17	19.5	428	428
		11.22	417	37.17	0	417	417
37spike	20.4	11.56	469	40.60	1	456	437
		11.81	439	37.21	1	418	
		12.22	495	40.48	9	454	448
		11.60	457	39.38	9	442	
		11.83	447	37.84	15	425	425
		11.38	431	37.87	15	425	
		11.22	417	37.17	0	417	417

Table 9: Biogenic N_2 measurements at Sites 6, 16 & 37 (these data by gas chromatography)

Date	Site	Chamber	Hours	mM N_2
8/6/95	6	4	0	481
			6	507
		5	0	481
			6	498
		6	0	481
			6	517
30/8/95	16	5	0	497
			4	507
		6	0	502
			4	504
	37	4	0	488
			22	497
			22	501
		5	0	499
			22	495
			22	502
		6	0	485
			22	495
			22	493

Table 10: N_2 data (by gas chromatography and mass spectrometry) for Sites 16 and 37 for the benthic chamber deployments of January/February 1996; the Weiss reference N_2 concentration at 19°C and 35 psu (435 µm) is for Port Phillip Bay water at the temperature and salinity at collection.

Site	Chamber	Hours	µM N_2 by GC	µM N_2 by MS
16	4	0.25	443.0	436.8
		2.5	491.0	437.2
		5.33	445.0	439.8
16	5	0.25	442.0	438.9
		2.5	460.0	436.7
		5.33	440.0	440.5
16	6	0.25	435.0	439.2
		2.5	447.0	439.1
		5.33	446.0	514.8
37	4	0.25	440.0	439.4
		24	459.0	453.6
37	5	0.25	440.0	437.8
		22	449.0	452.6
37	6	0.25	440.0	435.1
		22	449.0	450.9
Weiss Ref.			435.0	435.0

Table 11: Summary of benthic chamber seasonal variations in fluxes of oxygen, carbon dioxide, DIN, N_2 and denitrification efficiencies.

Site & Method	Date	Chamber	Hours	CO_2 flux mmol m^2 day-1	% N lost from DIN & CO_2 flux	Tot DIN as N_2 from CO_2	% N lost *vs* 1st draw $N_2/(N_2+DIN)$ measured	Chamber volume (L)	µM N_2 calculated from CO_2 flux	µM N_2 measured *vs* first draw	µM N_2 measured *vs* Weiss N_2	mM N_2 m^2 day^{-1} calculated from CO_2	mM N_2 m^2 day^{-1} vs draw 1	mM N_2 m^2 day^{-1} vs Weiss
6(GC)	8/03/95	6 Yellow	14	70.4	86	3.7	79.6	8	22	14	21	4.57	2.91	4.36
6(GC)	22/02/95	6 Blue	13	40.2	75	7.5	89.8	8.27	10	29	19	2.28	6.71	4.40
6(GC)	22/02/95	6 Yellow	13	55	74	4.0	73.0	9.47	12	11	22	3.07	2.91	5.83
6(GC)	8/06/95	4(6)	5	25.95	65	4.1	83.4	5.9	3	8	20	1.27	3.43	8.58
6(GC)	8/06/95	5(6)	5	15.7	65	0.4	0.0	5.9	2	0	8	0.77	0.00	3.43
6(GC)	8/06/95	6(6)	5	17.58	52	8.4	92.4	5.9	2	18	30	0.69	7.72	12.87
8(GC)	28/02/95	8 Yellow	16	24.4	92	1.5	90.0	7.3	10	8	8	1.69	1.33	1.33
8(GC)	28/02/95	8 Blue	14.5	18.2	72	0.4	0.0	7.3	5	0	0	0.99	0.00	0.00
14(GC)	3/03/95	14 Yellow	13	82.2	28	4.5	0.0	7.8	8	0	1	1.74	0.00	0.22
16(GC)	3/03/95	16 Blue	12.5	119.8	30	6.3	0.0	8	12	0	4	2.71	0.00	0.93
16(GC)	30/08/95	5	4	17.0	84	5.6	96.3	5.9	2	10	8	1.07	5.36	4.29
16(GC)	30/08/95	6	4	15.2	83	1.3	84.6	5.9	2	2	5	0.95	1.07	2.68
16(GC)	18/01/96	4	5.33	48.9	65	2.2	40.3	6.4	5	2	10	2.40	0.87	4.37
16(GC)	18/01/96	5	5.33	49.8	65	1.3	0.0	6.25	6	0	5	2.44	0.00	2.13
16(GC)	18/01/96	6	5.33	78.1	34	8.5	54.3	6.15	5	11	11	2.00	4.62	4.62
16(MS)	18/01/96	4	5.33	48.9	65	2.6	51.2	6.4	5	3	5	2.40	1.35	2.10
16(MS)	18/01/96	5	5.33	49.8	65	2.0	33.7	6.25	6	2	6	2.44	0.67	2.35
16(MS)	18/01/96	6	5.33	78.1	34	14.6	73.4	6.15	5	26	80	2.00	10.74	33.48
37(GC)	24/02/95	37 Blue	19.2	30.1	85	3.9	91.2	6.4	16	29	44	1.93	3.52	5.33
37(GC)	24/02/95	37 Yellow	19.5	20.7	83	0.3	0.0	6.6	11	0	20	1.30	0.00	2.46
37(GC)	8/03/95	37 B+NO3	15	23.2	80	5.1	93.1	7.4	8	27	51	1.40	4.75	9.15
37(GC)	1/09/95	4	22	12.97	81	1.3	85.2	5.9	8	11	21	0.79	1.07	2.05
37(GC)	1/09/95	5	22	20.87	70	0.5	0.0	5.9	11	0	21	1.10	0.00	2.05
37(GC)	1/09/95	6	22	13.8	82	1.1	82.4	5.9	9	9	16	0.85	0.88	1.56
37(GC)	23/01/96	4	24	15.5	78	2.0	86.8	5.9	10	19	24	0.91	1.70	2.15
37(GC)	23/01/96	5	24	17.8	72	1.1	66.0	5.35	12	9	14	0.97	0.73	1.13
37(GC)	23/01/96	6	24	16.2	75	1.1	72.5	5.9	10	9	14	0.92	0.80	1.25
37(MS)	23/01/96	4	24	15.5	78	1.5	83.1	5.9	10	14	19	0.91	1.27	1.66
37(MS)	23/01/96	5	24	17.8	72	1.6	76.2	5.35	12	15	18	0.97	1.21	1.43
37(MS)	23/01/96	6	24	16.2	75	1.7	82.2	5.9	10	16	16	0.92	1.41	1.42

FIGURE: 24. N_2 measurements in benthic chambers placed on sediments in Port Phillip Bay, January 1996. N_2 measurements were made by gas chromatography (■) and mass spectrometry (O). The entries marked [ ] indicate N_2 enrichment well beyond experimental expectations and appear to be due to some systematic error. Artificial seawater (ASW) was used as the internal standard with duplicate measurements preceding and following each Port Phillip Bay water sample.

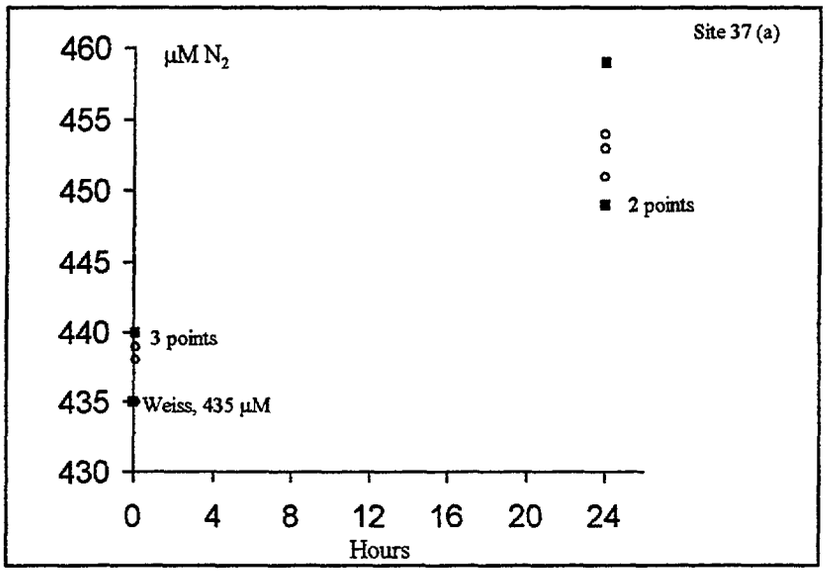

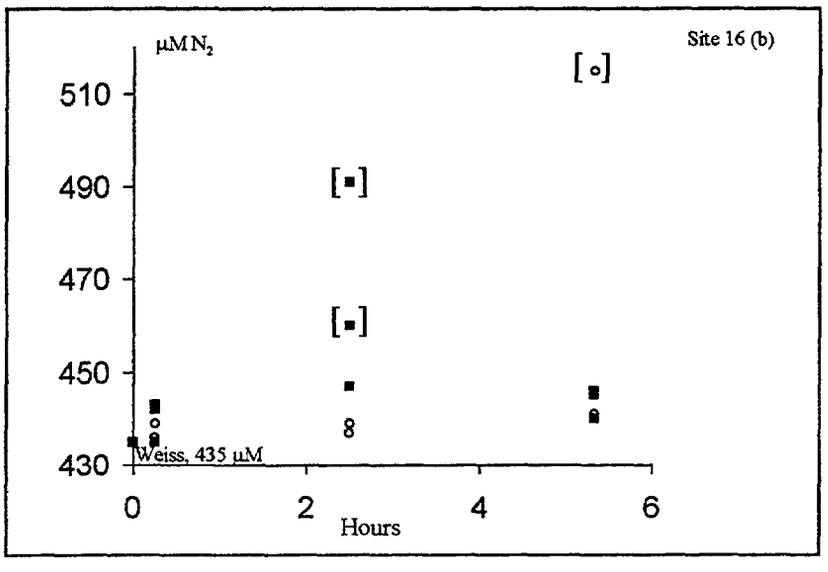

FIGURE: 25

N_2 (○), Total N (◇) and Redfield N from CO_2 (□) measurements in Yarra Estuary (Station 16) and Central Basin (Station 37) sediments of Port Phillip Bay. N_2 was measured by Mass Spectrometry. All data are as μmol N m^2 . The open triangle (△) represents the Total N corrected for the offset shown in the N_2 concentration of the first draw (at 15 mins) from the benthic chambers. The hatched area is representative of the DIN inventory (NH_4 +NO_3 + NO_2)

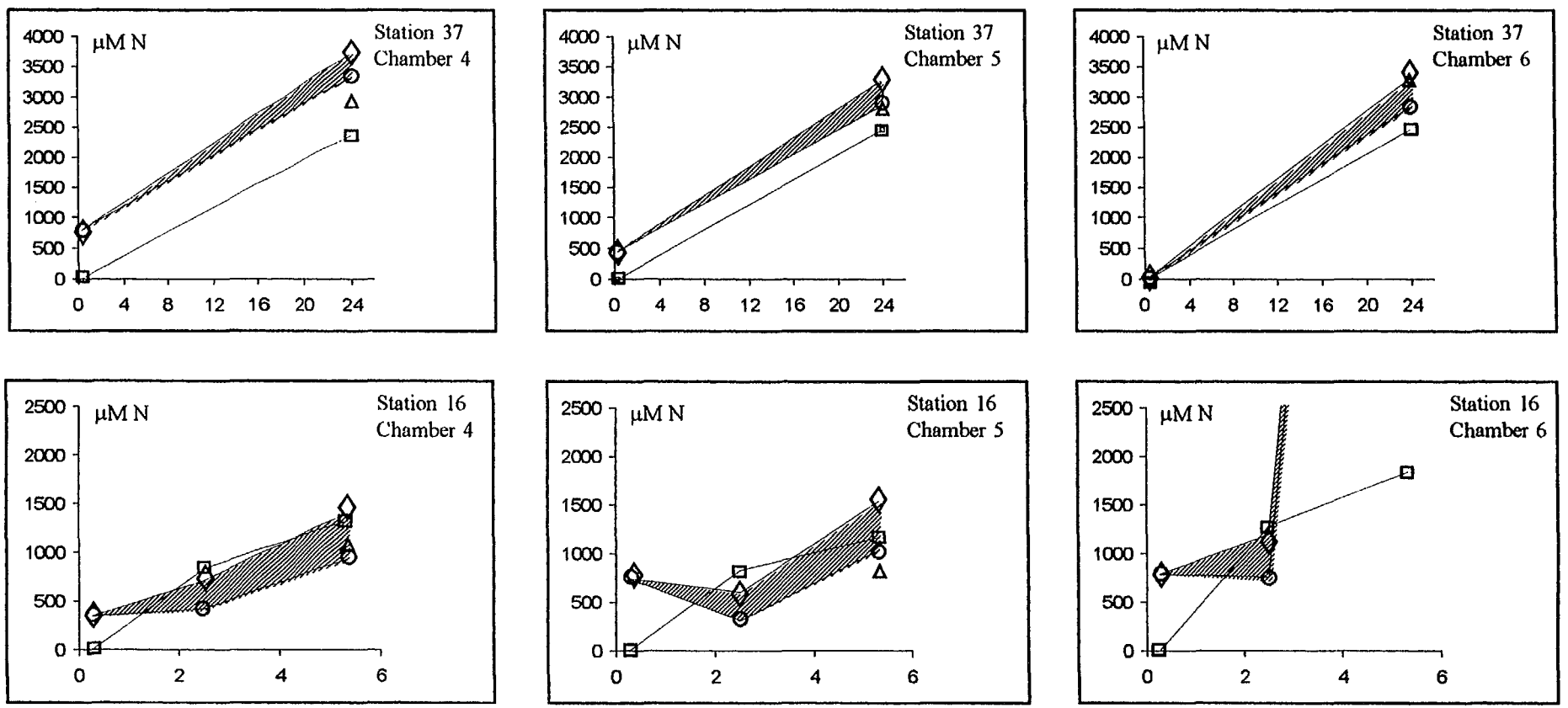

FIGURE: 26

N_2 (○), Total N (◇) and Redfield N from CO_2 (□) measurements in Yarra Estuary (Station 16) and Central Basin (Station 37) sediments of Port Phillip Bay. N_2 was measured by Gas Chromatography. All data are as µmol N m^2 . The open triangle (△) represents the Total N corrected for the offset shown in the N_2 concentration of the first draw (at 15 mins) from the benthic chambers. The hatched area is representative of the DIN inventory (NH_4 +NO_3 + NO_2)

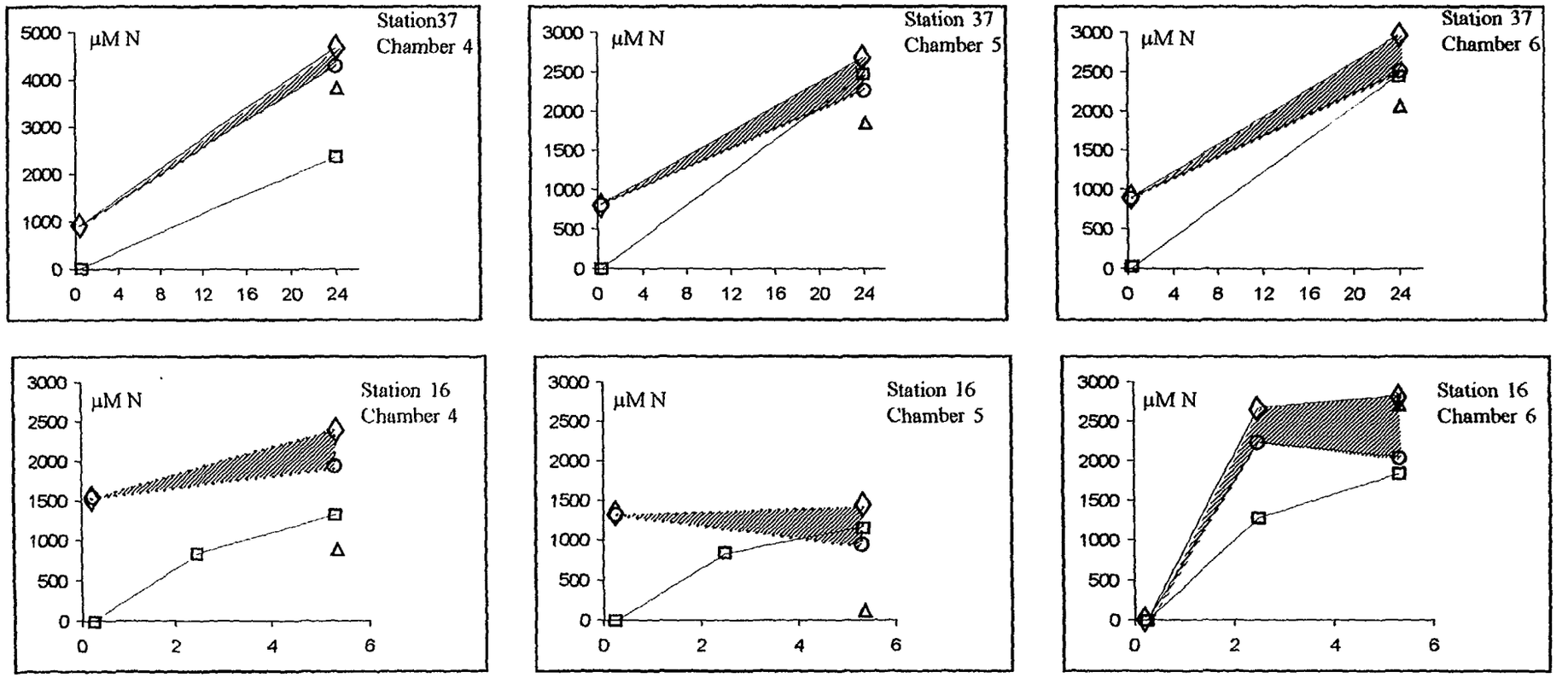

Figure: 27. A test of the Redfield model for N mineralisation in Port Phillip Bay: N predicted & N measured as N_2 and N_2 + DIN (as N_2) *vs* CO_2 oxidised in sediments. N_2 data plotted as (o)and N_2+DIN/2 as (□).

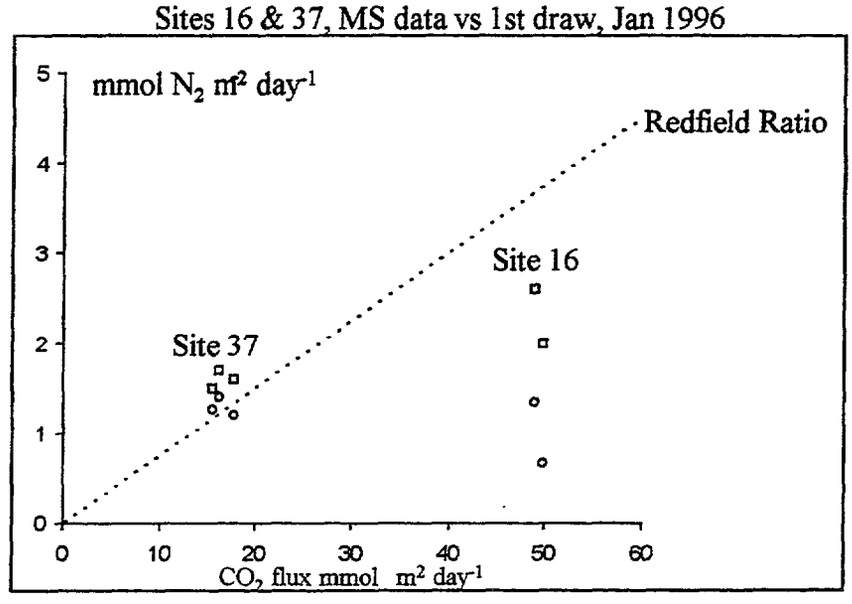

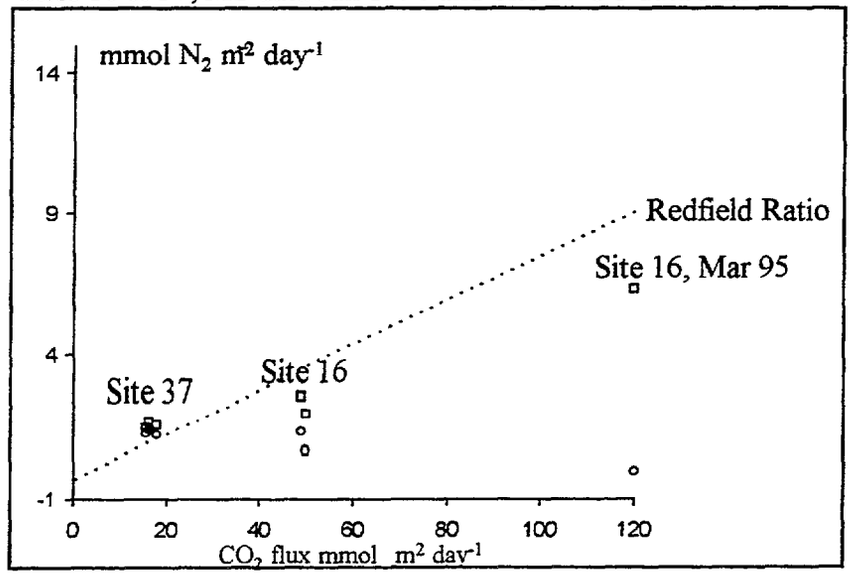

Figure 28: % denitrification measured N (N_2 /(N_2 + DIN) vs CO_2 flux

(a) Sites 16 & 37, MS data , Jan 1996

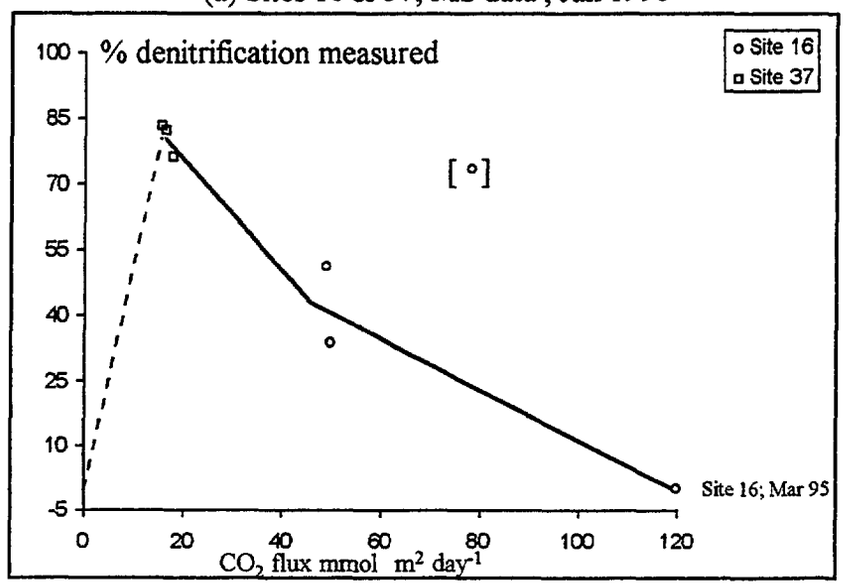

(b) Sites 16 & 37, all seasonal data.

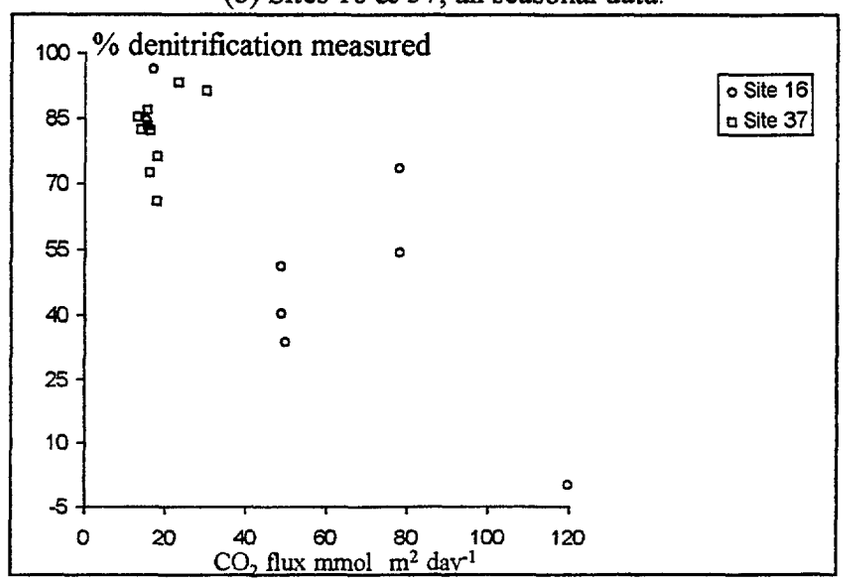

FIGURE: 29. Direct N_2 measurements in benthic chambers placed on sediments in Port Phillip Bay. N_2 measurements were made with a TCD Gas Chromatogram. Values for replicates are plotted as circles, squares and triangles. The N_2 concentration in bay water at the temperature and salinity (Weiss, 1970) at collection is recorded as a **O** at zerotime

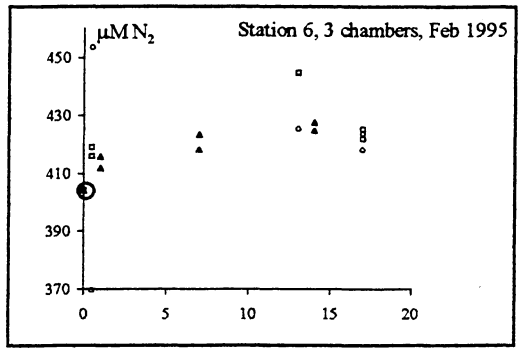

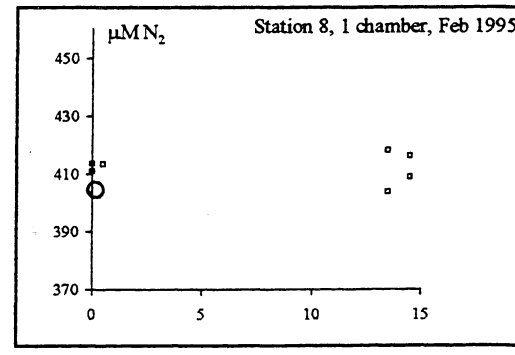

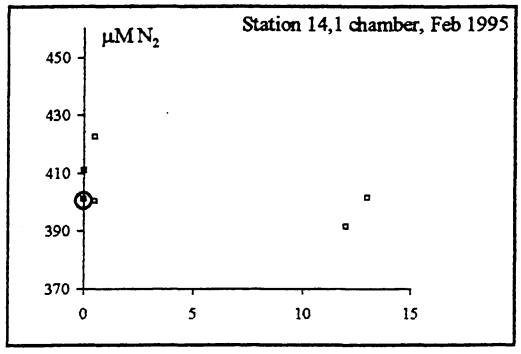

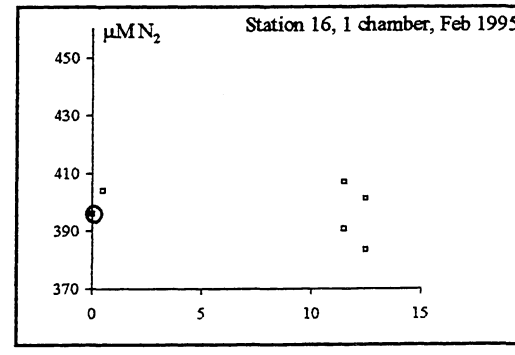

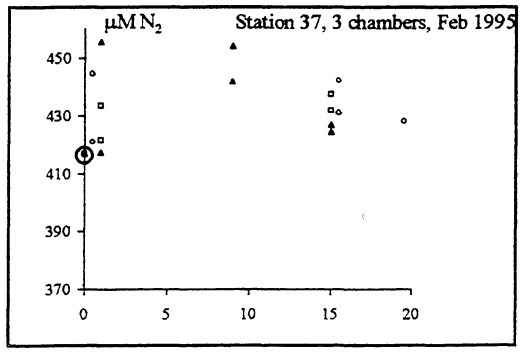

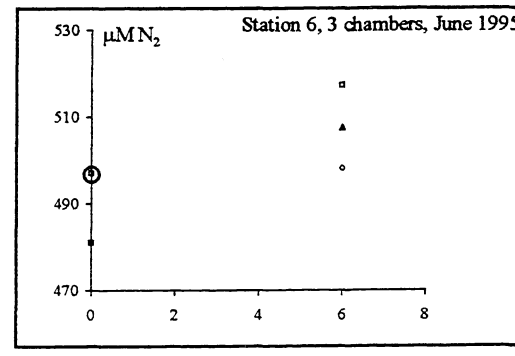

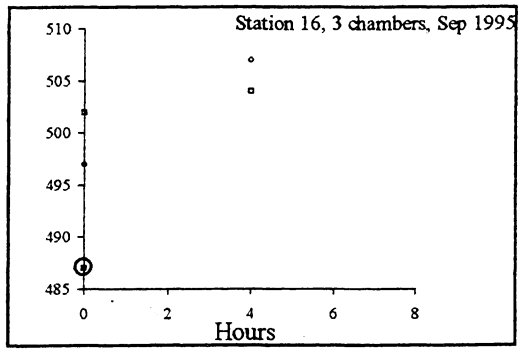

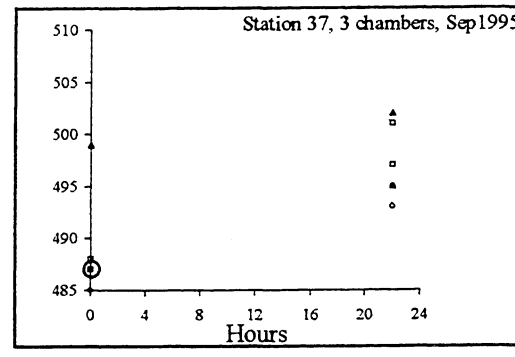

Figure: 30. Seasonal variations in denitrification; the Feb95 and the Aug/Sep 95 data are from GC measurements and the Jan 1996 data are from MS measurements.

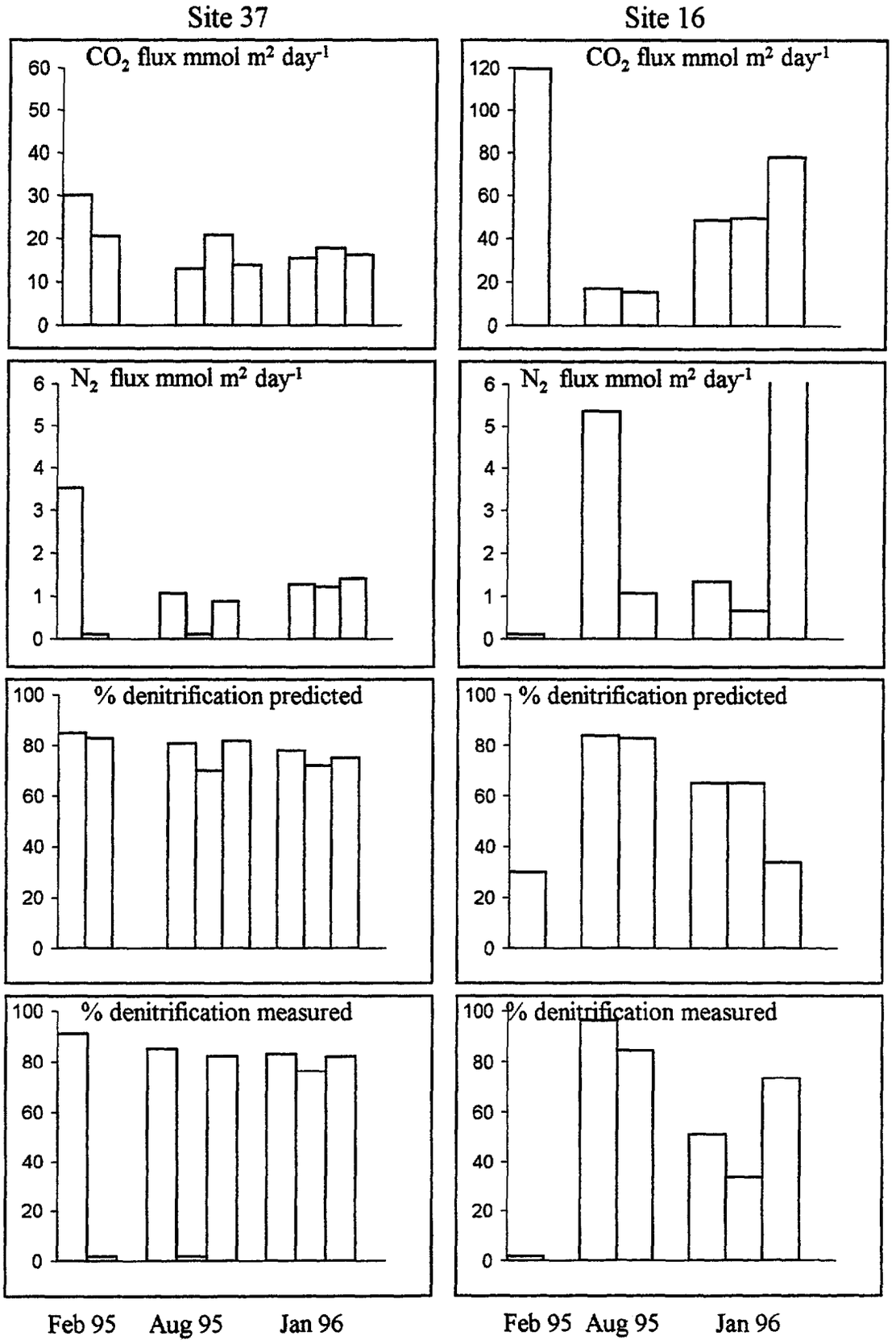

Figure 31a: N_2 enrichment in sediment porewaters in Port Phillip Bay

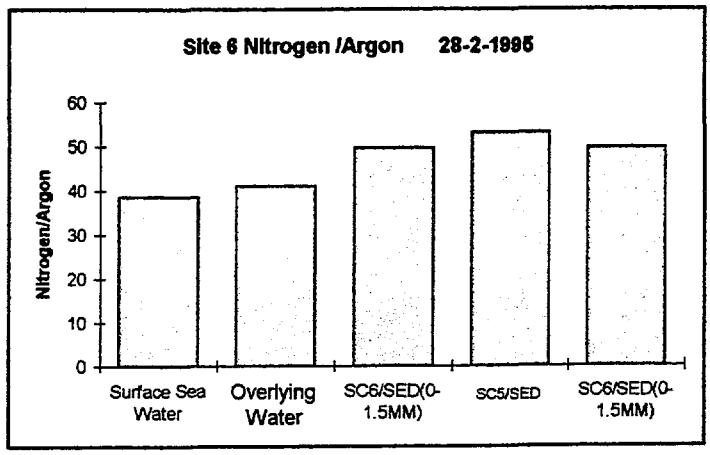

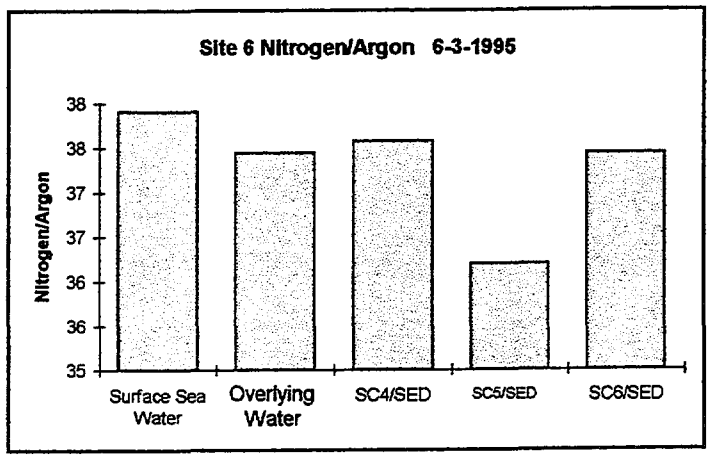

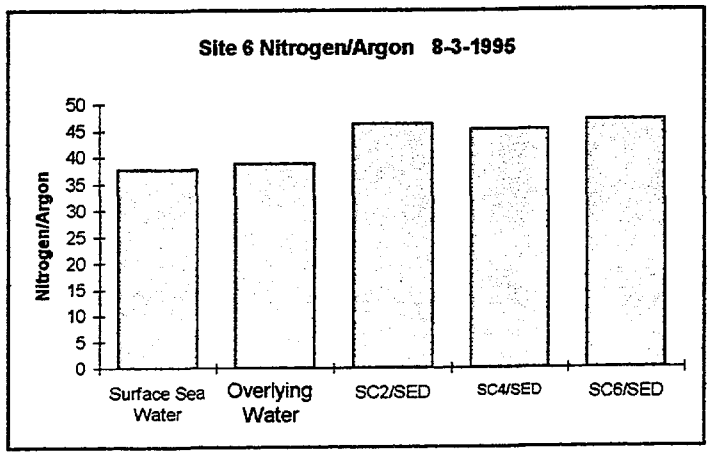

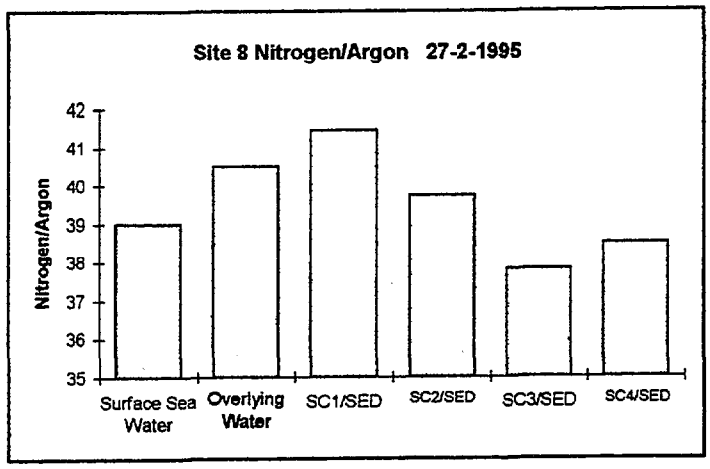

Figure 31b: N_2 enrichment in sediment porewaters in Port Phillip Bay

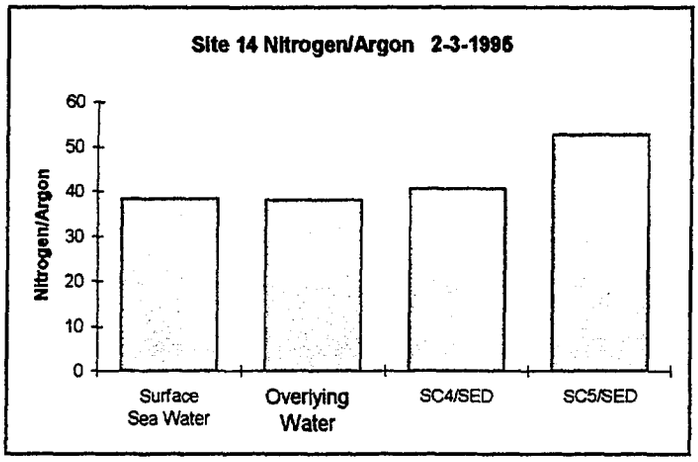

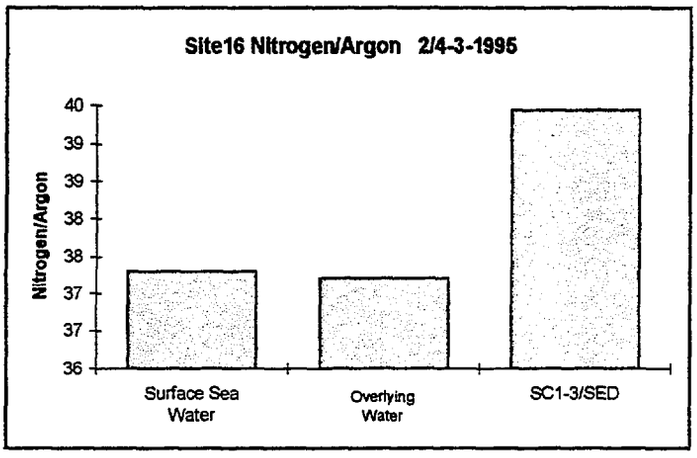

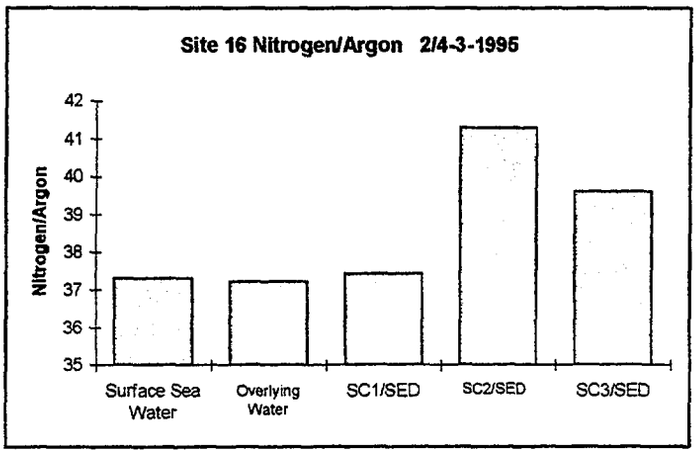

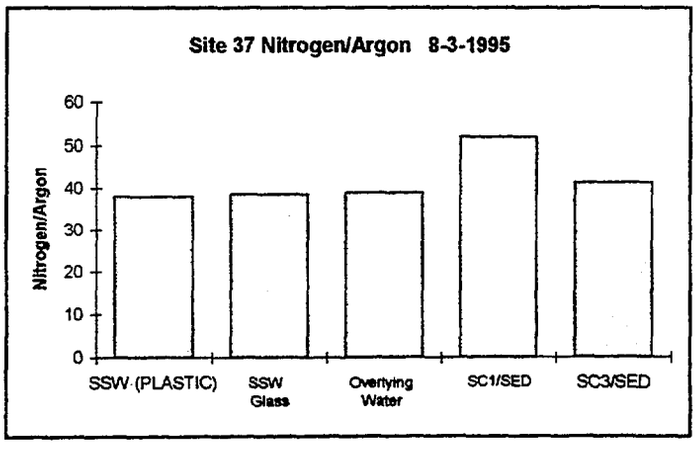

TRANSPORT PROCESSES AND TRACER KINETICS

Introduction

During the summer deployments of 1995 different tracers were added to the USC benthic chambers to determine the rate constants which characterise the transport processes across the sediment-seawater interface, and hence determine the relative importance's of diffusion and other transport process in moving solutes between the sediments and the overlying waters.

Methods

In addition to the Cs tracer, D_2O (heavy water) and NaBr (sodium bromide) solutions were prepared and a 'mixed' spike of all three tracers added to several chamber deployments.

Nine deployments were made and seven yielded useful data on both bromide and deuterium concentrations in the benthic chamber as a function of time. As an initial step in the data analysis, and to facilitate inter-comparison with the Cs tracer results obtained with the USC chambers (this report) and Nicholson et al. (1966) single exponentials were fitted to the concentration versus time D_2O and Br data at CSIRO Division of Environmental Mechanics.

Results

The results of these analyses are summarised in Table 12, and they indicate that there is very close agreement between the values obtained using Cs and those from the Br and D_2O experiments.

Table 12.
Results from fitting simple exponential function to concentrations versus time data for Cs, Br and D_2O

Size	Deployment Date	k (hr^{-1}) Cs	k_{Br} (hr^{-1})	k(hr^{-1}) D_2O	R^2 Br	R^2 D_2O
6 Blue	20.2.95	.067	.068	.058	.98	.994
6 Yellow	20.2.95	.074	.056	.059	.997	.997
8 Blue	27.2.95	.023	.030	.021	.996	.995
16 Blue	2.3.95	.19	.200	.178	.982	.986
37 Blue	23.2.95	.046	.032	.031	.994	.998
37 Blue	6.3.95	.031	.022	.028	.951	.963
37 Yellow	23.2.95	.034	.028	.026	.993	.995

Figure 32 displays the k values for all 3 tracers. The close congruence between all 3 data sets is immediately apparent, indicating the 'conservative' behaviour of Cs in this environment.

Summarised in Table 13 are the results of simple exponential curve-fits to the recent 1995 Cs data together with that collected in the previous field expedition in January 1994. The results

from 1994 vary over about a factor of five, indicating the transport process to be 'patchy'. The results for 1995 are generally similar to those measured in 1994 but are somewhat lower. However, the k value for Site 16 measured in 1995 seems anomalously high, being more than twice the next highest value at this Site and more than 4 times the k measured at the same site in 1994.

Table 13.
Comparison of first order rate constants for Cs disappearance, January 1994 & February/March 1995 k(hr^{-1})

Station	1994	1995
3B	.047	-
3Y	.046	-
6	.093	-
6B	-	.067
6Y	-	.074
8	.033	-
8*	.049	-
8B	-	.023
11	.030	-
13	.065	-
14	.044	-
16	.044	.19
19	.032	-
22	.045	-
32	.018	
37B		.046
37B*		.031
37Y		.034

A simple bioirrigation model

The simple wholly diffusive model is unable to fully explain the change of the tracer concentration with time. In this section we apply a simple bioirrigation model to the transport of the tracer from the benthic chamber to the sediments. This model treats all transport as occurring by the benthic organisms pumping water between the sediments and the overlying water. The model neglects transport due to diffusion - lumping it into the pumping transports. This assumption is justified in part by the reduced diffusive transport caused by the smaller concentration gradients within the sediments caused by the bioirrigation. The more severe assumption implicit in the model is that the exchange rate does not vary with depth. Using these assumptions it can be shown (McCaffrey et al, 1980) that the decrease in concentration (C_s) of a conservative tracer in the supernatant solution within the benthic chamber is described by

$$\frac{dC_s(f)}{dt} = -KC_s(f) + \frac{KV_s}{V_p}C_s(o) - K\frac{V_s}{V_p}C_s(f) \qquad (1)$$

Where $C_s(f)$ is the supernatant tracer concentration at time f; $Cs(o)$ the corresponding quantity at $f = 0$ (i.e. immediately after tracer injection, K- the exchange constant (hr^{-1}), V_S- the volume of the overlying solution and V_p the volume of the pore water reservoir exchanging with the supernatant solution. The first term right hand side of (i) refers to the flow of water into the sediments while the other turn 2 terms are for the outflow. The solution of this equation is:

$$C_s(t) = \frac{C_s(o)}{\left(\frac{V_s}{V_p}+1\right)}\left\{\frac{V_s}{V_p} + \exp(-Kt)\left(\frac{V_s}{V_p}+1\right)\right\} \qquad (2)$$

Rearranging (2) gives

$$\ln\left[\frac{C_s(f)}{C_o}\left(1+\frac{V_s}{V_p}\right)-\frac{V_s}{V_p}\right] = +K\left(1+\frac{V_s}{V_p}\right)t \qquad (3)$$

or

$$\frac{1}{\left(1+\frac{V_s}{V_p}\right)}.\ln\left[\frac{C_s(t)}{C_v}\left(1+\frac{V_s}{V_p}\right)-\frac{V_s}{V_p}\right] = Kt \qquad (4)$$

Thus plotting the left hand side of (4) against t using various values of V_s/V_p gives a best fit value of K. Table 14 shows the best fit values of K and V_s/V_p. Note that because of the exponential term on equation (2) the estimated value of V_s/V_p is not especially sensitive to changes in K and *vice versa*. Accordingly the reported values of V_s/V_p should be regarded as having an error of ±15%.

The biopumping rate (p) is given by

$$p = K \times L \qquad (5)$$

Where L is the height of the chamber. Values of p are reported in Table 15 also.

Table 14.

Values of K and $\frac{V_s}{V_p}$ estimated from data for Br and D_2O tracers

Station	Br		D_2O		
	-K(hr^{-1})	$\frac{V_s}{V_p}$	-K(hr^{-1})	$\frac{V_s}{V_p}$	p^*Br/D_2O ($cm^3cm^{-2}hr^{-1}$)
6B	.095	0.35	.07	.35	1.1/0.9
6Y	.063	.30	.066	.30	0.8/0.9
8B	.03	.3	.025	.3	.3/.3
16B	.25	.1	.22	.1	2.9/2.5
37B	.033	.35	.028		.3/.3
37*B	.028	.13	.03	.13	.3/.3
37Y	.03	.8	.028	.8	.3/.3

* Rates for Br and D_2O indicated.

The Sites fall into 3 categories (1) those where the pumping rate is 0.3 cm^3 cm^{-2} hr^{-1} (8B, 37B, 37*B, 37Y), (2) a smaller group with a higher rate of about 1cm^3 cm^{-2} hr^{-1} (6B and 6Y), and (3) an outlier at about 3 cm^3 cm^{-2} hr^{-1} (16B). To set these values in context we give in Table 15 pumping rates measured in other estuarine environments. The lowest rate of Port Phillip Bay is of about the same as the value observed in San Francisco Bay. The other 2 groups of stations from Port Phillip Bay have rates about 3 and 10 times larger than those measured from elsewhere.

Table 15.
Pumping rates for various estuarine environments

Location	k(sec^{-1})	Reference
Port Phillip Bay:	$x10^{+7}$	
* Stations 8B, 37B, 37*B and 37Y	83	This work
* Stations 6B and 6Y	278	This work
* Station 16B	830	This work
Narragansett Bay	5 - 13	Leudtke & Bender, 1979
Narragansett Bay	4.6 - 12.7	McCaffrey et al, 1980
San Francisco Bay	87*	Hammond & Fuller, 1979

Summary of tracer experiments

1. All three tracers display very similar disappearance kinetics (Figure 32). As they include a cation (Cs, anion (Br) and a neutral molecule (D_2O) with properties virtually identical to water we conclude that they are being removed by a physical, rather than a chemical, process (or that the chemical processes are slow relative to the physical removal processes).

2. Within the limitations imposed by the simple model of bioirrigation (- depth independent exchange rate, no diffusion), this simple model provides a good description of the time course of tracer loss from the chambers
3. Although the model provides an estimate of the V_s/V_p (ratio of chamber volume to the porewater volume with which it is exchanging) it provides no guidance as to where that volume is physically located. As can be seen from Table 15 this pore water volume is 1.2 to 10 times the volume of the chamber. Using the porosity for site 6 (0.47) this translates to sediment depths of 25 cm to approximately 2 metres. The one core we have, however, does not indicate exchange to such depths. This contradiction can be resolved by postulating a shallow bioirrigation exchange together with an exchange to regions deep within the sediments beyond the coring range.
4. The biological aspects of the various sites should be integrated with the physical data reported here. What are the benthic organisms which produce such high pumping rates, and is their relative abundance consistent with the order of magnitude variation in pumping rate, and the apparent smooth decline in tracer concentration?

Acknowledgements

Will Berelson, Colin Tindall, David Heggie, Andy Longmore and Geoff Nicholson carried out the benthic chamber deployments and collected the water samples and their contribution is gratefully acknowledged. We thank Keith Newgrain (CSIRO Division of Wildlife & Ecology) for the mass spectrometric analysis of the samples for deuterium. Helpful conversations with Dr Ian T Webster (CSIRO, DEM) are gratefully acknowledged.

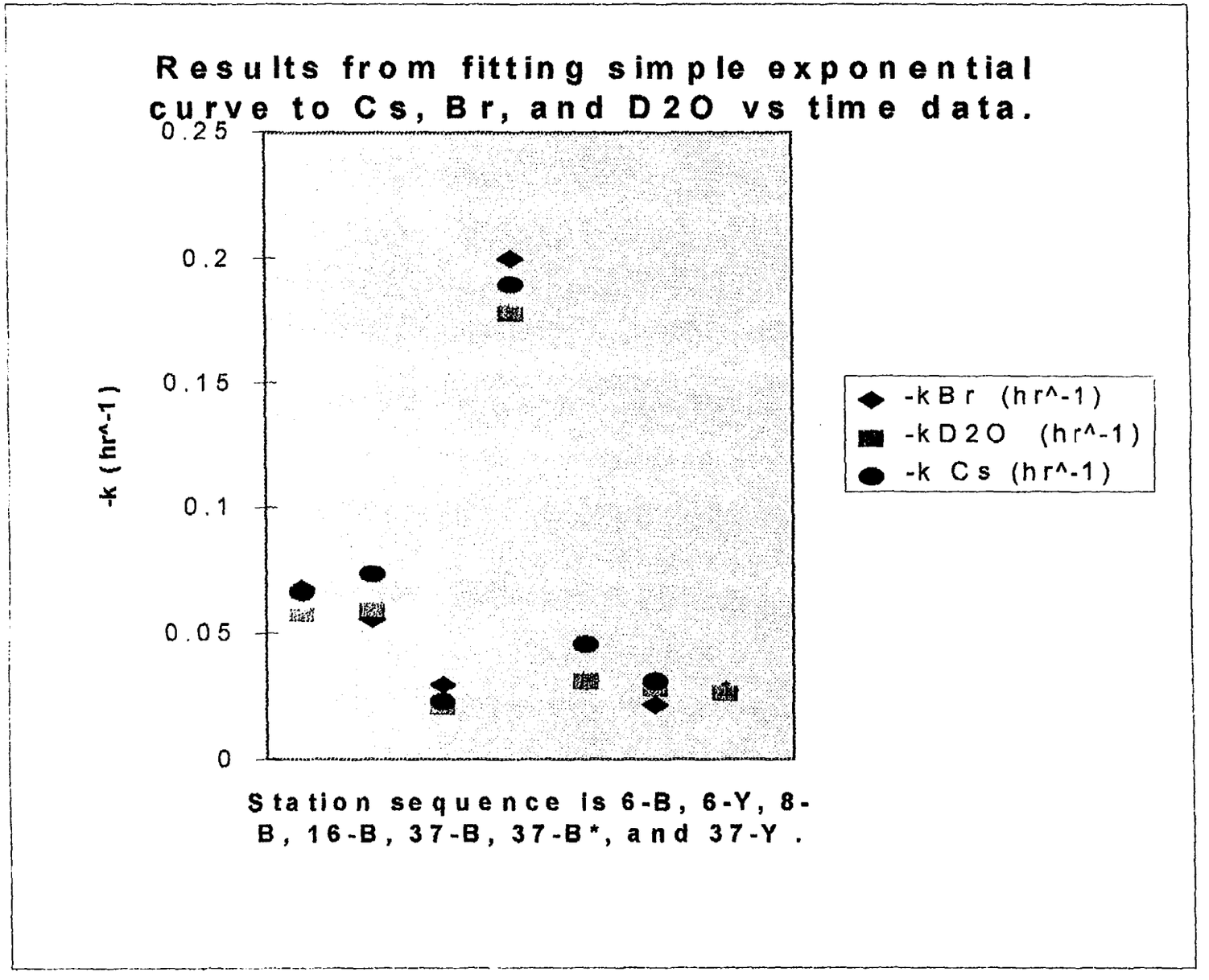
Results from fitting simple exponential curve to Cs, Br, and D2O vs time data.
0.25
0.2
0.15
0.1
0.05
0
-k (hr^-1)
-k Br (hr^-1)
-k D2O (hr^-1)
-k Cs (hr^-1)
Station sequence is 6-B, 6-Y, 8-B, 16-B, 37-B, 37-B*, and 37-Y .

Figure 32

References

Berelson, W.M. & D.E. Hammond, (1986), The calibration of a new free vehicle benthic flux chamber for use in the deep sea, Deep Sea Research, v. 33, 1439-1454

Berelson, W. M., D. E. Hammond & A. Eaton (1987c), A technique for the rapid extraction of radon-222 from water samples and a case study. In: Radon in Groundwater, ed. B. Graves, National Water Well Association, 271-281

Berelson, W. M., D. E. Hammond & G. Cutter, (1990), In situ measurements of calcium carbonate dissolution in deep-sea sediments. Geochim. Cosmochim. Acta, v. 54, 3013-3020

Berelson, W.M., D.E. Hammond & K.S. Johnson (1987a), Benthic fluxes and the cycling of biogenic silica and carbon in two southern California borderland basins. Geochimica et. Cosmochimica Acta, v. 51, 1345-1363

Berelson, W.M., D.E. Hammond, McManus, J. & T. Kilgore. (1994), Dissolution kinetics of calcium carbonate in equatorial Pacific sediments. Global Biogeochemical Cycles, v. 8, 219-235

Berelson, W.M., M.R. Buchholtz, D.E. Hammond & P.H. Santschi (1987), Radon fluxes measured with the MANOP Lander. Deep-Sea Research, v. 34, 1209-1228

Buchholtz ten Brink, M.R. (1987), Radioisotope mobility across the sediment water interface in the deep sea. Ph.D. Thesis, Columbia University, 451 pp

Burke, C.M., (1995), Microprofiles of oxygen concentration in Port Phillip Bay, Department of Aquaculture, University of Tasmania, Launceston

Hammond, D.E. & C. Fuller, 1979, Use of Radon-222 to estimate benthic exchange and atmospheric exchanges in San Francisco Bay, in San Francisco Bay - The Urbanized Estuary, (Ed. T.J. Conomos) AAAS, San Francisco, pp. 213-230

Leudtke, N., & M. Bender, 1979, Radiotracer studies of metal behaviour at the sediment-water interface of Narragansett Bay, Estuarine Coastal Marine Research, 9, 643-651

Longmore, A.R., Cowdell, R.A., & Flint, R., 1996, Nutrient Status of the water in Port Phillip Bay, Technical Report No. 24, CSIRO Port Phillip Bay Environmental Study, Melbourne, Australia.

McCaffrey, R.L., L.A. Myers, E. Davey, C. Morrison, N. Bender, M. Leudtke, D. Cullen, P. Froelich, & G. Klinkhammer, 1980, The relation between porewater chemistry and benthic fluxes of nutrients and manganese in Narrangansett Bay, Rhode Island, Limnol. Oceanog. 24, 31-44.

Nicholson, G.J., Longmore, A.R. & Cowdell (1996) Nutrient status of sediments in Port Phillip Bay, Technical Report No. 26, CSIRO Port Phillip Bay Environmental Study, Melbourne, Australia.

List of figure captions

Figure 1. Study area. This map shows the 1994 and 1995 sites. The latter are shown as stars.

Figure 2. Benthic chamber schematic. The unit consists of a PVC chamber (a), supported by an aluminium frame (o) that is approximately 1.2m x 0.5m x 0.5m. Other components include: chamber stirring paddle (b), hinged lid to top of chamber (c), pressure case with magnet-turning motor (d), pressure case with micro-processor (e) and batteries (f) with burn wire leads (g), bulb that draws 300 mL samples (h), sample tubes (k, j, i) and tubing leading out of chamber (l).

Figure 3-12. Analyte versus time plots for the chambers deployed. Concentrations are μM except alkalinity (μeq/L) and Cs (ppm). Values are corrected for the dilution which takes place during successive sampling. Analytical uncertainties statistics are given in Tables 1-10. Points plotted on the Y-axis are bottom water values measured on Niskin samples.

Figure 13 & 14. Oxygen electrode output. Electrode readings are made every 6 minutes. The plateau in output prior to time=0 suggests equilibration with the ambient bottom water. Ambient bottom water oxygen values were determined by Winkler titration on Niskin samples. The ambient oxygen electrode operated successfully during 4 deployments, and the chamber-electrode operated well in all deployments. The vertical tic-marks denote the timing of sample draws; six in total. The horizontal dashed line denotes the portion of the incubation deemed representative of a constant flux condition. The arrows against the X-axis denote local time, at 6 hour intervals.

Figure 15 & 16. Radon-222 versus incubation time plots. Data are from measurements of the last three samples drawn. The lines through the data define the flux of radon from bay sediments as a function of input and decay.

Figure 17 & 18. A comparison of benthic fluxes from Port Phillip Bay. Measurements made with the USC benthic chambers in January, 1994 and February, 1995. The data represent averages of chambers deployed at a given site (excluding the nitrate spiked experiments), or single chamber flux determinations. Uncertainties are s.d. of the averages or s.d. of the flux.

Figure 19. Oxygen uptake versus organic carbon oxidised (C_{OX}), for two scenarios described in the text. The dashed lines labelled 1.0 and 1.3 define the O_2/C_{OX} flux ratios.

Figure 20. Plots of nitrogen and phosphate fluxes versus total carbon oxidised. The top two panels include a line that defines the expected flux of N for a given flux of CO_2. The top panel includes the sum of nitrite, nitrate and ammonia fluxes, the middle panel adds DON to the three other N fluxes. The bottom panel shows the phosphate flux versus. the TCO_2 flux and the line denotes the expected relationship if the organic matter oxidised is typical marine phytoplankton.

Figure 21a) Cs concentration versus time after injection. The fits to these data are an exponential and the fitting parameter, "b", given on each plot, defines the curvature. Plots of delta deuterium versus time after injection. The fitting function is the same and the fitting

parameter, b, is given for each station. Plots of spikes of added nitrate versus time in two chambers are also given. The fitting function is the same as for previous figures.

Figure 22. The Cs fitting parameter, b, versus the measured radon flux. The rate of Cs loss from the chamber correlates positively with the magnitude of radon emanation from the sediments. Two sets of three points clustered together represent Sites 6 and 37.

Figure 23. Dissolved silica flux versus radon flux. Data from 1994 and 1995 are included on this plot. The relationship between these parameters is systematic and positive although two points with very large silicate fluxes fall off the trend. These two points are from Hobsons Bay and indicate very high dissolution rates of biogenic silica in 1995 compared to 1994.

Figure 24. Plots of N_2 measurements in benthic chambers deployed at Sites 16 and 37 during January/February 1996. Mass spectrometirc measurements are shown in open circles and gas chromaograph mesuremtns are shown in closed squares. Also shown are bottom water concentrations and the predicted bottom wter claclulated from Weiss's solubility tables.

Figure 25. N_2 (as N), Total N and Redfield N from CO_2 measurements in the Yarra estuary (Site 16) and the Central Basin (Site 37) sediments of Port Phillip Bay. N_2 was measured by mass spectrometry. All data are as µmol/m2. The open triangle represents the total N corrected for the offset shown in the N_2 concentration of the first draw (at 15 mins) from the benthic chambers.

Figure 26. N_2 (as N), Total N and Redfield N from CO_2 measurements in the Yarra estuary (Site 16) and the Central Basin (Site 37) sediments of Port Phillip Bay. N_2 was measured by gas chromatography. All data are as µmol/m2. The open triangle represents the total N corrected for the offset shown in the N_2 concentration of the first draw (at 15 mins) from the benthic chambers.

Figure 27. Plots of carbon dioxide fluxes and N fluxes (shown as N_2 -N denitrification flux) and DIN flux compared to the predicted N release flux calcualted from the CO_2 data and the Redfield ratio. This is another way of examining the denitrification hypothesis more directly as a function of different rates of organic matter metabolism in the sediments.

Figure 28a. Plot of the calculated denitrification efficiency versus measured CO_2 flux at Sites 16 and 37 during summer 1996. Also shown is the calculated denitrification efficiency at Site 16 during March 1995, a period when the temperatures were similar to those in January/February 1995.

Figure 28b. Plot of denitrification efficiency at Sites 16 and 37 for all seasonal data, February 1995, June 1995, September 1995 and January/February 1996.

Figure 29. Direct N_2 measurements in benthic chambers placed on the sediments in Port Phillip Bay during February, June and September 1995, N_2 measaurements were made with a TCD detector . The N_2 concentrtion in Bay water at the temperature and salinity (Weiss, 1970) at collection is recorded as 0 at zerotime.

Figure 30. Seasonal variations in the CO_2 flux, the measured N_2 flux, the % denitrification predicted (from Redfield model) and the % denitrification measured for Sites 16 and 37 during January/February 1996..

Figure 31. Histogram representations of N_2/Ar ratios in sediments at Sites 6 and 8, compared to surface waters, collected on various occasions.

Figure 32. Rate constants describing the removal of the three tracers from the benthic chambers deployed at several Sites in the Port Phillip Bay.

List of tables